

Probabilistic Treatment of the Sliding Wedge

By

Ping Feng

A Thesis

**Submitted to the Faculty of Graduate Studies
in Partial Fulfillment of the Requirements
for the Degree of**

MASTER OF SCIENCE

**Department of Civil and Geological Engineering
University of Manitoba
Winnipeg, Manitoba
Canada**

© Copyright by Ping Feng June, 1997



National Library
of Canada

Acquisitions and
Bibliographic Services

395 Wellington Street
Ottawa ON K1A 0N4
Canada

Bibliothèque nationale
du Canada

Acquisitions et
services bibliographiques

395, rue Wellington
Ottawa ON K1A 0N4
Canada

Your file Votre référence

Our file Notre référence

The author has granted a non-exclusive licence allowing the National Library of Canada to reproduce, loan, distribute or sell copies of this thesis in microform, paper or electronic formats.

L'auteur a accordé une licence non exclusive permettant à la Bibliothèque nationale du Canada de reproduire, prêter, distribuer ou vendre des copies de cette thèse sous la forme de microfiche/film, de reproduction sur papier ou sur format électronique.

The author retains ownership of the copyright in this thesis. Neither the thesis nor substantial extracts from it may be printed or otherwise reproduced without the author's permission.

L'auteur conserve la propriété du droit d'auteur qui protège cette thèse. Ni la thèse ni des extraits substantiels de celle-ci ne doivent être imprimés ou autrement reproduits sans son autorisation.

0-612-23300-6

**THE UNIVERSITY OF MANITOBA
FACULTY OF GRADUATE STUDIES
COPYRIGHT PERMISSION**

PROBABILISTIC TREATMENT OF THE SLIDING WEDGE

BY

PING FENG

**A Thesis submitted to the Faculty of Graduate Studies of the University of Manitoba
in partial fulfillment of the requirements of the degree of**

MASTER OF SCIENCE

Ping Feng © 1997

**Permission has been granted to the LIBRARY OF THE UNIVERSITY OF MANITOBA
to lend or sell copies of this thesis, to the NATIONAL LIBRARY OF CANADA to microfilm this
thesis and to lend or sell copies of the film, and to UNIVERSITY MICROFILMS to publish an
abstract of this thesis.**

**This reproduction or copy of this thesis has been made available by authority of the copyright
owner solely for the purpose of private study and research, and may only be reproduced and
copied as permitted by copyright laws or with express written authorization from the copyright
owner.**

Abstract

Rock slope stability problems are often encountered in engineering environments. In nature, most variables governing rock slope stability problems such as the orientation of discontinuities, the strength parameters and the loading conditions are random variables. Therefore the safety factor itself is a statistic. This thesis analyzes the variation of all the parameters that enter into the standard stability analysis through the use of the Monte Carlo simulation technique.

To meet this goal, a Windows based program EzSlide written in Visual Basic 4.0 has been developed. EzSlide follows the concepts and procedures of an earlier DOS program, PROSLIDE/GEO SLIDE. Several new routines are added however. Now all the strength parameters and the loading conditions can be modeled using a theoretical probability distribution. Five common probability distributions: the normal, the lognormal, the Weibull, the exponential and the triangular can be chosen by the user to model these variables. Three new routines for the optimization of the slope angle and the slope strike, and the slope height are added to evaluate their influence on the probability of failure.

An application of the program using field data from a highway rock cut along TransCanada highway 17A is undertaken. The factors that influence the safety factor and the probability of failure are investigated. The water pressure and strength parameter *JRC* have the most significant impact on the safety factor and the probability of failure. It is found that the probability of failure changes dramatically with slope strike. The shape of the safety factor distribution is also examined. The probability distribution of the safety factor is found to be multi-modal. Multimodality is caused by the fact that discontinuities are not continuously distributed, but occur in sets and that only certain combinations of the discontinuities form sliding wedges.

Acknowledgments

I would like to express my sincere gratitude to my advisor Professor Emery Lajtai for his substantial encouragement, insightful guidance and endless patience during the whole course of this project. His expertise in geological engineering and Visual Basic was most helpful. Without his leadership and support this thesis would not have been possible.

I am grateful also to the examination committee's members, Professor Stimpson and Professor Raghuvir for taking their time to review my work and offering constructive criticisms. Special thanks to Professor Stimpson for his valuable suggestions and discussions.

I would like to thank Laura Wytrykush's contribution for coding the stereonet procedures of EzSlide.

The program EzSlide has already been used by undergraduate students of the Geological Engineering Program. Many corrections and improvement were made following student feedback.

I also wish to extend my appreciation to Mrs. Lajtai for her wonderful pictures of the Kenora rock cuts.

Finally I wish to express my gratitude to my husband Liang for his invaluable discussions, suggestions and support. I would also like to thank my son Sam for his understanding during missed weekends and late nights, and my parents and my brothers for their consistent support and encouragement.

Contents

Abstract	i
Acknowledgment	ii
Table of Contents	iii
List of Figure	v
List of Table	viii
Symbols and Abbreviations	ix
Chapter 1 Introduction	1
1.1 The Deterministic Method	2
1.2 The Probabilistic Method	3
1.3 The Objective of the Thesis	8
Chapter 2 Monte Carlo Simulation	9
2.1 Basic Definitions in Probability Theory.....	9
2.2 Monte Carlo Simulation	11
2.2.1 Random variable processing	12
2.2.2 Estimation of parameters for a theoretical distribution	14
2.2.3 Variate generation	18
2.2.4 Variate generation in EzSlide.....	19
2.2.4.1 Variate generation from the uniform distribution	20
2.2.4.2 Variate generation from the exponential distribution.....	21
2.2.4.3 Variate generation from the Weibull distribution	21
2.2.4.4 Variate generation from the triangular distribution.....	22
2.2.4.5 Variate generation from the normal distribution	23
2.2.4.6 Variate generation from the log-normal distribution	24
2.2.3 The Monte Carlo Method in EzSlide	24
2.3.1 Random variable modeling	24
2.3.2 The simulation process in Ezslide.....	26
Chapter 3 The Windows Program Ezslide	28
3.1 Program Structure	29
3.2 Shear Strength Criteria	31
3.2.1 Linear Mohr - Coulomb criterion.....	31
3.2.2 Barton's non-linear shear strength for joints.....	32
3.3 Single Wedge Analysis	33
3.3.1 Data entry	36
3.3.2 Kinematic check.....	38
3.3.3 3D graphical view for a single wedge	39

3.4 Multi Wedge Analysis	41
3.4.1 Data entry and the Discontinuity List.....	41
3.4.2 Geological structure domains	44
3.4.3 Loading conditions	45
3.4.4 Running the probabilistic analysis	46
3.4.5 Selection of the random strength parameters	48
3.4.6 The probability of failure	49
3.4.7 Optimization routines in EzSlide	51
3.5 Post Analysis of Safety Factors	53
3.5.1 Cumulative distribution of the safety factor with Weibull fit	53
3.5.2 Histogram	54
3.6 Input and Output Files	55
Chapter 4 An Example For Ezslide	57
4.1 Geological Data Collection	57
4.2 Single Wedge Analysis	60
4.2.1 Influence of Barton's strength parameters <i>JCS</i> , <i>JRC</i> and ϕ_B on SF...	64
4.2.2 Estimating the Barton strength parameters	67
4.2.3 The influence of the Mohr-Coulomb strength parameters	67
4.2.4 The effect of the height of the slope.....	70
4.3 Probabilistic Analysis of A Multi Joint System	74
4.3.1 Probabilistic analysis.....	74
4.3.2 The factors influencing the probability of failure.....	77
4.3.2.1 The influence of water pressure	77
4.3.2.2 The effect of JRC	78
4.3.2.3 The effect of JCS	81
4.3.3 Slope angle and the probability of failure	82
4.3.4 Sensitivity of the probability of failure to slope strike	82
4.3.5 The effect of domain control	84
4.3.6 The effect of the probability distribution type.....	87
4.4 The Safety Factor Distribution	91
Chapter 5 Conclusions	98
Appendix	100
References	102

List of Figures

Figure 1.1	A typical highway rock cut with vertical slope face.....	2
Figure 1.2	The negative exponential distribution of joint spacing	5
Figure 1.3	The lognormal distribution of joint length.....	5
Figure 1.4	The Weibull (α , 1) distribution	6
Figure 1.5	A typical normal distribution	6
Figure 2.1	Probability density function (PDF)	10
Figure 2.2	Cumulative probability function (CPF).....	10
Figure 2.3	A continuous, piecewise-linear empirical distribution.....	13
Figure 3.1	The main and the sub-menus in the program EzSlide.....	30
Figure 3.2	The flow chart for the deterministic analysis of a single wedge	35
Figure 3.3	The window of the data entry and the display of the kinematic check. The tabbed file folder in the top left corner shows the "Slope" page. There two other pages containing the discontinuity and load data.....	37
Figure 3.4	The water level is entered as a percentage of distance AB, i.e. the depth above the discontinuity at the crest.....	38
Figure 3.5	The summary display for the single-wedge.....	40
Figure 3.6	The flow chart of probabilistic analysis for a multi wedge system	43
Figure 3.7	The Discontinuity List with the discontinuities displayed as poles in the stereonet.....	45
Figure 3.8	The Start Probabilistic Analysis window	47
Figure 3.9	The form for the specification of the lowest, the highest, most likely value and the probability distribution of the strength parameter JRC..	49
Figure 3.10	Summary display for the results of the probabilistic analysis	51
Figure 3.11	The Optimization result window with graph and table	52
Figure 3.12	The window shows the cumulative distribution with Weibull fit for safety factors listed in the spreadsheet	54
Figure 3.13	The window for displaying histogram of safety factors	55
Figure 4.1	The rock joint system on the south side of highway 17A West of the intersection with highway 659	59
Figure 4.2	A partially failed single wedge on the north side of highway 17A west of the intersection with highway 659	59
Figure 4.3	The Plane A and Plane B of the Kenora partially failed wedge and the joint system are displayed in the stereonet.....	61

Figure 4.4	The deterministic analysis result of the single wedge shown in Figure 4.2	63
Figure 4.5	The effect of <i>JCS</i> on the safety factor	64
Figure 4.6	The effect of basic friction angle on the safety factor	66
Figure 4.7	The effect of <i>JRC</i> on the safety factor	66
Figure 4.8	The effect of the unit cohesion and the friction angle on The safety factor of the Kenora wedge.....	68
Figure 4.9	Possible combinations of the unit cohesion and the friction angle to yield a safety factor of unity	69
Figure 4.10	A rock slope with vertical excavation surface.....	70
Figure 4.11	The height effect on the safety factor	73
Figure 4.12	The effect of water level on the probability of failure.....	77
Figure 4.13	The effect of <i>JRC</i> on the probability of failure	78
Figure 4.14	The shift in the cumulative distribution of safety factors with <i>JRC</i> in the wedge and the plane sliding modes	79
Figure 4.15	The cumulative distribution of safety factors with different <i>JCS</i> values in the wedge and plane sliding modes.....	80
Figure 4.16	The effect of <i>JCS</i> on the probability of failure.....	81
Figure 4.17	The probability of failure changes slightly with the slope angle.....	83
Figure 4.18	The probability of failure changes dramatically with slope strike	83
Figure 4.19	The cumulative distribution of safety factors with “domain control” and “no domain control” in the wedge sliding mode	84
Figure 4.20	The histograms of safety factors in wedge sliding mode under “domain control” and “no domain control”	85
Figure 4.21	A typical failed wedge whose plane A and B come from the same set	86
Figure 4.22	The cumulative distribution of the safety factor in the $0 < SF < 1$ range. The distributions are not truncated.....	88
Figure 4.23	The cumulative distribution of the safety factor in the $0 < SF < 1$ Range. The distributions are truncated at $1 < JRC < 8$	88
Figure 4.24	The probability of failure under different distributions of <i>JRC</i> with The same most likely value at 4, but different ranges of <i>JRC</i>	90
Figure 4.25	The probability of failure under different distributions of <i>JRC</i> with the same range $1 < JRC < 8$, but different most likely value of <i>JRC</i> , one is 2 and the other is 4.....	90

Figure 4.26	The cumulative distribution and the histogram of total safety factor 4 with $-99.99 < SF < 99.99$	92
Figure 4.27	The cumulative distribution and the histogram of total safety factor with $0 < SF < 15$.....	93
Figure 4.28	The cumulative distribution and histogram of safety factors in wedge failure mode with $0 < SF < 15$.....	94
Figure 4.29	The cumulative distribution and the histogram of safety factors in the plane sliding mode with $-99.99 < SF < 99.99$	96
Figure 4.30	The cumulative distribution and the histogram of safety factor in the plane sliding mode with $3.1 < SF < 4.8$. Only discontinuities of the same set are forming the sliding plane	97

List of Tables

Table 3.1	File recordings in the EzSlide	56
Table 4.1	Some possible combinations of the strength parameters for the partially failed Kenora wedge.....	67
Table 4.2	Input for the random variables	75
Table 4.3	Monte Carlo simulation.....	76
Table A.1	The Discontinuity List of the rock joint system located on the south side of highway 17A west of the intersection with 659 near Kenora, Ontario (Figure 4.1).....	100
Table A.2	The geometry and the estimated strength parameters of the partially failed wedge located on the north side of highway 17A (Figure 4.2) ..	101

Symbols & Abbreviations

$F_X(x)$	Cumulative distribution function
$f_X(x)$	Probability density function
\bar{x}	Sample mean
x_i	Individual random variables (observations)
s^2	Sample variance
s	Standard deviation
MLE	Maximum-likelihood estimators
α	Shape parameter
β	Scale parameter
γ	Location parameter; unit weight of the rock
$Expone(\beta)$	Exponential distribution
$Weibull(\alpha, \beta)$	Weibull distribution
$N(\mu, \sigma)$	Normal distribution
$LN(\mu, \sigma)$	Lognormal distribution
$Triang(a, b, c)$	Triangular distribution
$U(0,1)$	A variate continuously distributed uniformly between 0 and 1
$U(a,b)$	A variate continuously distributed uniformly between a and b
τ	Peak shear strength
σ_n	Normal stress of joint surface
c	Unit cohesion
ϕ	Internal friction angle
JRC	Joint Roughness Coefficient
JCS	Joint Wall Compressive Strength
σ_c	Uniaxial compressive strength of the rock
ϕ_B	Basic friction angle
δ	Slope angle
SF	Safety factor
D	Driving force
R	Resisting force
N	Number of discontinuities
N_A	Normal force to the plane A
p_i	Relative frequency of occurrence that wedges tending to failure mode i
n_i	Number of free wedges tending to failure mode i
N_T	Total number of analyzed wedges (equals to Simulation times)
$P_{f,i}$	Probability of failure in failure mode i
$n_{f,i}$	Number of failed wedges tending to failure mode i
N_K	Total number of kinematic free wedges
N_F	Total number of failed wedges
$P_{f,sys}$	Probability of failure for a rock joint system
k	Number of bins in a histogram

Chapter 1

Introduction

Rock slope excavations are common in engineering environments in the form of rock cuts for highways, railways, powerhouses, and spillways in civil engineering excavations and open pit mines. Figure 1.1 is a typical highway rock cut (on TransCanada highway 17A near Kenora, Ontario). Before undertaking excavations in a jointed rock mass, a stability analysis of the rock slopes formed by the natural discontinuities and the excavation free surface should be performed.

Rock slope designs, particularly in hard rock, are based on the limiting equilibrium method that considers the equilibrium of the forces acting on a potentially unstable rock block. The comparison of the resisting force that opposes sliding and the driving force in the form of a safety factor is the usual measure of stability. Most of the parameters that enter into the standard stability analysis are subject to statistical variation. Therefore the safety factor itself is a statistic. Defining its statistical distribution in the geological environment of the rock slope is the main object of this work.



Figure 1.1 A typical highway rock cut with vertical slope face (near Kenora, Ontario).

1.1 The Deterministic Method

Deterministic analysis, using a single set of parameters, is still the dominant approach in rock slope design and stability analysis. The orientation of potential sliding surfaces and their shear strengths, the unit weight of rock, water pressure and external support forces are pre-determined and then treated as constant parameters producing a single value of the safety factor.

Although all the geological parameters are subject to variation, the deterministic method uses fixed values of the rock properties. In practical design, engineers tend to choose conservative, low values of strength parameters for the discontinuities, and higher groundwater and external force levels to compensate for the inherent uncertainty

presented by the variable nature of the rock mass. Consequently, the method should result in a conservative design that tends to increase the cost of a project. In spite of this, the deterministic method may overestimate stability; failures of rock slopes do take place.

There are three sets of variables governing rock slope stability. They are the geometry of discontinuities, the strength parameters of discontinuities and the external loading conditions. In fact, most of these variables are characterized by uncertainty; they are not constants. The orientations of rock joints surveyed from field investigation vary even within the same set. The strength properties of rock mass are inherently uncertain since in material testing single values are seldom measured. External forces such as water level and earthquake loading are changing all the time. The deterministic method is really unsuitable in this situation.

1.2 The Probabilistic Method

To overcome the deficiency of the deterministic method, several researchers have used probability theory to quantify uncertainties in rock properties. Probabilistic analysis was introduced to rock slope stability by McMahon (McMahon, 1971). Subsequently, many scientists have investigated the statistical characteristics of joint sets, their length, spacing, and orientation. Priest and Hudson (1976), Call et al. (1976), Einstein and Baecher (1983) proposed that the distribution of joint lengths and spacing have the shape of the negative exponential distributions (Figure 1.2). McMahon (1974) presented a lognormal distribution for fracture lengths (Figure 1.3). Singh et al. (1985) summarized the collection of geotechnical and mining data relating to slope instabilities in British surface coal mines and concluded that in many cases the normal or lognormal

distributions have been found to be the most satisfactory models to describe the characteristics of failed wedges.

Kim & Gao (1995) analyzed mechanical properties obtained from laboratory and field tests. The results suggested that the distribution of test data follows the Weibull distribution (Figure 1.4). However, many engineers assume that a probability distribution of strength parameters follows the normal distribution (Figure 1.5).

Existing probabilistic methods can be divided into two categories: analytical methods and simulation techniques. Analytical methods are based on closed-form expressions of the main descriptors, such as the mean and the standard deviation of the random variable. Since many assumptions need to be made in their formulation, they are very difficult to use, especially when the function is nonlinear and algebraically complex. Therefore simulation techniques are more widely preferred. Among them, the Monte Carlo simulation is the most convenient. It is a numerical method of solving mathematical problems by random sampling. It has become popular and practical with the advent of computers.

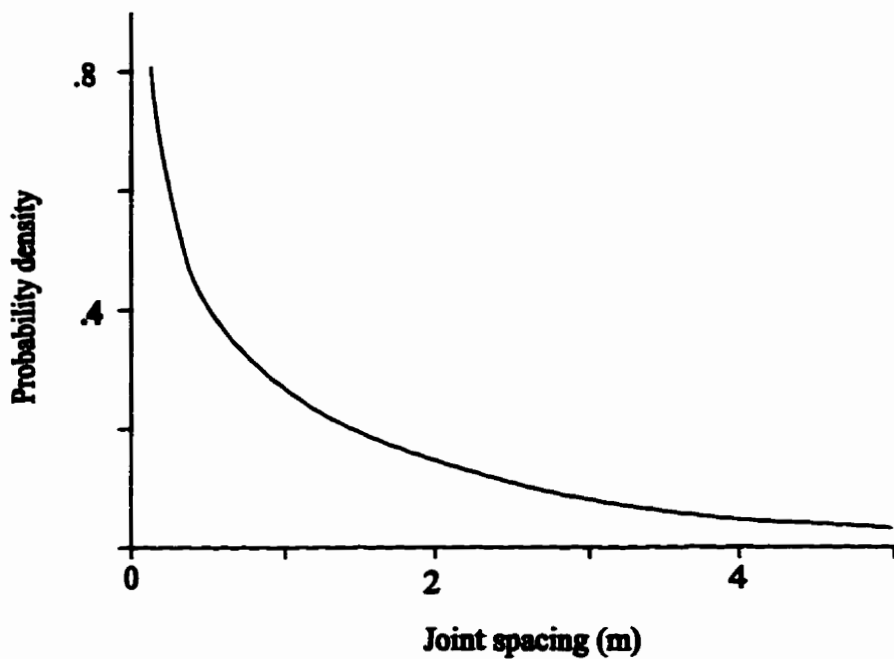


Figure 1.2 The negative exponential distribution of joint spacing

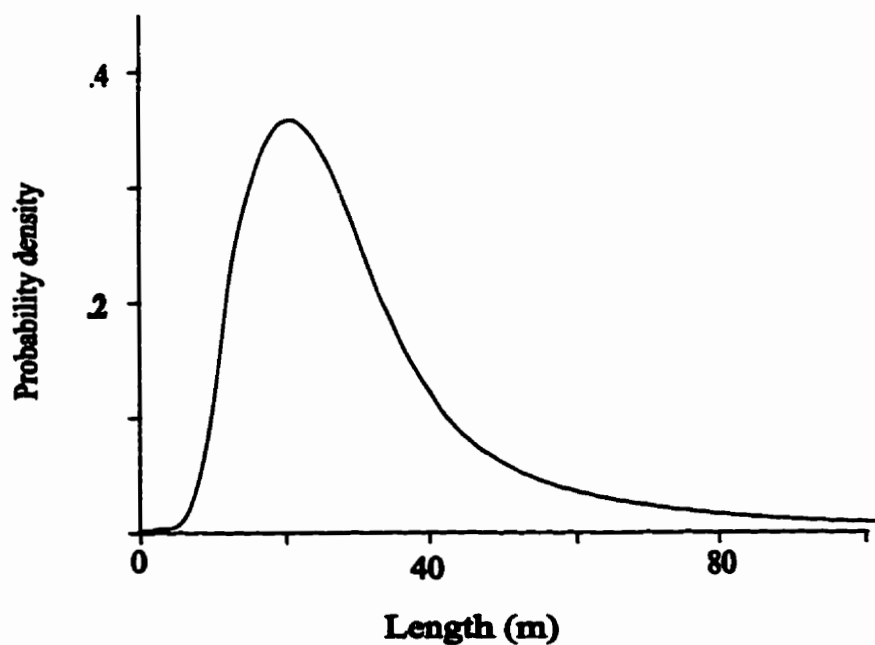


Figure 1.3 The lognormal distribution of joint length

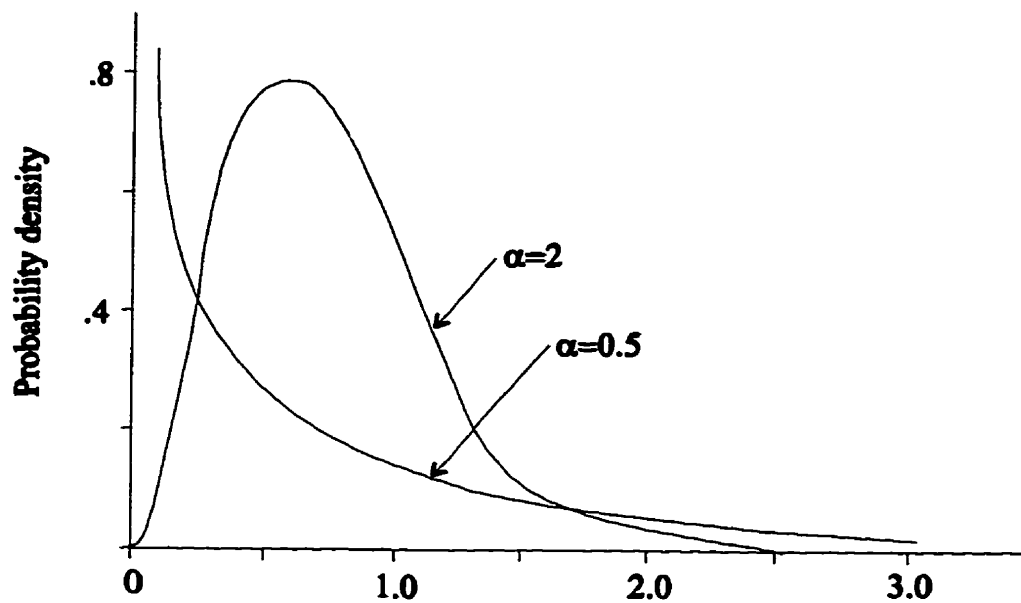


Figure 1.4 The weibull (α , 1) distribution.

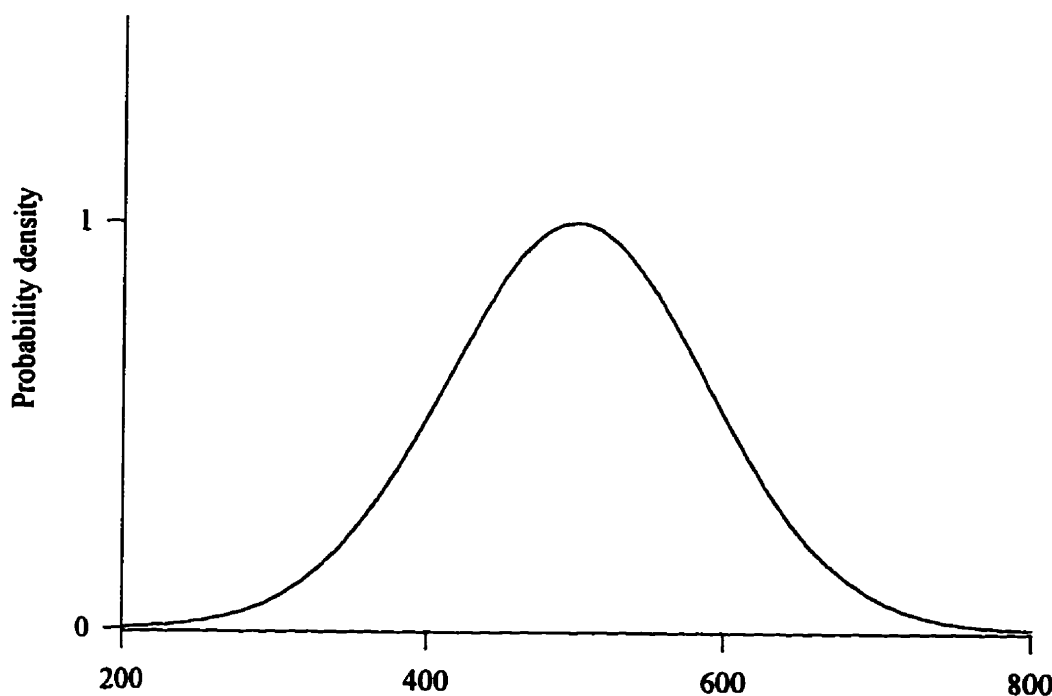


Figure 1.5 A typical normal distribution.

Several computer programs have been written for conducting probabilistic analysis on rock slope stability using Monte Carlo simulation technique (Lajtai and Carter 1989; Singh et al. 1985; Tamimi et al. 1989; Piteau et al. 1985, Leung & Quek 1995). Some of them consider only plane sliding (Tamimi 1985; Singh et al. 1985), others include wedge sliding as well (Leung and Quek 1995; Lajtai and Carter 1989; Piteau et al. 1985).

Lajtai and Carter developed two DOS-based programs, GEOSLIDE and PROSLIDE, to conduct a deterministic and a probabilistic analysis, respectively (Lajtai and Carter 1989). The analysis uses 3D vector algebra, in essence following the routine described in Hoek and Bray (1977). This thesis is the continuation of this work. The new Windows program EzSlide has been developed using the Object - Oriented programming language - Visual Basic, professional edition Version 4.0, and it runs under either Windows 95 or Windows NT. EzSlide is a multiple-document application comprising three major parts: deterministic analysis for a single wedge, probabilistic analysis for a multi wedge system and a collection of utilities for the post-analysis of the results. It builds on the GEOSLIDE/PROSLIDE by making use of all transferable functions and subroutines. However, there are several significant additions. In GEOSLIDE/PROSLIDE, only the geological data are statistic; the external forces are entered as constants. In EzSlide, all the parameters are distributed. In addition, several useful routines have been added. The most important is the sensitivity analysis of the slope geometry where the slope strike, dip and the height can be varied within the same simulation run.

1.3 The Objective of the Thesis

The aim of this thesis is try to provide an effective tool for the design and stability analysis of rock slopes in jointed rocks. In many regards, EzSlide follows the concepts and procedures in GEOSLIDE/PROSLIDE. It has however a number of new features:

1. Strength parameters can use either the Coulomb – Mohr or the Barton specification. The loading conditions can be considered as random variables. Five common probability distributions can be chosen to model these variables. They are the normal, the lognormal, the Weibull, the exponential and the triangular distributions.
2. Three new routines for the optimization of slope dip and slope strike, and for the evaluation of the effect of slope height are added. They are useful in evaluating the sensitivity of these parameters and thus allow the selection of the optimum (lowest failure probability) slope orientation and slope angle.
3. A post analysis feature that gives the cumulative distribution of the safety factor with the Weibull distribution fitted to it. The histograms of the safety factors in each failure mode (wedge sliding along the intersection, wedge sliding along a single plane and plane sliding) can be displayed as well.
4. All the inputs and the results are now stored in convenient text files that can be read, constructed and edited with any text editor (e.g. Wordpad). All graphs can now be saved as Windows metafiles.
5. The thesis includes a practical application of EzSlide using field data from a highway rock cut along TransCanada highway 17A, just north of Kenora, Ontario.

Chapter 2

Monte Carlo Simulation

In the probabilistic analysis of a rock slope system, either some or all parameters describing joint properties are considered as random variables. During the simulation, the random values are generated from their theoretical distributions. In this chapter the relevant probability theory and the simulation technique used in EzSlide are introduced.

2.1 Basic Definitions in Probability Theory

Random variables: Parameters such as the strength parameters of rock joints, the orientation of discontinuities and the water level in the rock mass do not have fixed values. Hence these parameters are called random variables.

Probability Density Function: A probability density function (PDF) describes the relative likelihood that a random variable will assume a particular value. A typical PDF is plotted in Figure 2.1 in which the random variable is continuously distributed (i.e., it can take on all possible values). The area under the PDF is always unity.

Cumulative Distribution Function (CDF) is just another way to describe the information included in the PDF. CDF gives the probability that the variable will have a value less than or equal to the selected value (Figure 2.2). There is an inherent relationship between PDF and CDF such that CDF is the integral of the corresponding PDF, i.e. the ordinate at X_1 , on the cumulative distribution, is equal to the area under the probability density distribution to the left of X_1 . It is noted that the symbol $f_X(x)$ is used for the ordinate of the PDF and $F_X(x)$ for the CDF. In Figure 2.2, CDF is an increasing continuous function between $F_X(-\infty) = 0$ and $F_X(\infty) = 1$.

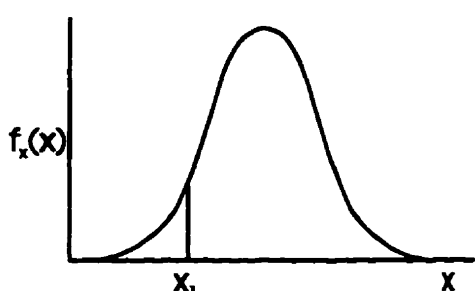


Figure 2.1 Probability density function (PDF)

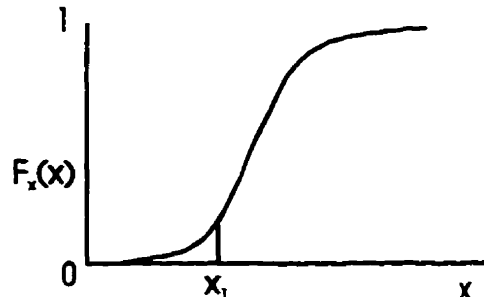


Figure 2.2 Cumulative distribution function (CDF)

For a set of data, there are three parameters used to describe the dominant features of the distribution of the data. They are the sample mean, the variance and the standard deviation.

Sample Mean: the mean indicates the center of gravity of a probability distribution. Assuming there are n observations with variate values x_1, x_2, \dots, x_n , the mean of the sample is denoted \bar{x} and is given by:

$$\bar{x} = \frac{1}{n} \sum_{i=1}^n x_i \quad (2.1)$$

Sample variance s^2 : the variance of a set of n variates x_1, x_2, \dots, x_n with mean \bar{x} is the sum of the squared deviations divided by $n-1$:

$$s^2 = \frac{1}{n-1} \sum_{i=1}^n (x_i - \bar{x})^2 \quad (2.2)$$

Standard deviation s : the standard deviation of a set of variates is defined to be the positive square root of the variance s^2 . A small standard deviation will indicate a tightly clustered data set about the mean while a large s will show a large scatter about the mean.

$$s = +\sqrt{\frac{1}{n-1} \sum_{i=1}^n (x_i - \bar{x})^2} \quad (2.3)$$

2.2 Monte Carlo Simulation

With the development of modern computers, simulation techniques are becoming an increasingly popular and economic tool for probabilistic analysis. The Monte Carlo simulation is the most widely used simulation techniques for solving certain stochastic problems. The method was developed during World War II and was applied to the problem related to development of the atomic bomb. It is generally defined as a numerical method to solve mathematical problems by the simulation of random variables. Basically, Monte Carlo simulation involves constructing the sample space of the random variables and repeating an analysis over and over using random variables, which in turn are derived from the distribution of the variable using a random number generator. There are several random number generators used with modern computers. Visual Basic has a built-in random number generator written in the form of the numerical function **Rnd** which returns a double precision random number between 0 and 1 denoted $U(0,1)$. Based on U

(0,1), random variables can then be generated from the appropriate probability distribution.

2.2.1 Random Variable Processing

The first step in the simulation is the selection of a theoretical distribution for the random variable in question. When it is possible to collect data on a random variable of interest, there are three possible approaches to specify a distribution (Law & Kelton, 1991):

1. The data values are used directly in the simulation. This is called “trace-driven simulation”.
2. The data values are used to define an empirical distribution function.
3. Standard techniques of statistical inference are used to fit a theoretical distribution, e.g., triangular or Weibull, to the data.

Approach 1 is suitable when a large number of data is available. If the database is small, only a small number of simulations can be accommodated. In this case, the trace-driven simulation may not be reliable.

Approach 2 defines a piecewise – linear empirical distribution based on the actual values of the original data. First the original observations X_1, X_2, \dots, X_n are sorted in increasing order $X_{(1)} \leq X_{(2)} \leq \dots \leq X_{(n)}$ where $X_{(i)}$ is the i th smallest value. The cumulative distribution $F(x)$ is given in the general form (2.4):

$$F(x) = \begin{cases} 0 & \text{if } x < X_{(1)} \\ \frac{i-1}{n-1} + \frac{x - X_{(i)}}{(n-1)(X_{(i+1)} - X_{(i)})} & \text{if } X_{(i)} \leq x < X_{(i+1)} (i = 1, 2, \dots, n-1) \\ 1 & \text{if } X_{(n)} \leq x \end{cases} \quad (2.4)$$

An example for a continuous piecewise linear empirical distribution is shown in Figure 2.3.

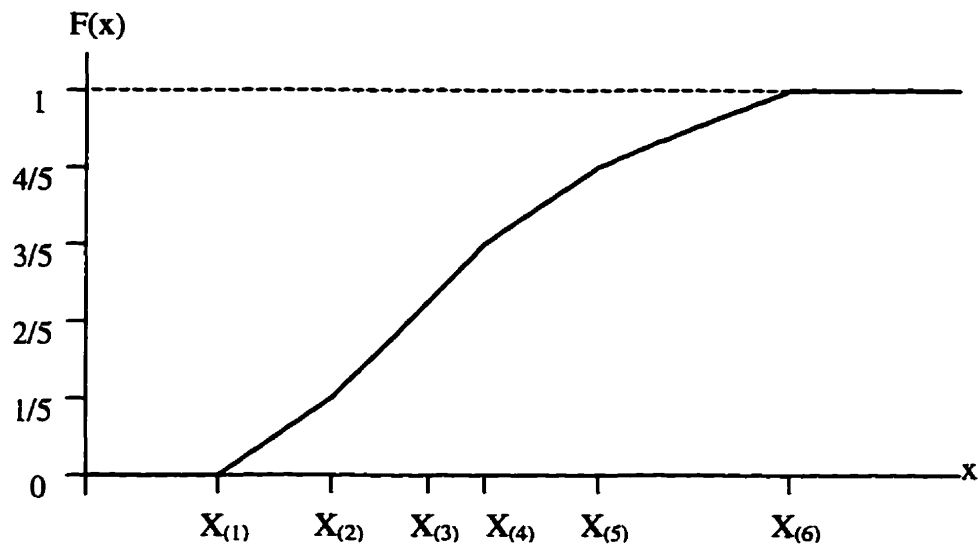


Figure 2.3 A continuous, piecewise-linear empirical distribution.

Approach 2 is used when the observed data can't fit a theoretical distribution adequately. From a continuous distribution, any value between the minimum and the maximum observed data can be generated. However, an empirical distribution may have certain "irregularities", particularly if a small number of data is available. In addition, values outside the range of the observed data can't be generated in a simulation using an empirical distribution. Therefore, if a theoretical distribution can be found that fits the

data reasonably well, it is preferable to use approach 3. A theoretical distribution offers a compact way to represent a set of data values. Furthermore, values outside the range of the observed data can be generated from a theoretical distribution.

Once a candidate theoretical probability distribution is specified for the random variable, the next step is to find the statistical parameters for the probability distribution from observed data.

2.2.2 Estimation of parameters for a theoretical distribution

For a specific theoretical distribution, there are three parameters to define its physical and geometric features. They are the location parameter, γ , the scale parameter, β , and the shape parameter, α . A *location parameter* γ specifies the x-axis location point of a value. Usually, γ is at the midpoint or at the low-tail endpoint of the distribution's range. The scale parameter, β , determines the scale or unit of measurement of the values in the range of the distribution. A change in β compresses or expands the associated distribution without altering its basic form. The shape parameter, α , determines the basic form or shape of a distribution. A change in α alters a distribution's shape properties such as its skewness.

Once a probability distribution has been selected, we must specify their parameters. Here the *maximum-likelihood estimator* method (MLE) for estimating statistical parameters of a particular distribution is applied. In this method, the observed data X_1, X_2, \dots, X_n , are used to estimate the statistical parameters. An *estimator*, which is a parameter of a probability distribution, is a numerical function of the data.

Suppose we have hypothesized a continuous distribution X_1, X_2, \dots, X_n that has only one unknown parameter, θ . If $f_\theta(x)$ denotes the hypothesized probability density function, the *likelihood function* is defined (Law and Kelton, 1991):

$$L(\theta) = f_\theta(X_1)f_\theta(X_2)\cdots f_\theta(X_n) \quad (2.5)$$

This function gives the probability of the data if θ is the only unknown parameter. The MLE of the unknown value of θ , which denoted by θ' , is defined to be the value of θ that maximizes $L(\theta)$. Namely $L(\theta') \geq L(\theta)$ for all possible values of θ . Thus, θ' “best explains” the collected data (Law & Kelton, 1991).

Five probability distributions are used in EzSlide for modeling the properties of rock joints. The following listing gives their probability density function and the cumulative distribution, together with the description of the parameters, their range and the MLE.

1. Exponential distribution $Expone(\beta)$

Density function	$f(x) = \frac{1}{\beta} e^{-x/\beta}$	if $x \geq 0$	(2.6)
-------------------------	---------------------------------------	---------------	-------

Cumulative Distribution	$F(x) = 1 - e^{-x/\beta}$	if $x \geq 0$	(2.7)
--------------------------------	---------------------------	---------------	-------

Parameter	Scale parameter $\beta > 0$		
------------------	-----------------------------	--	--

MLE	$\hat{\beta} = \bar{X}(n)$	(mean value)	(2.8)
------------	----------------------------	--------------	-------

2. Weibull distribution $Weibull(\alpha, \beta)$

Density function	$f(x) = \alpha \beta^{-\alpha} x^{\alpha-1} e^{-(x/\beta)^\alpha}$	if $x > 0$	(2.9)
-------------------------	--	------------	-------

Cumulative Distribution	$F(x) = 1 - e^{-(x/\beta)^\alpha}$	if $x > 0$	(2.10)
--------------------------------	------------------------------------	------------	--------

Parameter

Shape parameter $\alpha > 0$, scale parameter $\beta > 0$

MLE

The following two equations must be satisfied:

$$\frac{\sum_{i=1}^n X_i^{\hat{\alpha}} \ln X_i}{\sum_{i=1}^n X_i^{\hat{\alpha}}} - \frac{1}{\hat{\alpha}} = \frac{\sum_{i=1}^n \ln X_i}{n} \quad (2.11)$$

$$\hat{\beta} = \left(\frac{\sum_{i=1}^n X_i^{\hat{\alpha}}}{\frac{n}{n}} \right)^{1/\hat{\alpha}} \quad (2.12)$$

Equation (2.11) can be solved for $\hat{\alpha}$ numerically by the Newton's method.

Equation (2.12) gives $\hat{\beta}$ directly. The general recursive step for the Newton iteration is:

$$\hat{\alpha}_{k+1} = \hat{\alpha}_k + \frac{A + 1/\hat{\alpha}_k - C_k / B_k}{1/\hat{\alpha}_k^2 + (B_k H_k - C_k^2) / B_k^2} \quad (2.13)$$

where

$$A = \frac{\sum_{i=1}^n \ln X_i}{n}, \quad B_k = \sum_{i=1}^n X_i^{\hat{\alpha}_k}, \quad (2.14)$$

$$C_k = \sum_{i=1}^n X_i^{\hat{\alpha}_k} \ln X_i, \quad H_k = \sum_{i=1}^n X_i^{\hat{\alpha}_k} (\ln X_i)^2$$

The starting point for the iteration is estimated as:

$$\hat{\alpha}_0 = \left\{ \frac{\frac{6}{\pi^2} \left[\sum_{i=1}^n (\ln X_i)^2 - \left(\sum_{i=1}^n \ln X_i \right)^2 / n \right]}{n-1} \right\}^{-1/2} \quad (2.15)$$

With this choice of $\hat{\alpha}_0$, an average of only iterations are needed to achieve four-place accuracy.

3. Normal Distribution $N(\mu, \sigma)$

Density function $f(x) = \frac{1}{\sqrt{2\pi\sigma^2}} e^{-(x-\mu)^2/2\sigma^2}$ for all real numbers of x (2.16)

Cumulative Distribution no closed form

Parameter Location parameter $\mu \in (-\infty, \infty)$, scale parameter $\sigma > 0$

MLE $\hat{\mu} = \bar{X}(n)$ (mean), $\hat{\sigma} = \left[\frac{\sum_{i=1}^n [X_i - \bar{X}(n)]^2}{n} \right]^{1/2}$ (2.17)

4. Log-Normal Distribution $LN(\mu, \sigma)$

Density function $f(x) = \frac{1}{x\sqrt{2\pi\sigma^2}} \exp \frac{-(\ln x - \mu)^2}{2\sigma^2}$ if $x > 0$ (2.18)

Cumulative Distribution no closed form

Parameter Shape parameter $\sigma > 0$, scale parameter $\mu \in (-\infty, \infty)$

MLE $\hat{\mu} = \frac{\sum_{i=1}^n \ln X_i}{n}$, $\hat{\sigma} = \left[\frac{\sum_{i=1}^n (\ln X_i - \hat{\mu})^2}{n} \right]^{1/2}$ (2.19)

5. Triangular Distribution $\text{Triang}(a, b, c)$

Density function

$$f(x) = \begin{cases} \frac{2(x-a)}{(b-a)(c-a)} & \text{if } a \leq x \leq c \\ \frac{2(b-x)}{(b-a)(b-c)} & \text{if } c < x \leq b \\ 0 & \text{otherwise} \end{cases} \quad (2.20)$$

Distribution

$$F(x) = \begin{cases} 0 & \text{if } x < a \\ \frac{(x-a)^2}{(b-a)(c-a)} & \text{if } a \leq x \leq c \\ 1 - \frac{(b-x)^2}{(b-a)(b-c)} & \text{if } c < x \leq b \\ 1 & \text{if } b < x \end{cases} \quad (2.21)$$

Parameter a, b , and c are real numbers with $a < c < b$, a is a location parameter, $b-a$ is a scale parameter, c is a shape parameter

MLE no relevant MLE.

2.2.3 Variate generation

The Monte Carlo simulation involves sampling and random variate generation from the probability distribution. After a theoretical distribution is specified, random variates must be generated for the simulation. There are many techniques for generating random variates. In general, any method of generating random variates from any distribution needs the IID (Independent Identical Distribution) $U(0,1)$ random numbers, which are uniformly distributed in the interval $[0,1]$. In EzSlide the inverse transform method has been used.

The cumulative distribution function $F_X(x)$ is an increasing function within the range of $0 < F(x) < 1$. The inverse function F_X^{-1} of any distribution is defined by:

$$F_X^{-1}(y) = \inf[x : F_X(x) \geq y] \quad 0 \leq y \leq 1 \quad (2.22)$$

This means that $F_X^{-1}(y)$ is the smallest value of x for which $F_X(x) \geq y$. Thus, if $U(0,1)$ is uniformly distributed in the interval $(0,1)$ and X is a random variate that has distribution function F_X , we can obtain the random variate X by operating on the uniform distribution $U(0,1)$ with the inverse transform F_X^{-1} as follows:

$$X = F_X^{-1}(U) \quad (2.23)$$

Therefore, the algorithm for generating a random variate X is:

1. Generate random variate from $U(0,1)$;
2. Return $X = F_X^{-1}(U)$.

To apply the inverse transform method, the function F_X^{-1} must exist in closed analytical form and a statistically and a reliable $U(0,1)$ random number generator should be available. The latter requirement is easy to satisfy since the **Rnd** function that returns a random variate from $U(0,1)$ is built into Visual Basic. However, if a close form of F_X^{-1} does not exist, the inverse transform method is not applicable. In this case, other methods will be used.

2.2.4 Variate generation in EzSlide

This section constructs all the functions needed to generate the six types of distribution variates in EzSlide. The uniform distribution is used for the random selection of two discontinuities from the Discontinuity List. The other five distributions are for the

random strength variables and the loading conditions. In EzSlide, the user is asked to enter three representative values for each random variable, a low, a high and a most likely value. The program then calculates the statistical parameters using MLEs for the specified probability distribution. After this the program calls the corresponding Visual Basic functions and passes on the computed statistical parameters to generate the random variate.

2.2.4.1 Variate generation from the uniform distribution

The distribution that is uniform between values (a, b) is denoted $U(a, b)$ and has probability density function:

$$f_x(x) = \begin{cases} 1/(b-a) & a \leq x \leq b \\ 0 & \text{otherwise.} \end{cases} \quad (2.24)$$

$$U = F_x(x) = (x - a) / (b - a) \quad (2.25)$$

The inverse transform method can be trivially used to produce variates from $U(a, b)$. The algorithm:

- (1) Generate U from $U(0,1)$,
- (2) $X \leftarrow U(a, b) = a + (b-a)*U(0,1)$.

The Visual Basic function that is used for generating random numbers between a and b in EzSlide is as follow.

```
Function uniformrandom (a As Integer, b As Integer)
    uniformrandom = a + (b - a) * Rnd
End Function
```

If the number of joints in the Discontinuity List is N , any two random numbers between 1 and N can be generated during the simulation. Therefore the parameters for the function are $a = 1$ and $b = N$. The function returns a random integer between 1 and N .

2.2.4.2 Variate generation from the exponential distribution

The exponential variate has the PDF as shown in equation (2.6); it is denoted $E(\beta)$. The inverse transform method can be used to produce a variate from $E(\beta)$ since the close form F_X exists as shown in equation (2.7). This is given as

$$U = 1 - e^{-x/\beta} \quad (2.26)$$

Solving for X , we obtain

$$X = -\beta \ln(1 - U) \quad (2.27)$$

Since $(1-U)$ and U have the same $U(0,1)$ distribution, equation (2.27) can be changed to:

$$X = -\beta \ln U \quad (2.28)$$

The function for producing variates from $E(\beta)$ is shown below. The value β is calculated using MLE that is the mean value (equation (2.8)) of the three representative values entered by the user.

```
Function exponrandom(beta As Double)
    exponrandom = -beta * Log(Rnd)
End Function
```

2.2.4.3 Variate generation from the Weibull distribution

The PDF and CDF of Weibull distribution are given in equation (2.9) and (2.10).

The inverse transform of the Weibull distribution is:

$$U = F_X(x) = 1 - e^{-(x/\beta)^\alpha} \quad (2.29)$$

$$X = \beta(-\ln(1-U))^{1/\alpha} \quad (2.30)$$

Now $1-U$ is also from $U(0,1)$, so

$$X = \beta(-\ln U)^{1/\alpha} \quad (2.31)$$

Note that when $\alpha=1$, $\beta=1$, $W(1,1) = E(1)$. Equation (2.31) and equation (2.28) are the same. Hence we can generate $W(\alpha,\beta)$ from $E(1)$ by generating V from $E(1)$, and then deliver X from $X \leftarrow \beta V^{1/\alpha}$. The *Alfa* and *beta* are calculated by Newton iteration using equations from (2.11) to (2.15). The Visual Basic function used in EzSlide is:

```
Function weibullrandom (Alfa As Double, beta As Double)
    Dim V As Double
    V = exponrandom (1)
    weibullrandom = beta * V ^ (1 / Alfa)
End Function
```

2.2.4.4 Variate generation from the triangular distribution

Triangular distribution is fully specified by three values entered by the user: the minimum a , the mode c , and the maximum b . Its PDF and CDF are shown in equation (2.20) and (2.21). From the inverse transform method, the variate from the triangular distribution can be obtained as follow:

$$X = a + \sqrt{U(b-a)(c-a)} \quad U \leq (b-a)/(c-a) \quad (2.32)$$

$$X = b - \sqrt{(1-U)(b-a)(b-c)} \quad \text{Otherwise}$$

The Visual Basic function to generate variates from the triangular distribution is:

```
Function Tri (a As Double, b As Double, c As Double)
    Dim t1 As Double, t2 As Double, U1 As Double
    t1 = c - a
    t2 = b - a
    U1 = Rnd
    If U1 > (t2 / t1) Then
        Tri = b - Sqr ((1 - U1) * (b - c) * t2)
    Else
        Tri = a + Sqr ((U1 - 1) * (b - a) * (c - a))
    End If
End Function
```

```

    Else
        Tri = a + Sqr(U1 * t1 * t2)
    End If
End Function

```

2.2.4.5 Variate generation from the normal distribution

The normal distribution is the most widely used distribution in the Monte Carlo simulation. Its density function is shown in equation (2.16). There is no analytical closed form solution for the CDF. Hence the inverse transform F_x^{-1} does not exist. In EzSlide, the polar method is used to generate variates from the normal distribution denoted by $N(\mu, \sigma)$ defined by Walker (1987). The Visual Basic function for generating a normal distribution variate used in EzSlide is listed below. The *mu* and *sigma* are the MLEs of the normal distribution listed in equation (2.17). They are the sample mean and the standard deviation respectively.

```

Function normrandom(mu As Double, sigma As Double)
    Dim iset As Integer, R As Double, U1 As Double, U2 As Double
    Dim V1 As Double, V2 As Double, Z As Double, Gset As Double
    iset = 0
    If iset = 0 Then
        Do
            U1 = Rnd
            U2 = Rnd
            V1 = 2 * U1 - 1
            V2 = 2 * U2 - 1
            R = V1 ^ 2 + V2 ^ 2
        Loop While (R >= 1# Or R = 0)
        Z = Sqr(-2# * Log(R) / R)
        Gset = V1 * Z * sigma + mu
        iset = 1
        nrandom = V2 * Z * sigma + mu
    Else
        nrandom = Gset
        iset = 0
    End If
End Function

```

2.2.4.6 Variate generation from the lognormal distribution

The lognormal distribution has a close relationship to the normal distribution such that if Y is distributed as $N(\mu, \sigma)$ then e^Y is distributed as $LN(\mu, \sigma)$. Therefore variates form $LN(\mu, \sigma)$ can be generated from the normal distribution $N((\mu, \sigma))$. The Visual Basic function for generating variate with $LN(\mu, \sigma)$ distribution is listed below. The *mu* and *sigma* are the MLEs, the mean and the standard deviation, listed in equation (2.19).

```
Function lograndom(mu As Double, sigma As Double)
    Dim y As Double
    y = nrandom(0, 1)
    y = mu + y * sigma
    lograndom = Exp(y)
End Function
```

2.3 The Monte Carlo Method in EzSlide

2.3.1. Random variable modeling

Practically all the parameters governing rock slope stability such as the joint orientation, the joint strength parameters, and the external loading conditions are random variables. In order to treat their properties as realistically as possible, in EzSlide a combination of the approach 1 and approach 3 (section 2.2.1) are utilized.

Discontinuities such as faults, joints and bedding planes within the rock mass have a very important influence on the stability of rock slopes. Since the early 1930s', there have been many attempts to use theoretical distributions to describe joint orientation. Many distributions, such as uniform, bivariate normal and bivariate Fisher etc. distributions have been proposed. However, according to Dershowitz and Einstein (1988), "based on the comparison of field data none of the currently used distributions

provide a statistically acceptable fit" (Dershowitz, Einstein 1988). It is often simpler and more effective to use the measured orientation data directly (Approach 1).

In EzSlide, the orientation data collected from field investigation are entered in the Discontinuity List. During the Monte Carlo simulation, the computer picks two discontinuities from the List in a random fashion. A wedge is formed by slope face, top slope and these two discontinuities. If there are N discontinuities in the List, the maximum number of discontinuity combinations, or the maximum number of potential wedges is $N \times (N - 1)/2$, where N is the number of discontinuities in the Discontinuity List.

With the exception of joint orientation data, there is seldom enough strength data to define a theoretical or empirical distribution. The strength parameters and loading conditions involving in rock slope stability analysis are usually estimated from a few tests or through the back-analysis of failed slopes. In a joint survey, geologists measure the orientation of discontinuities and normally attach some kind of description to the joint profile and to joint surface characteristics. With some care and experience, the profile and texture characteristics can be quantified. For the Mohr-Coulomb law, they must be turned into estimates of unit cohesion and friction angle. The friction angle has a narrow range; a reasonable estimate is possible. There is really no sure way to estimate unit cohesion. The non-linear shear strength specification of Barton has an advantage in this regard. All its parameters, JRC , JCS and the basic friction angle ϕ_B have a limited range and their estimate is possible through comparison with standard profiles (JRC), the uniaxial compressive strength (JCS) and with literature listings for specific rock types (ϕ_B).

If the strength parameters can be established during the joint survey and each joint is assigned a set of strength parameters, “Approach 1”, the use of parameters as they are, is perhaps the best method. This is how PROSLIDE does the Monte Carlo simulation. This option is still available in EzSlide.

If strength parameters are not listed for each discontinuity in the Discontinuity List, “Approach 3”, using a theoretical distribution based on a rough estimate of the parameters, is perhaps the most useful. EzSlide does this by asking the user for an estimate of the low and high ends of the range plus the most likely value. In addition, a theoretical distribution must be specified. EzSlide uses the given limits and the most likely value to construct the specified theoretical distribution. It is this distribution from which the random variates are generated through the random number generator.

2.3.2 The simulation process in EzSlide

The Monte Carlo simulation employed in EzSlide has the following steps:

1. Generate two random numbers between 0 and 1 from a uniform distribution $U(0,1)$ using the **Rnd** function and convert them to random numbers between 1 and N to correspond to the discontinuity numbers in the Discontinuity List.
2. A wedge is formed by the slope face, the top slope and the two discontinuities and its kinematic freedom established.
3. If the wedge is free to slide, the strength properties are determined depending on the selected options. If “Approach 1” is used, the strength parameters come directly from the Discontinuity List. If “Approach 3” is used, the strength parameters are generated from the theoretical distribution. If the wedge is not free to slide, the wedge is

discarded, classified as “not free” and another pair of discontinuities is picked by repeating steps 1 and 2.

4. For the kinematically free wedge, the safety factor is calculated using the strength parameters from Step 3. In addition to the safety factor, the wedge is classified according to the sliding modes (plane sliding, wedge slide on the intersection of two discontinuities, or wedge slide on a single plane).

The four steps are repeated as many times as requested provided the entered field data are large enough to support it. When the simulation is finished, a set of safety factors for all the kinematically free wedges will be produced. The safety factors which are larger than 1 indicate that the wedges are stable, otherwise the wedges have failed. After the simulation, the probability of failure in each failure mode is computed. Finally, the probability of system failure is calculated. Detailed description of the computation for the probability of failure will be given in Chapter 3.

Chapter 3

The Windows Program EzSlide

Since the release of Windows 3.0 in 1990, Windows programs and applications are becoming more and more popular. In order to carry out a deterministic and/or probabilistic analysis of rock slope, a Windows based program EzSlide has been developed using the Object-Oriented Programming language Visual Basic, version 4.0. EzSlide is a multiple-document interface application with a user-friendly GUI (Graphical User Interfaces). The program consists of three major parts: 1. Deterministic analysis for the single wedge; 2. probabilistic analysis for multiple wedge systems; 3. post analysis of the safety factor distribution.

EzSlide builds on GEOSLIDE, PROSLIDE by making use of all transferable functions and subroutines. However, there are several significant additions. The program allows for the variability of the externally applied loads, surcharge, earthquake loading and water pressure. The strength parameters of recorded joints can be used either as listed in the Discontinuity List or varied following a selected distribution function. Slope orientation, strike and dip, and slope height can now be varied in a single operation.

3.1 Program structure

EzSlide has been developed using Microsoft Visual Basic version 4.0 and it runs under Windows 95 or Windows NT. It has a standard Windows interface complete with multiple windows, menus, toolbar, push buttons, dialog boxes and various other controls. There is an editable data input/output spreadsheet component and 2D/3D graphics package for data presentation. The program is easy to manipulate with mouse clicks or from the keyboard. Since this program comprise three different tasks, a multiple document interface (MDI) had to be developed. An MDI application in Visual Basic consists of a single parent window and a number of child windows or regular windows. The parent window has the main menu and a toolbar, which control the child and the regular windows as well. Under each main menu item, sub-menus are attached to carry out specific tasks. Figure 3.1 shows the main menu and sub-menus and the toolbar in the parent window. In the child and regular windows, the user communicate with the program through text boxes, check boxes, radio buttons and command buttons. In the text boxes, the user enters the value of optional parameters. Check boxes turn features on and off. Radio buttons are circle shaped buttons that allow the user to choose one of two or several options. A command button in EzSlide performs tasks or opens dialog boxes where the user gives instructions. Most of the code is contained in code modules. There is a help menu that provides information about program capabilities. Context-sensitive help is available as required on each form separately.

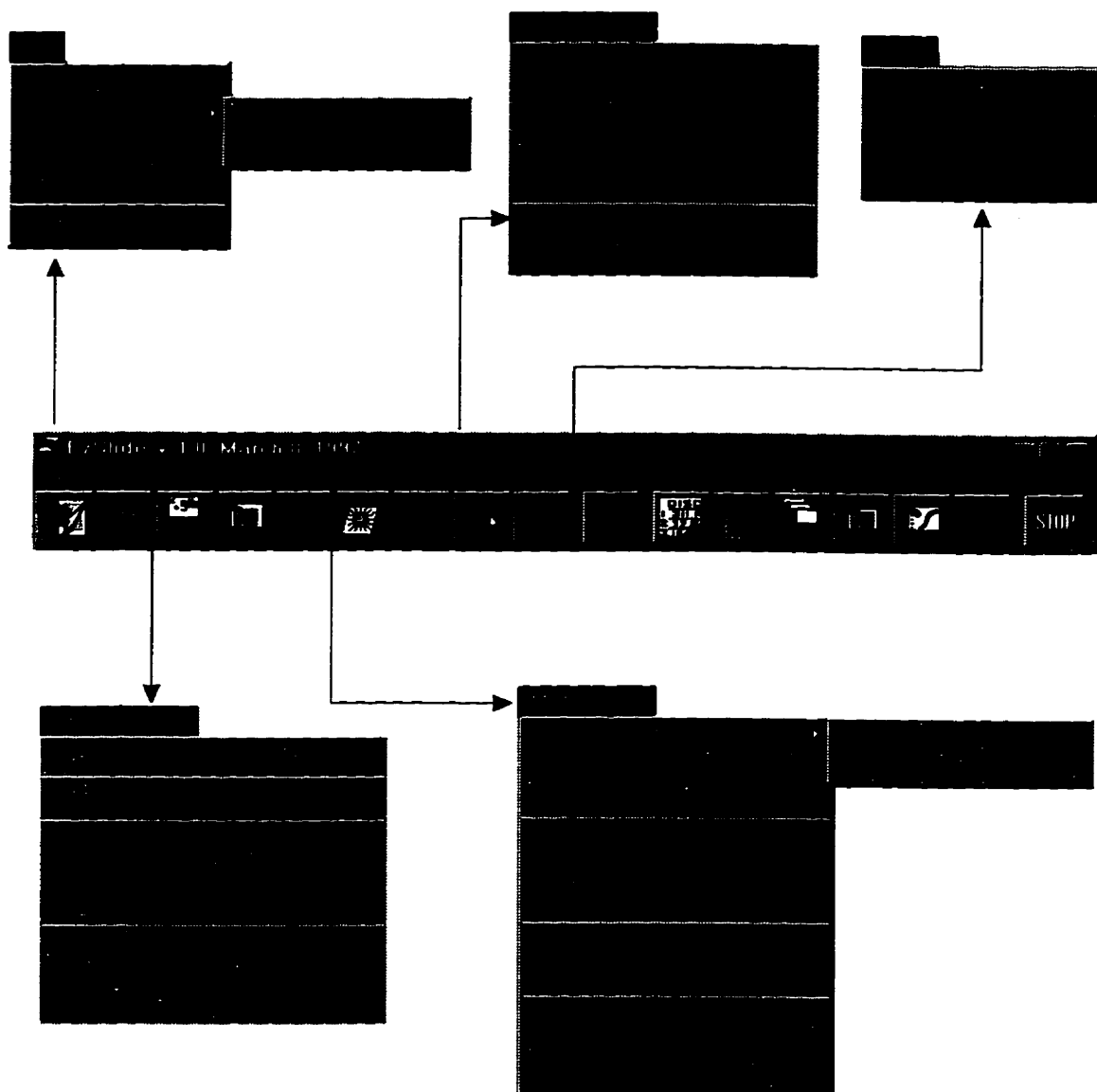


Figure 3.1 The main and the sub-menus in the program EzSlide

3.2 Shear Strength criteria

The method of Limiting Equilibrium, used in the stability analysis, requires the measurement of the shear strength of rock joints. In the program GEOSLIDE/PROSLIDE, the Coulomb-Mohr strength parameters of unit cohesion and friction angle are used to describe strength along a discontinuity. EzSlide offers an option. In addition to the Coulomb-Mohr description, the user can now work with the nonlinear strength parameters of Barton (1976).

3.2.1 Linear Mohr - Coulomb criterion

The Mohr - Coulomb shear strength criterion is used widely to describe the strength properties of rock joints. It represents a linear relationship between shear strength and the normal stress on a rock joint and can be expressed in the form of:

$$\tau = c + \sigma_n \tan \phi \quad (3.1)$$

Where τ is the peak strength, σ_n is the effective normal stress on the surface, c is the effective unit cohesion, and ϕ is the angle of friction.

The Mohr-Coulomb strength parameters, cohesion and friction angle, would ideally be determined by conducting in situ direct shear tests on the appropriate discontinuity of the rock mass. This however is rarely done. Back analysis of failed or existing stable slopes is really the only effective way to determine the two strength parameters. Test results from both in-situ and laboratory shear tests show that typically the friction angle varies between 27° and 47° for most rock joints (Hoek and Bray, 1977, Lama & Vutukuri, 1978). According to Lama, cohesion values are low in rock joints, usually under 1.0 MPa.

3.2.2 Barton's non-linear shear strength for joints

A non-linear shear strength for rough joints was proposed by Barton (Barton, 1976). Based on tests and observations carried out on artificially produced rough joints, Barton established the following empirical equation for shear strength (τ):

$$\tau = \sigma_n \tan \left(JRC \log_{10} \left(\frac{JCS}{\sigma_n} \right) + \phi_B \right) \quad (3.2)$$

Here JRC is defined as *Joint Roughness Coefficient* based on a sliding scale from 0 for the smoothest to 20 for the roughest surface. JCS is the *Joint Wall Compressive Strength*. Barton suggested that JCS is equal to the uniaxial compressive strength σ_c of the rock if the joint surface is unweathered or the normal stress level is very high, and may reduce to $1/4 \sigma_c$ if the joint walls are weathered or the normal stress is moderate to low. ϕ_B is the basic *friction angle* that has a range from 25° to 35° for unweathered rock surfaces and is often assumed to be about 30° .

Barton's original studies were carried out at low normal stress levels relative to the joint wall compressive strength, which are thought to be more suitable for rock slope stability problems. However, when the value of the term in the bracket (equation 3.2) exceeds 70° , the shear strength envelopes are too steeply inclined and equation (3.2) is not applicable. Barton indicated that when the values of $\arctan \tau / \sigma_n$ larger than 70° the shear strength should be discounted (Barton, 1976). In the program EzSlide, when the value $\phi_B + JRC \log_{10}(JCS / \sigma_n) > 70^\circ$, the value $\phi_B + JRC \log_{10}(JCS / \sigma_n) = 70^\circ$ is substituted.

The major difference between the Barton and Coulomb – Mohr laws is that in the Barton specification the shear strength reduces to nil at $\sigma_n = 0$; in the Mohr – Coulomb criterion the shear strength is equal to the cohesion parameter at $\sigma_n = 0$.

3.3 Single Wedge Analysis

The stability analysis of the single wedge is the heart of both the single- and the multi-wedge problems. It is essentially a rigid-body analysis of a mass of rock delimited by four plane surfaces: the slope face, the slope crest and the two discontinuities. The analysis in EzSlide uses 3D vector algebra, in essence following the routine described in Hoek and Bray (1977) and as coded by Carter and Lajtai (1989) in the DOS-based program, GEOSLIDE. In the single wedge analysis, the kinematic freedom of the wedge to slide is evaluated first. Then the geometry of the wedge is developed; the edges, the angles, the areas and the volume are computed. The external forces (water, earthquake, anchor and other external forces) are vector-summed and the resultant resolved normal and parallel with the slide-direction.

If the Mohr-Coulomb criterion is selected, the safety factor for a typical wedge is computed as:

$$SF = \frac{c_A A_A + c_B A_B + N_A \tan \phi_A + N_B \tan \phi_B}{D} \quad (3.3)$$

In (3.3), c_A , c_B are the unit cohesion along plane A and B. A_A , A_B are the area of the plane A and B; N_A , N_B are the components of the resultant normal to plane A and B respectively. ϕ_A , ϕ_B are the friction angle of plane A and B. D is the driving force along

the slide direction. It is calculated by resolving the resultant force parallel with the slide direction. D is treated as a vector. It is positive when it points downslope, negative when pointing upslope. For the plane sliding mode, Equation (3.3) can also be used for the plane sliding mode by setting the non-applicable parameters to nil. EzSlide is designed to find the safety factor for the plane slide when the plane strikes parallel or nearly parallel (within $\pm 20^\circ$) with the strike of the slope surface.

If Barton's specification is used, the safety factor is given by:

$$SF = \frac{R_A + R_B}{D} = \frac{\tau_A A_A + \tau_B A_B}{D} \quad (3.4)$$

Here R_A, R_B are the resisting forces mobilized along plane A and B, τ_A, τ_B are the unit shear resistance of the plane A and B respectively as calculated from equation (3.2). The safety factor equals to 1.0 represents the limiting equilibrium condition. This exists when the resisting forces and driving forces are equal. A safety factor less than one signals failure. Because D may assume a negative sign, a negative safety factor between 0 and -1 signals failure by sliding upslope. When $SF < -1$, the slope is safe again.

The single wedge analysis in EzSlide consists of four parts: data input, kinematic freedom check, calculation of safety factor, and the display of the results with 3D visualization. The flow chart for the deterministic analysis of a single wedge is shown in Figure 3.2.

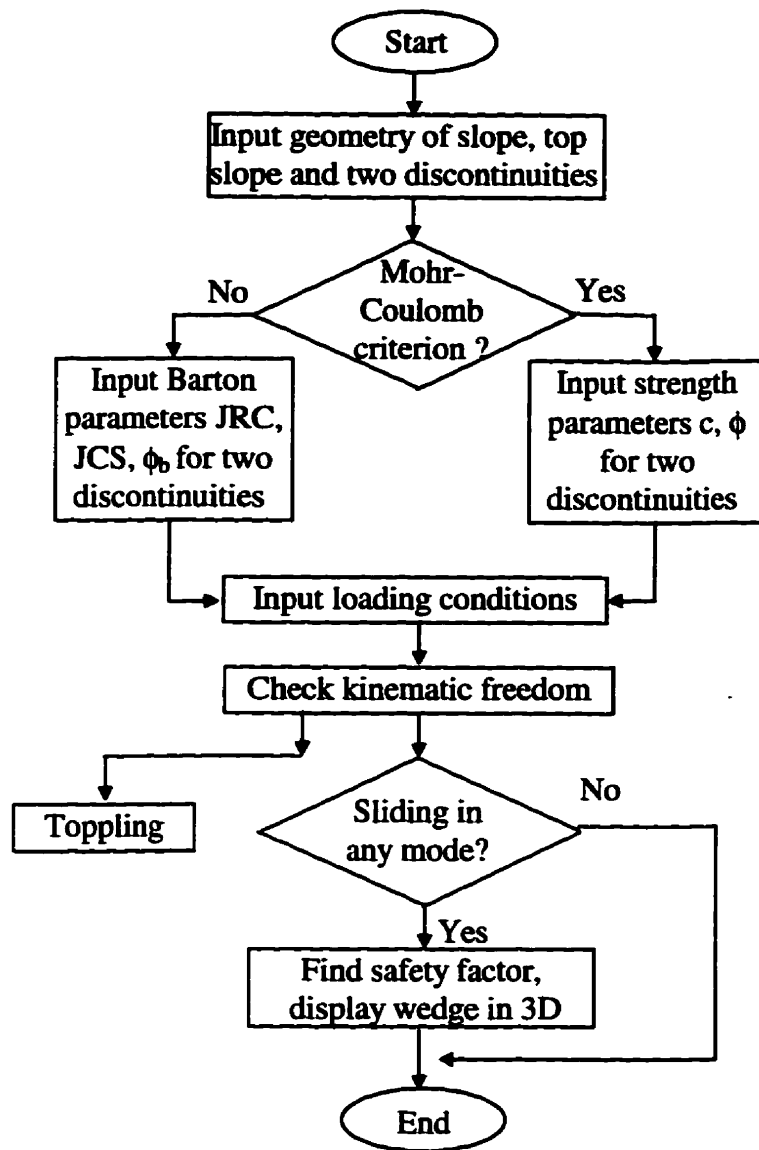


Figure 3.2 The flow chart for the deterministic analysis of a single wedge

3.3.1 Data entry

A typical 3D wedge is made up of four planes. They are the slope face, the two discontinuities and slope crest. Before conducting a single wedge stability analysis, the user has to input the geometry data, the strength parameters for two joints, and the value of the external forces that act on the wedge. Geometry data include the orientation and the height of slope surface, and the orientation of the two discontinuities, plane A and B. The strength parameters of two discontinuities are entered as the unit cohesion c and the friction angle ϕ if the Mohr-Coulomb criterion is selected. Otherwise, JRC , JCS and ϕ_B are entered for the Barton criterion. Entering the external loads such as water pressure, anchor forces, surcharges and earthquake-loading etc. are optional depending on design requirements. The data entry window is shown in Figure 3.3.

The mathematical analysis is based on 3D-vector algebra in EzSlide. The slope surface and the discontinuities are handled as “poles” (normal to planes). The orientation of a plane is entered through the azimuth and plunge of the normal vector. The azimuth of a vector is defined as the direction of its horizontal projection measured clockwise from the north, while the plunge is the maximum inclination to the horizontal. Following the geological convention, the plunge is considered positive when the normal points downward.

External forces are entered as vectors as well; both direction (azimuth and plunge) and magnitude must be entered. For forces that point upwards the plunge is negative. The water level is input as a percentage of the distance AB, which defined as the head above the discontinuity at the crest, as shown in Figure 3.4. Alternatively, the Hoek and Bray

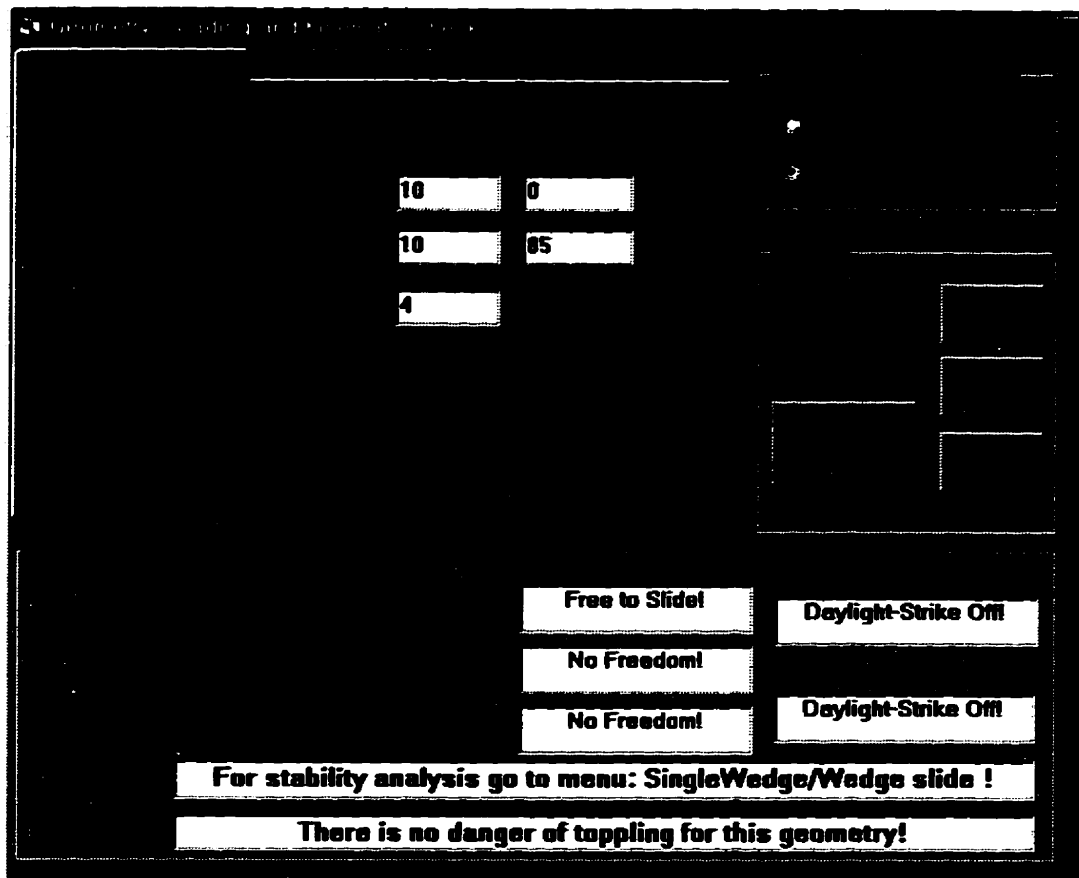


Figure 3.3 The window of the data entry and the display of the kinematic check results. The tabbed file folder in the top left corner shows the “Slope” page. There are two other pages containing the discontinuity and the load data.

condition (triangular pressure distribution with maximum head equal to one half of the slope height) can be selected (Hoek and Bray, 1977 p. 205).

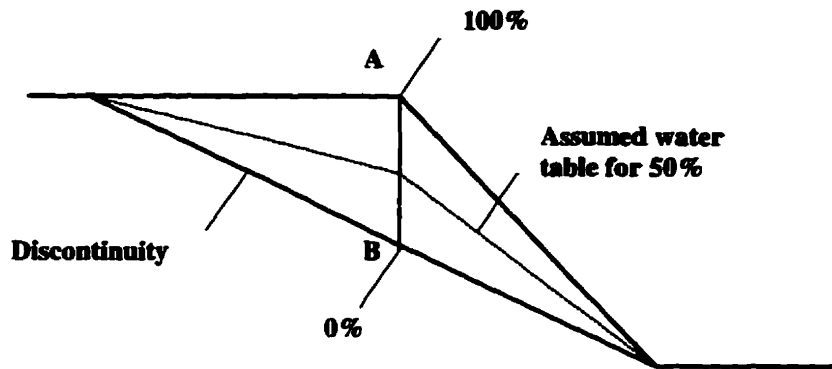


Figure 3.4 The water level is entered as a percentage of distance AB, i.e. the depth above the discontinuity at the crest.

3.3.2 Kinematic check

Kinematic analysis determines the possibility of sliding for a single wedge. If sliding is possible, it defines the mode of sliding. After the entry of the geometry of the four planes, the check for the “kinematic freedom” is undertaken using the techniques outlined by Hoek and Bray (Hoek & Bray, 1977) and Goodman (1976). There are three steps involved in the analysis: the daylighting check, the identification of the slide type and the toppling check.

The kinematic analysis examines the relationship between the strike and dip of the slope and the two discontinuities. A wedge sliding along the line of intersection of two discontinuities is possible when the plunge of this line is less than the apparent dip of the

slope, measured in a vertical plane containing the slide direction. Whether a wedge slides along the line of intersection or on a single plane is determined using Hocking's refinement (Hoek and Bray, 1977, p.59). Plane sliding occurs when the strike of the sliding plane is within $\pm 20^\circ$ of the strike of the slope and the dip of the plane is less than the dip of the slope.

Toppling failure involves the overturning of rock blocks and is associated with steep slopes and sub-vertical joints dipping steeply back into the slope. The toppling check follows the Goodman technique (Goodman, 1976, p. 265). Toppling occurs when the strike of the joints nearly parallel to the strike of the slope (within the 30°), and the plunge of the plane is less than the difference between the slope dip and the friction angle of the plane.

3.3.3 3D graphical view for a single wedge

If the wedge is free to slide in any of the three sliding modes, the program calculates the volume and the weight of wedge, finds the resultant force, its driving and normal components, and finally computes the safety factor. EzSlide offers summary tables for both the input and the output of the analysis, and a view of the sliding wedge in 3D as shown in Figure 3.5. The 3D view of the wedge can be manipulated. User can zoom in and out, stretch the size of a wedge in different directions and rotate it along three coordinate axes to get a better look at the wedge geometry in 3D space. Some of the intermediate computations, such as areas of each plane, the volume and the weight of the wedge, the resultant, the driving and the resisting forces are listed as well. The user can also print the results or save them to a file that can be opened by any text editor.

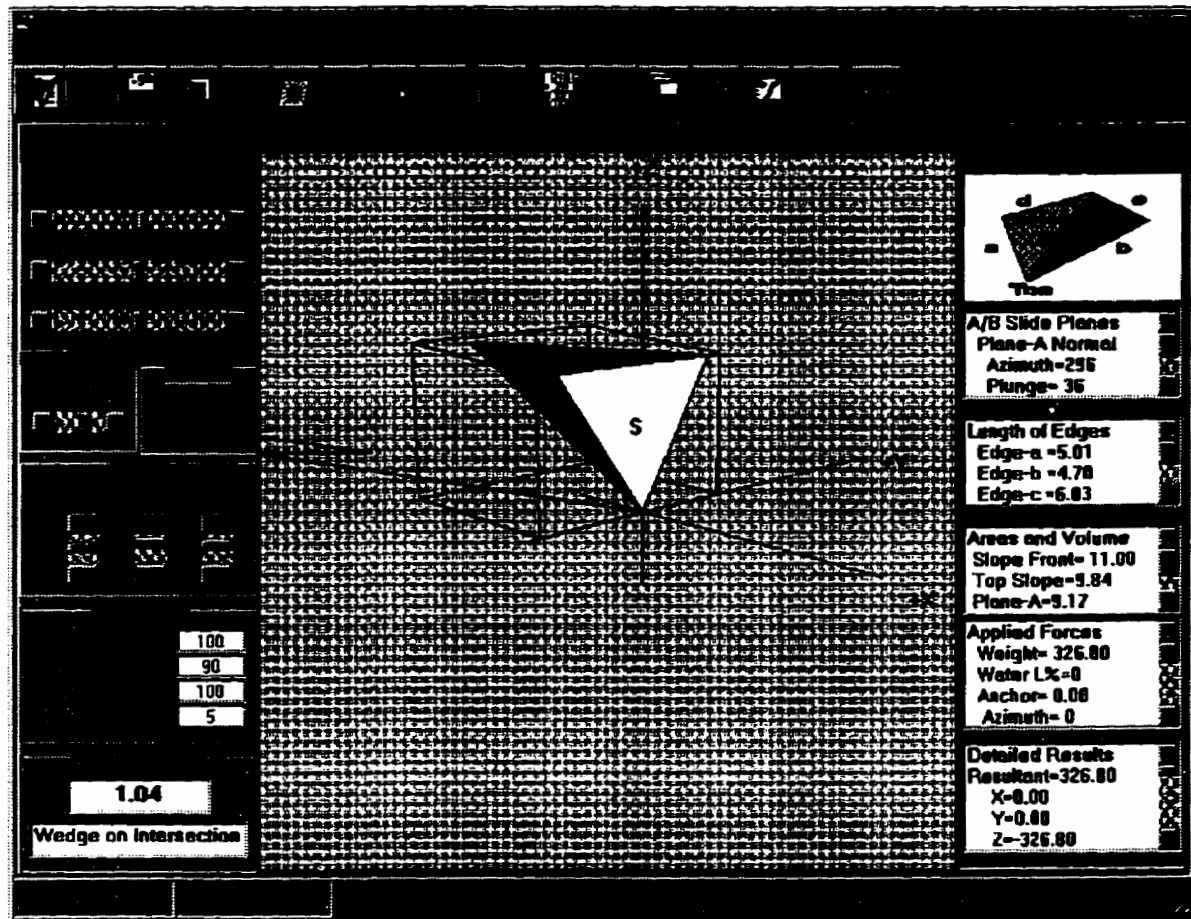


Figure 3.5 The summary display for the single – wedge.

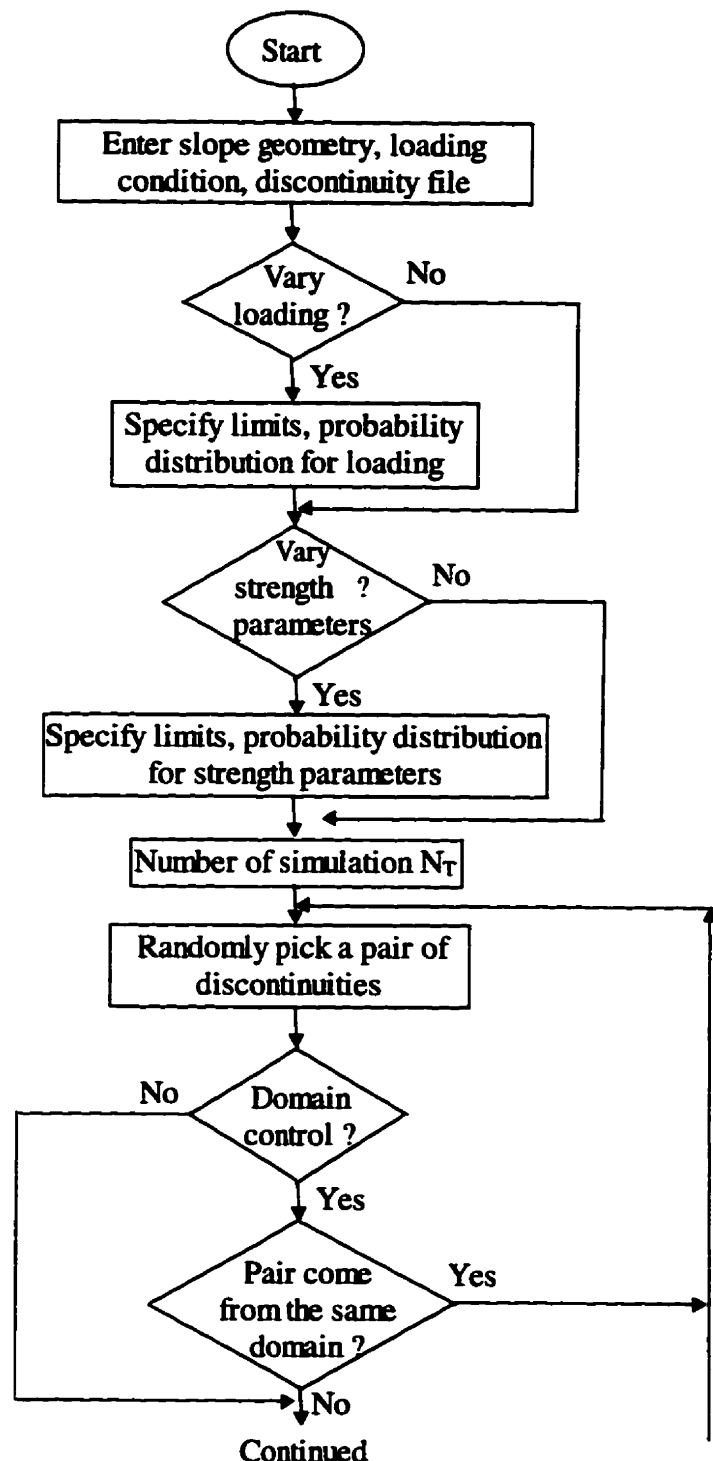
3.4 Multi Wedge Analysis

The multi wedge analysis is conducted using the Monte Carlo simulation technique. The whole process includes: data entry for slope geometry and the discontinuities, the random variable processing for strength parameters or external forces, and the actual simulation run.

When the simulation is done, a set of safety factors for all the kinematically free wedges is produced, and the failure probability for each failure mode and the probability of system failure are calculated. The flow chart of the multi-wedge analysis for a rock joint system is shown in Figure 3.6.

3.4.1 Data entry and the Discontinuity List

For the standard multi-wedge run, the dip, dip direction and the height of the slope are considered as constant. Their entry is through File-StartNew or File-OpenGeo menu items. For a given slope geometry, the joint data are entered as a Discontinuity List, which includes all the measured joint orientations and strength parameters. This may be entered directly from the keyboard or retrieved from a text file by selecting menu MultiWedge - Discontinuity List. If the Mohr-Coulomb criterion is used, the items for each discontinuity are the azimuth, the plunge, the domain number, the unit cohesion and the friction angle. When the Barton specification is selected, six parameters are needed for each discontinuity. They are the azimuth, the plunge, the domain number, *JRC*, *JCR* and the basic friction angle. If the joints have not been sorted into sets, the domain should be 1 for all the discontinuities. EzSlide however has the facility of grouping joints into sets later.



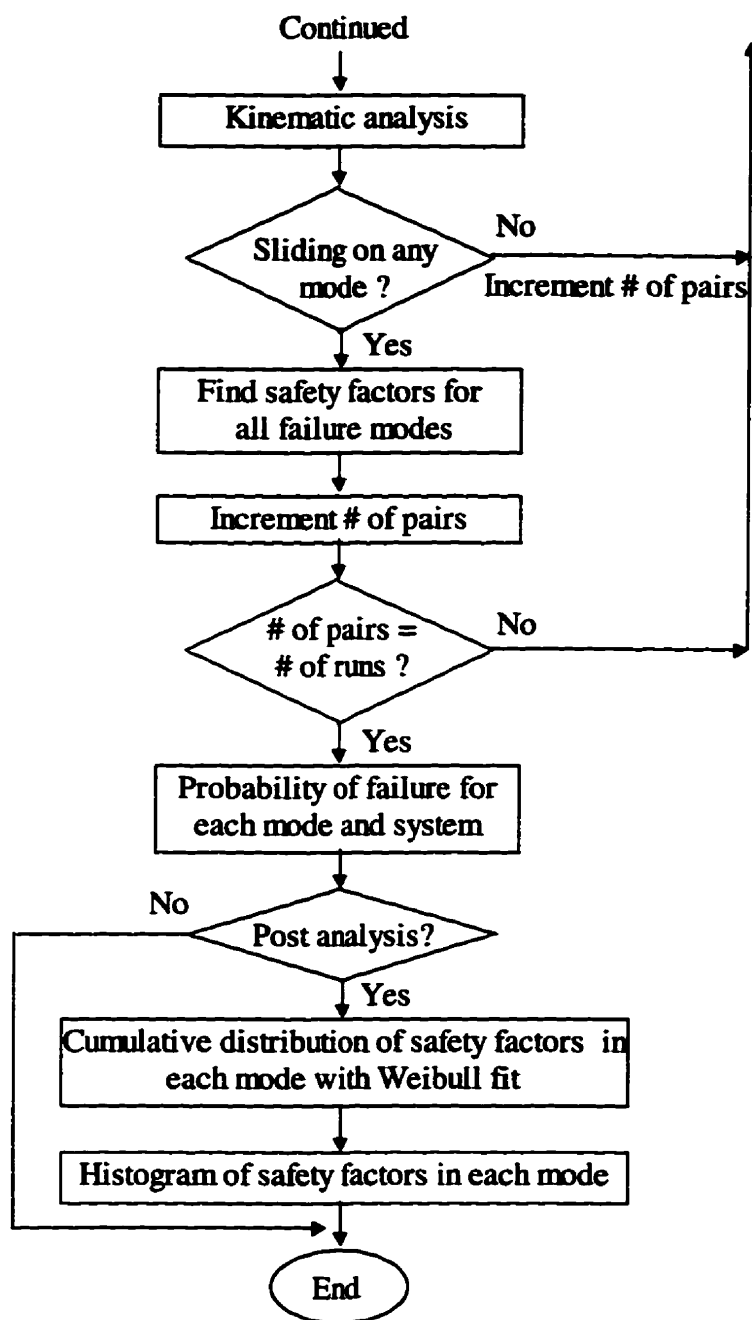


Figure 3.6 The flow chart of probabilistic analysis for a multi wedge system

3.4.2 Geological structural domains

Joints that have almost the same orientation form a joint set and various joint sets form a joint system. Because joints belonging to the same joint set usually have similar geological and strength characteristics (Herget, 1977), joints are often grouped into joint sets (domains).

When the user has an unsorted discontinuity file, the domain number for all the joints should be the same. EzSlide provides functions for plotting the orientation of joint data as poles on a lower equal area stereonet and then separating the data into domains (sets). To group the joints into joint sets, the user first clicks the button Display Poles to display the joints as poles in the lower hemisphere stereonet. Usually several clusters are observable suggesting the existence of sets (Figure 3.7). The sorting process is not automatic. The user must give a seed for each domain by double clicking a representative pole in the display (Figure 3.7) or by pressing the button Give Seeds for Domains and enter the azimuth and the plunge of the seed manually. After that, the program takes over. Clicking the button Show Domain, the poles belonging to different domains are displayed in different colors and a corresponding domain number in the “Discontinuity List” is inserted.

The maximum number of domains for a joint system can't exceed 6 in EzSlide. The joint data including the domain numbers can also be edited in the “Discontinuity List”. The program reads the list in the table once OK is pressed.

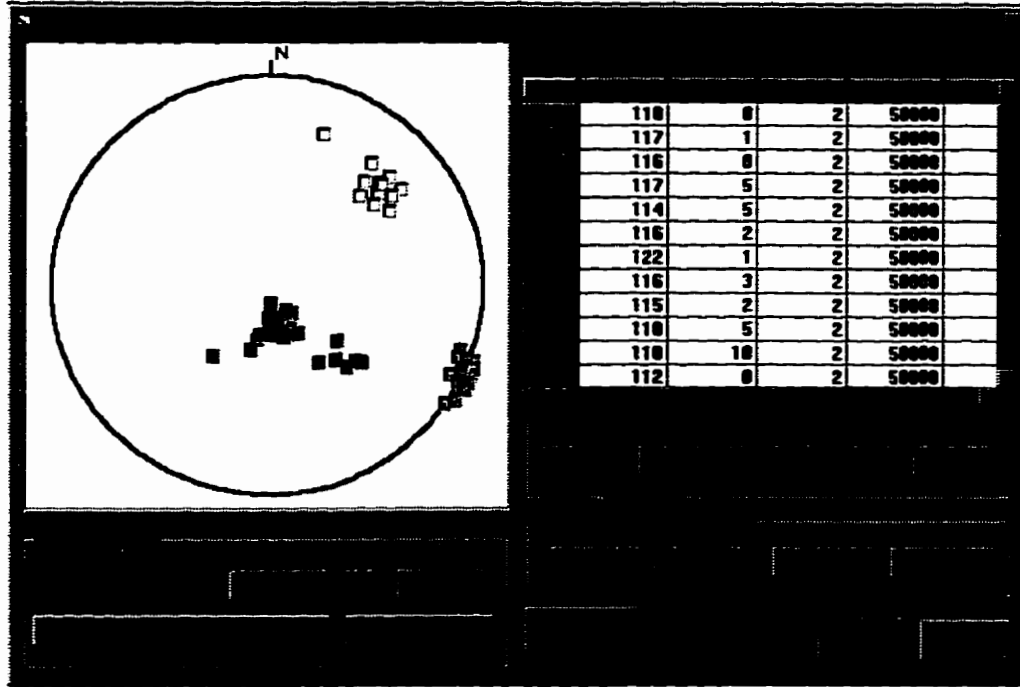


Figure 3.7 The Discontinuity List with the discontinuities displayed as poles in the stereonet.

3.4.3 Loading conditions

Once the Discontinuity List is ready, the next step is to enter the external loading condition. The loading condition in rock slope stability problems includes the water pressure, the anchor force, the external forces, the earthquake loading and the surcharge. The external forces are entered in one of two ways.

The first way handles forces by assuming that they are constant. This is the method used in PROSLIDE. In EzSlide, constant forces are entered in the Geometry, Loading and Kinematic Check form (Figure 3.3) on the Loading page of the tabbed file folder. This is opened through menu item File-StartNew, File-OpenGeo or Edit.

The second method is to consider external loading parameters as random variables. Since the direction of the external forces is usually fixed, only their magnitude is open for statistical variation. The direction of the external forces is entered in the Loading page of the tabbed file folder (Figure 3.3). The magnitudes of the external forces as random variables are entered when the user selects menu item MultiWedge – Run Multi-Wedge Analysis, and then checks the loading box. This opens the dialog box where the user is asked to enter three representative values and to specify the probability distribution. If the three inputted values for low, high and most likely are kept the same, the force is taken to be deterministic (constant).

3.4.4 Running the probabilistic analysis

When all the parameters have been entered, the program will take over by doing the Monte Carlo simulation. The simulation is undertaken in two ways in EzSlide. The major difference is in the treatment of the variability of joint strength parameters and the loading conditions.

The first method follows the procedure used in PROSLIDE using only the Discontinuity List with its orientation and strength parameters. The selection process has two options. If the no-replacement check box is checked, a wedge is used only once. The maximum number of discontinuity combinations to form a wedge from the discontinuity population N is $N*(N-1)/2$. If the no-replacement box is unchecked, the same wedge may be reused several times. This is not desirable while using the Discontinuity List as the source for the strength parameters. In this procedure, there is still the provision to vary the loading condition by checking the loading box (Figure 3.8).

The second method for the Monte Carlo simulation uses theoretical distributions to produce variates for loading and/or strength. The orientation of joints is still taken from the Discontinuity List, but the strength parameters in the listing are ignored, and the strength parameters are derived from the theoretical distribution. In this procedure of simulation, the same wedge may be reused several times, since the strength parameters are now random variables. The simulation number can be as large as desirable.

The number of simulation (N_T) to do is either selected by the user or the program. The program may overrule the user, if the number of discontinuities is too small to produce the required number of discontinuity combination. As a help to the user, the number of combinations for the selected option is indicated as shown in Figure 3.8.

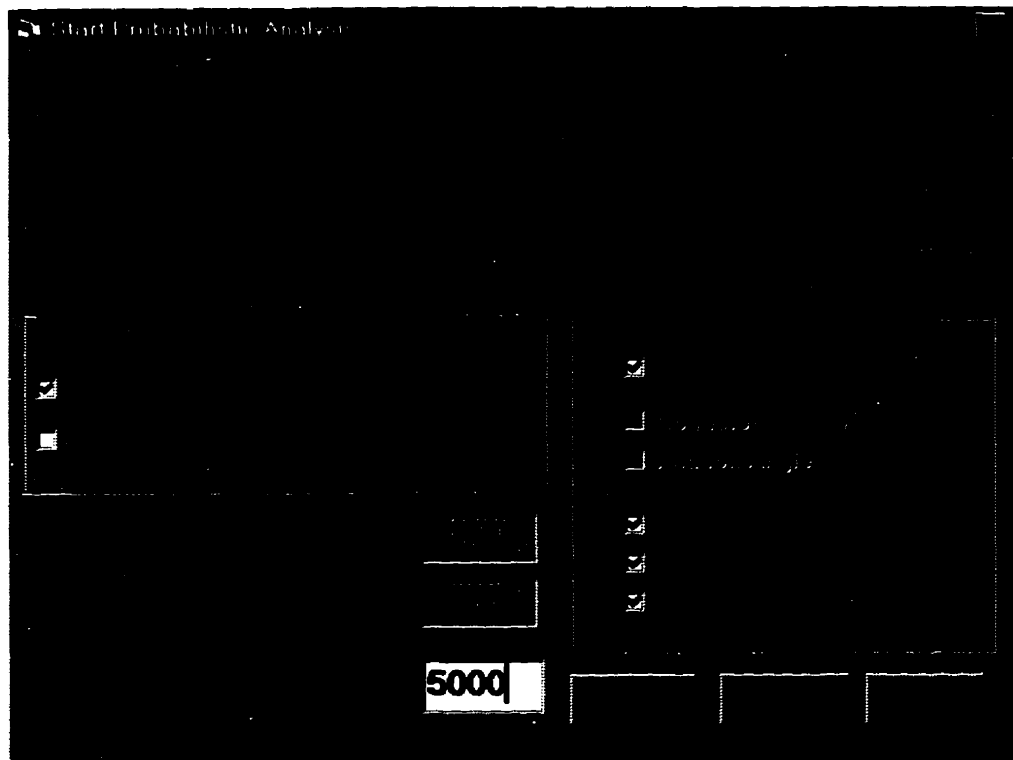


Figure 3.8 The Start Probabilistic Analysis window.

3.4.5 Selection of the random strength parameters

Determination of strength parameters is an important as well as the most difficult part of the stability analysis because relatively small changes in shear strength parameters can result in significant changes in the safety factor. It is recognized that joints in different sets have different strengths. Since many factors, such as the degree of weathering, joint roughness, normal stress and presence of water will influence the shear strength of the joints, the strengths measured within a single joint set can also vary. Therefore it is quite natural and reasonable to model strength parameters as random variables in rock slope problems.

The appropriate probability distribution of strength parameters and their varying ranges in each joint set need to be specified. To do this, the user clicks the submenu Run Multi-Wedge Analysis from the MultiWedge menu, then checks the boxes of the strength parameters. This opens a dialog box and asks the user enter three representative values and a probability distribution for the strength parameter (Figure 3.9). The user is asked to specify three representative values for the parameters: the anticipated lowest, highest and the most likely value, and then asked to pick a theoretical probability distribution. Five probability density functions are available for selection, they are the normal, the Weibull, the lognormal, the exponential and the triangular distributions. The normal or the triangular distribution is recommended if the user doesn't know the appropriate distribution. The program takes the three entered values to calculate probability distribution using the *Maximum-Likelihood Estimators'* method as described in Chapter 2. If the strength parameters are considered constant, all three values should be the same.

EzSlide Specification - II

4	8	5	Normal
3	9	5	Normal
4	7	5	Normal
0	0	0	Normal
0	0	0	Normal
0	0	0	Normal

Figure 3.9 The form for the specification of the lowest, the highest, most likely values and the probability distribution of the strength parameter *JRC*.

3.4.6 The probability of failure

Failures, involving the movement of rock blocks on discontinuities in hard rock, may involve three basic modes: plane sliding, wedge sliding and toppling. Multi wedge analysis in EzSlide includes only the first two. Wedge sliding itself is of two types: sliding on the line of intersection and sliding along the dip direction of one plane. The safety factors are classified under the three failure types: (1) Plane sliding along a single plane; (2) wedge sliding along the intersection of two planes; (3) wedge sliding along the dip direction of one of the two planes (Hoek & Bray, 1978). The probability of failure is the relative frequency of safety factors that are less than unity.

The relative frequency of occurrence (p_i) of the failure mode i is:

$$p_i = \frac{n_i}{N_T} \quad (3.5)$$

where n_i is the number of kinematically free wedges in failure mode i and N_T is the total number of wedges analyzed (total number of simulations including both the kinematically free and the not-daylighting wedges).

The probability of failure for each mode $p_{f,i}$ is the ratio of number of failed wedges to the number of kinematically free wedges in that mode:

$$p_{f,i} = \frac{n_{f,i}}{n_i} \quad (3.6)$$

where $n_{f,i}$ is the number of wedges with safety factor less than 1 in mode i.

The probability of system failure $p_{f,sys}$ is calculated from (Quek and Leung, 1995):

$$P_{f,sys} = \sum_{i=1}^3 p_{f,i} \times p_i = \frac{N_F}{N_T} \quad (3.7)$$

where N_F is the total number of failed wedges.

N_T refers to the total number of wedges analyzed. One can however interpret this in two ways: N_T is either the total number of discontinuity combinations that were looked at or only those combinations that form a kinematically free wedge. The computed probability of failure for the system will be quite different.

Lajtai and Carter (1989) used the number of the kinematically free wedges (N_K) for N_T :

$$P_{f,sy} = \frac{N_F}{N_K} \quad (3.8)$$

For the Kenora example, the failure probability using N_T is around one half of the same probability using N_K (Figure 3.10). EzSlide computes both, leaving the problem of definition to the user.

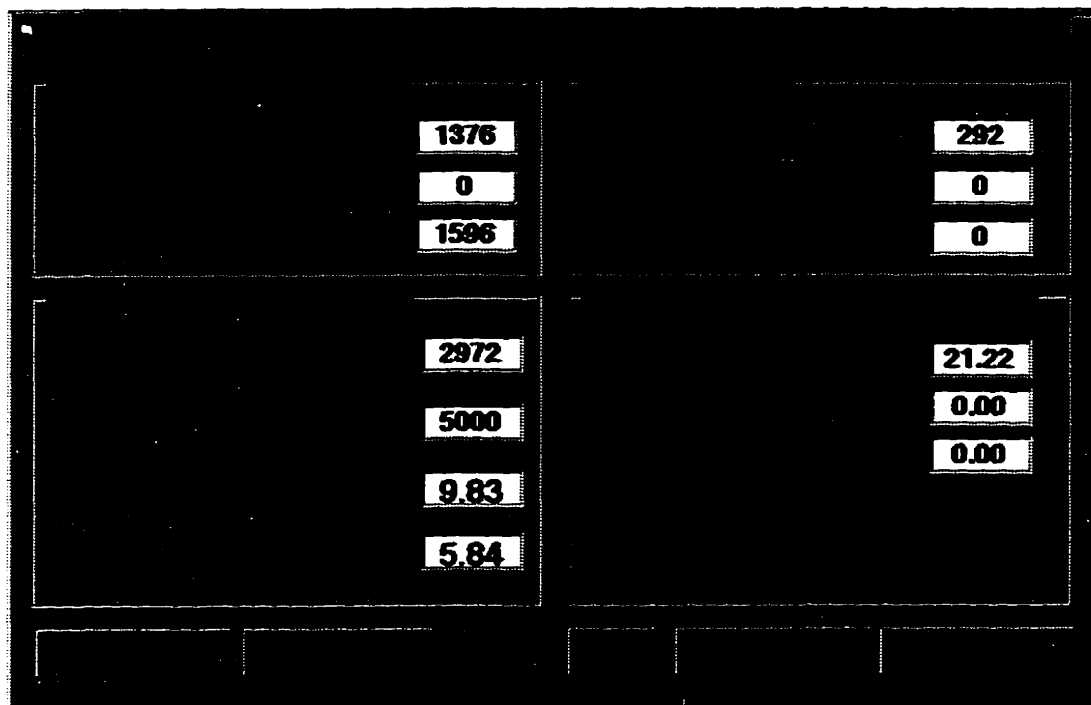


Figure 3.10 Summary display for the results of the probabilistic analysis.

3.4.7 Optimization routines in EzSlide

During the design stage, it may be possible to alter the strike or dip of the slope to reduce the probability of failure. EzSlide provides the tool for this purpose. There are three routines for optimized computation in EzSlide. One allows the horizontal rotation of the slope strike. This is useful in cases where the orientation of the rock slope or rock

cut is not fixed through other considerations. The second routine examines the influence of the slope angle on the safety factor of the slope. The third one tries to find the effect of slope height on the failure probability. These routines are part of the probabilistic analysis of the multi-wedge system.

The optimization process involves the running of the multi wedge routine over and over again using 19 stations within a specified range of the slope strike, dip or height. At each station, a full Monte Carlo simulation is conducted (Figure 3.6). The percentage of the kinematically free wedges and the system failure probability are displayed in a table (Figure 3.11). The sensitivity of the slope strike, slope dip or slope height on the probability of failure is shown in the graph.

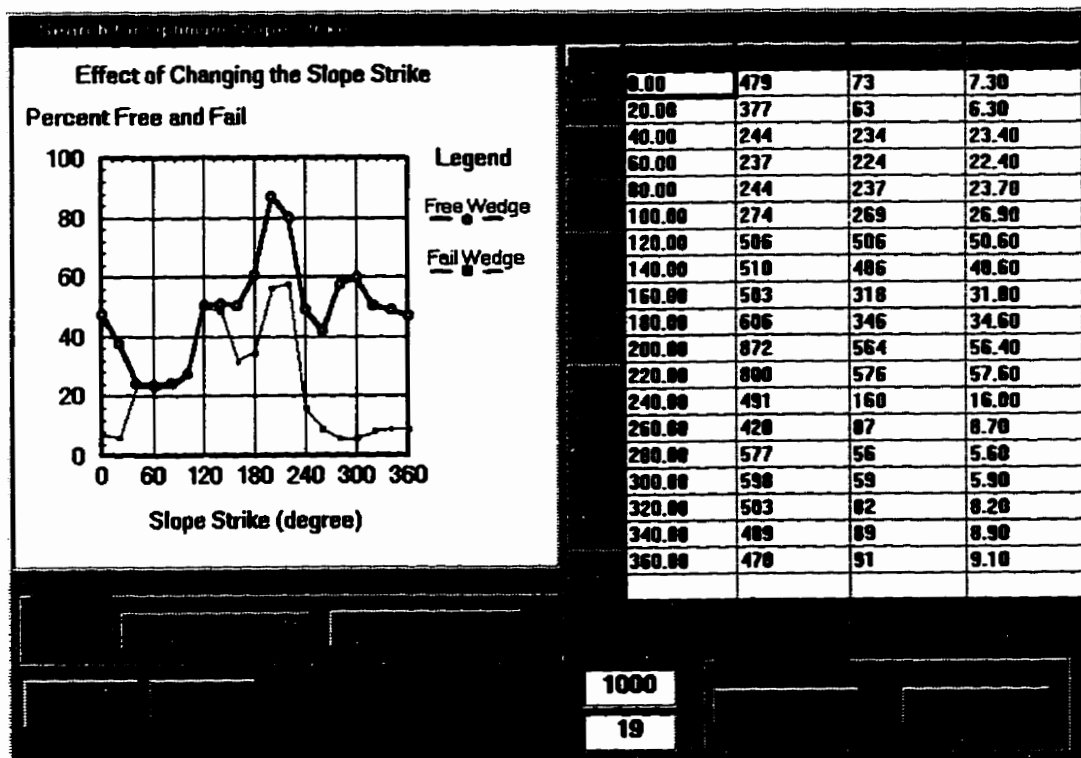


Figure 3.11 The optimization result window with graph and table.

3.5 Post Analysis of Safety Factors

Post analysis involves the plotting of the safety factor data in a cumulative distribution form (Figure 3.12). Alternatively, a histogram may be constructed as well. The Weibull distribution is fitted to the cumulative data automatically.

Most workers have analyzed the safety factors based on the assumption that the distribution of safety factors is normal (Piteau et al, 1985; Call et al, 1976 etc.). In fact the distribution of the safety factors is often skewed. The Weibull distribution can accommodate this condition. Unfortunately, there is a greater problem: the distribution is often multi - modal. The most useful values of the safety factors are around 1 and less. Therefore Ezslide in the default state truncates the data to the range of $-1.99 < SF < 2.99$. The user can however change the limits (menu item: Post Analysis/Limits for Weibull fit). One obvious cause for multi - modality is the fact that at least three sliding modes are involved. EzSlide, therefore, allows the analysis of the safety factor for each failure mode separately as well.

3.5.1 Cumulative distribution of the safety factor with Weibull fit

The Weibull parameters are found by using the Newton Iteration Method as introduced in section 2.2.2. However, the Weibull distribution is not suitable for negative values. In the solution process (transparent to the user), the safety factor scale is shifted to make all values positive. The default range for the Weibull fit is $-1.99 < SF < 2.99$. The user can change the range to seek for the best fit by trial and error.

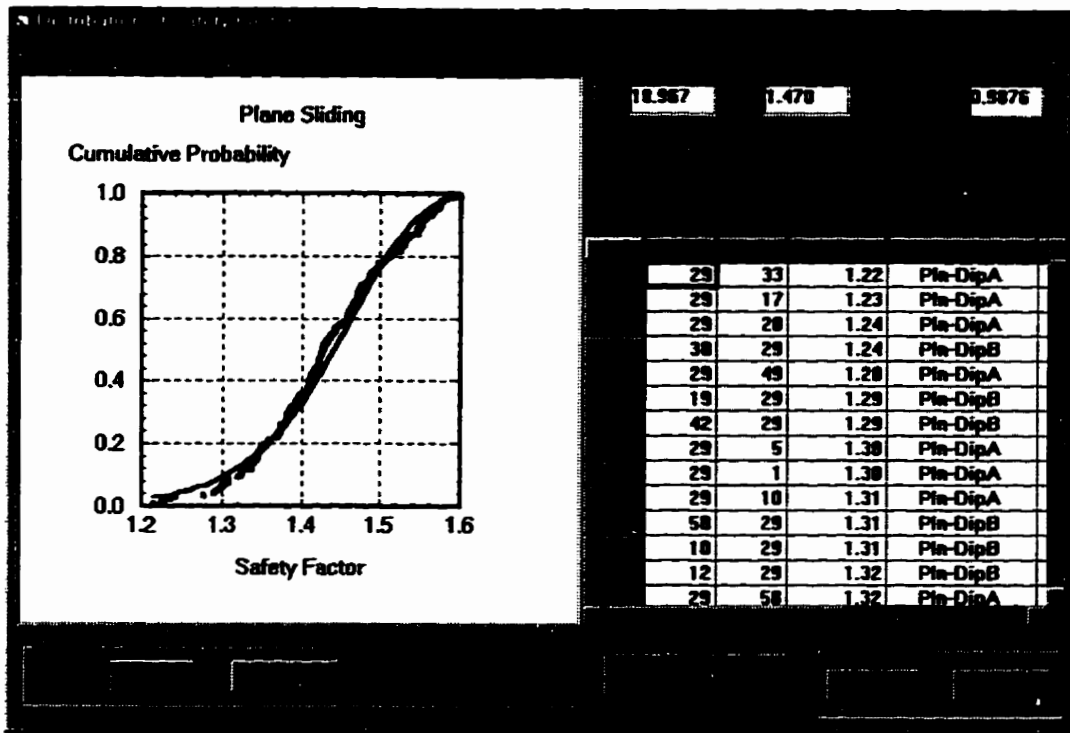


Figure 3.12 The window shows the cumulative distribution with Weibull fit for safety factors listed in the spreadsheet.

3.5.2 Histogram

The histogram is a graphical estimate for the underlying density function. In EzSlide, a histogram is made by dividing the range of safety factors into k (number of bins) adjacent intervals of the same width (Figure 3.13). Choosing a reasonable number of bins (k) is still difficult. In EzSlide, the default bin number is $\frac{1}{4}$ of the number of safety factors in the specified range. The program allows the user to change the number of bins and the limits to reconstruct the histogram.

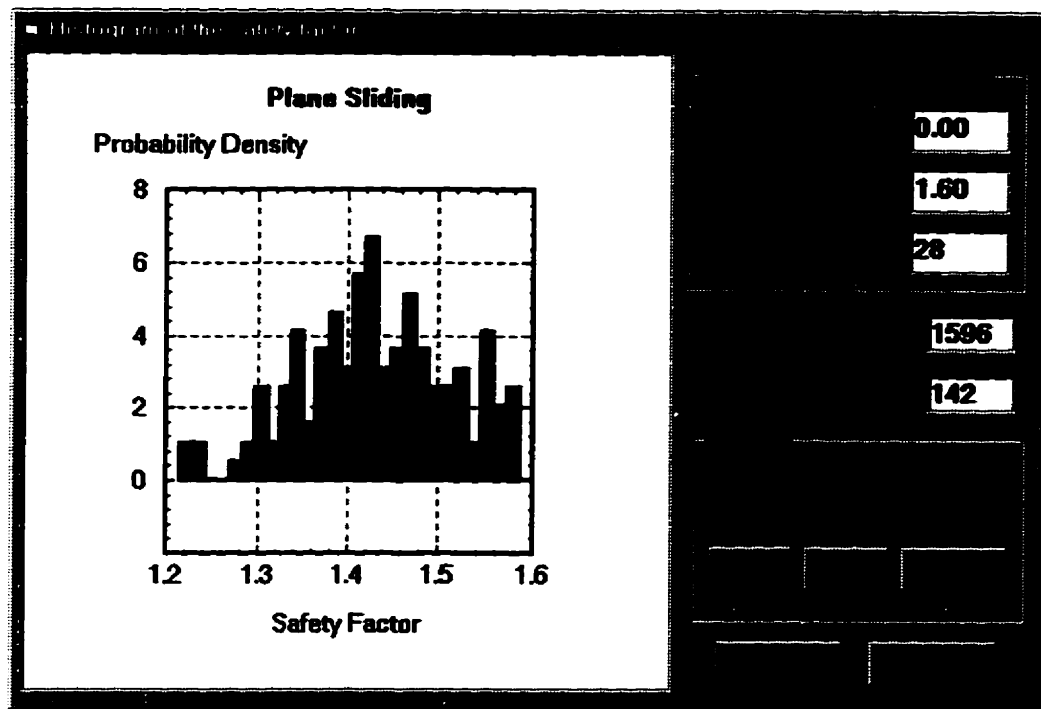


Figure 3.13 The window for displaying histogram of safety factors.

3.6 Input and Output Files

EzSlide stores input and output data in text files. Any text editor, like Notepad or Wordpad, can read and edit text files. The nature of the stored data is reflected in the file extension. Table 3.1 gives a brief description of the files and their default extensions in EzSlide.

Table 3.1 File recordings in the EzSlide

	File Description	File Name Extension
1	Geometry, strength parameters, loading conditions	.gfm (Mohr Coulomb criterion) .gfb (Barton nonlinear criterion)
2	Discontinuity list	.dlm (Mohr Coulomb criterion) .dlb (Barton nonlinear criterion)
3	Single wedge analysis summary	.swr
4	Multi wedge analysis summary	.mws
5	All safety factors	.sfs
6	Safety factor for wedge sliding along the intersection	.sfi
7	Safety factor for wedge sliding along the dip of a single plane	.sfw
8	Safety factor for plane sliding	.sfp
9	Results of the optimization for slope strike	.str
10	Results of the optimization for slope dip	.dip
11	Results of changing the slope height	.hei

Chapter 4

An application using EzSlide

This chapter presents the results of a real - life slope problem using EzSlide. The emphasis is on the investigation of the factors that influence the safety factor and the probability of failure. First, the effect of the strength parameters on the safety factor is discussed. Following this, the sensitivity of the safety factor and the probability of failure to change in water pressure, slope angle and slope strike is evaluated. Next the significance of the two control options: domain control and no domain control are demonstrated. The chapter closes with an examination of the different types of probability distributions of the random variable that can be used with the distribution of safety factor in the three failure modes.

4.1 Geological Data Collection

To conduct an analysis of a rock slope stability using EzSlide, a vertical highway rock cut near Kenora, Ontario was selected. The site is located at the south side of the Trans - Canada highway 17A just before its intersection with highway 659 (Figure 4.1). The rock is Precambrian gneiss with a strong vertical foliation. The orientation of 60

joints was measured (Table A.1 of Appendix). The joint roughness coefficient (*JRC*) of joints were estimated by comparison with standard profiles (Barton, 1976).

When the orientations of joints are plotted as poles in the lower hemisphere, equal area stereonet, three sets of joints can be distinguished (Figure 4.3). The 60 joints and domain designations are listed in Table A.1 (Appendix). The slope of the rock cut is nearly vertical, i.e. the plunge of the normal to the slope is 0°. The measured azimuth of the normal to slope is 190°. The top surface retains its natural shape. It is not far from being horizontal. Thus, the azimuth and plunge of the normal to the top slope surface are 190° and 90° respectively.

On the north side of the highway 17A just opposite to the measured joint system, a partially failed wedge, about 4m high and 3m wide was observed (Figure 4.2). The azimuth and plunge of the normal to the slope are 10° and 0° respectively. The azimuth and plunge of the normal to the top slope are 10° and 85° respectively. The orientation of the two discontinuities forming the wedge are listed in the Table A.2 and shown in Figure 4.3. Only one of the two sliding planes belongs to the three major sets found in the southern road cut.

From Coulson's test results (Barton, 1976), the basic friction angle for gneiss is between 23° (wet) and 29° (dry). The uniaxial compressive strength of gneiss is between 100 MPa and 200 MPa (Hoek and Bray, 1972). As a first step, the value $\sigma_c = 100$ MPa and value $\phi_B = 26^\circ$ were chosen for all the joints. As suggested by Barton (Barton, 1976), the *JCS* of a rock joint varies from $\frac{1}{4} \sigma_c$ (weathered joint surface) to σ_c (unweathered



Figure 4.1 The rock joint system on the south side of highway 17A west of the intersection with highway 659.

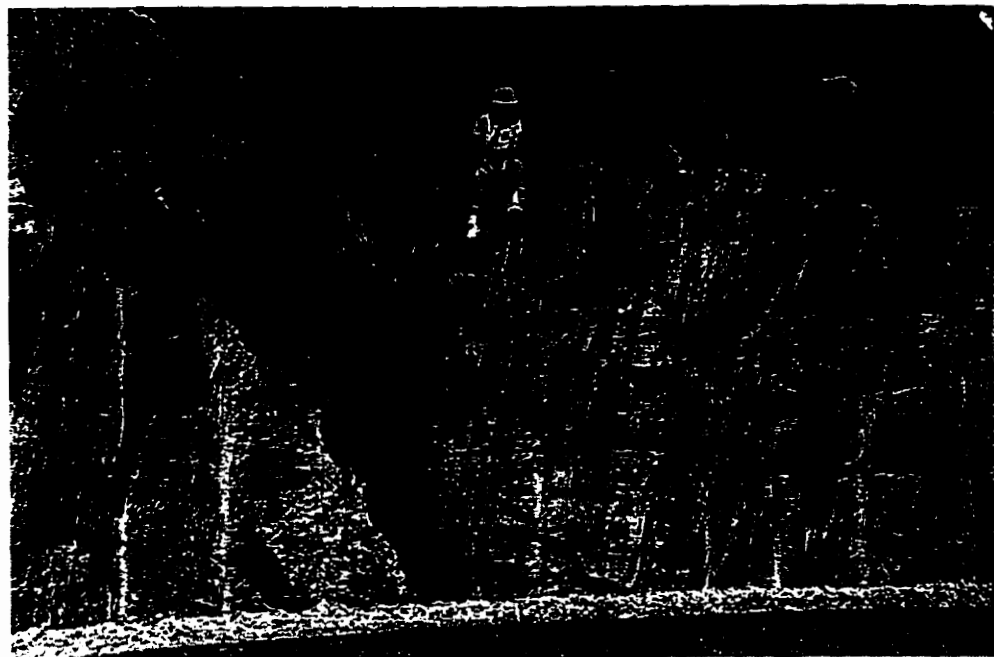


Figure 4.2 A partially failed single wedge on the north side of highway 17A west of the intersection with highway 659.

joint surface). Here the *JCS* of joints is taken as $\frac{1}{2} \sigma_c = 50$ MPa, because some weathering of the joint surfaces was noted. JRC values, as based on field observations, fall in the range of 3 to 9.

4.2 Single Wedge Analysis

As an example, the case of the partially failed wedge (Table A.2 in Appendix A) will be examined using the single wedge analysis routine in EzSlide. To conduct a single wedge analysis with EzSlide, one starts with the menu item File - Start New or the File-Open GeoFile. Since this is a new case, one starts with “File - Start New”. The “Geometry, Loading and Kinematic Check” (Figure 3.3) form opens. The slope, discontinuity and loading data are entered into a three page tabbed file folder. The geometry data and the strength parameters of the partially failed wedge are entered as listed in Table A.2 of the Appendix. There are no external forces acting on the wedge, the site is dry; hence only the weight of the wedge is considered.

After finishing all the inputs, the next step is to check the kinematics of the wedge. By pressing the button Check for Daylighting, the sliding possibilities of the wedge in three sliding modes are analyzed. The report on the kinematic freedom indicates “Free to Slide” along the intersection of the two planes as expected on basis of the field observation. There is “No Freedom” for wedge sliding along the plane A or plane B alone. The results on the plane slide on A and on B show “Daylighting-Strike off”, which means that the planes are daylighting but the difference in the strikes of the two planes and the strike of the slope is greater than 20°. In another words, the plane sliding along these two planes is unlikely. There is also a report on the possibility of toppling. Toppling

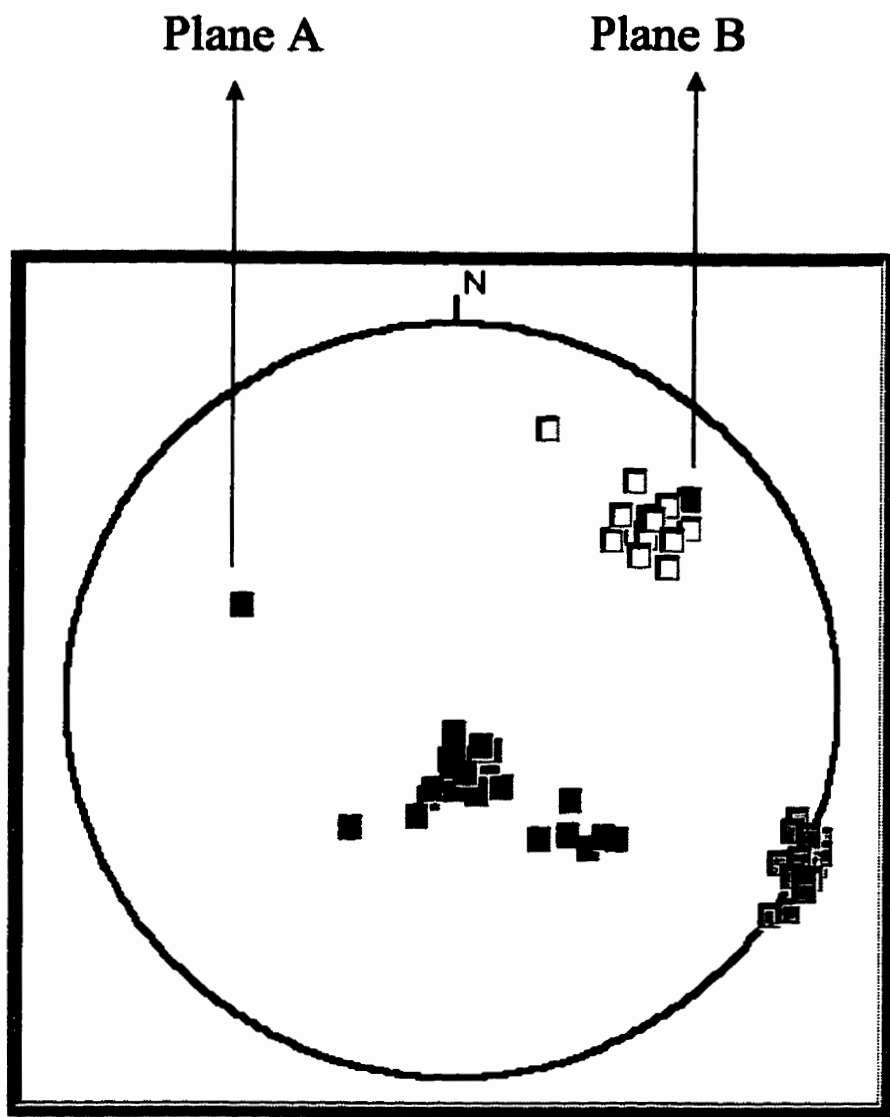


Figure 4.3 The Plane A and Plane B of the failed single wedge and the joint system are displayed in the stereonet.

is suggested when the joints are steeply dipping back into the slope. For this wedge, the toppling check shows that "There is no danger of toppling for this geometry". Based on the kinematic check, the program suggests that "For stability analysis go to menu: Single Wedge/Wedge Slide".

The kinematic freedom check showed that the wedge sliding along the intersection of the two planes is expected as observed in the field. Clicking the menu Single Wedge – Wedge Slide, yields a safety factor of 1.24 under dry condition. A 3D view of the wedge is displayed and some intermediate computation results are listed. Detailed results are shown in Figure 4.4 which is a hardcopy obtained by pressing menu Print Single Wedge Summary of main menu Single Wedge. The safety factor is obviously larger than the unity, which is the expected safety factor of the partially failed slope. The computed safety factor at 1.24 indicates that initial estimates for strength parameters of two planes are too high, or the loading of the wedge is too low. Keeping the loading condition the same, the strength parameters can be adjusted until the desired result of SF = 1 is achieved.

The method of this type of back-analysis is a useful supplement to the estimation of joint strength. The back-analysis automatically includes the effect of scale, which is difficult to represent from laboratory testing. The measured single wedge shown in Figure 4.2 provides a good opportunity to estimate strength of joints in that local area based on back-analysis. However, before estimating the strength of joints, it is advisable to investigate the influence of the Barton and the Coulomb-Mohr's strength parameters on the safety factor.

EzSlide - Single Wedge Summary

6/29/97 4:19:11 PM

Geometry File:

C:\pfa\pic\bigwg.gfb

Slope Normal, Azimuth = 10	Plunge = 0	Slope Height = 4
Top Slope Normal, Azimuth = 10	Plunge = 85	
Discontinuity A Normal, Azimuth = 296		Plunge = 36
Discontinuity B Normal, Azimuth = 46		Plunge = 20
Discontinuity A, JCS = 50000	Basic Fi = 26	JRC = 5
Discontinuity B, JCS = 50000	Basic Fi = 26	JRC = 5

Installed Forces:

Anchor, Azimuth = 10	Plunge = 0	Magnitude = 0
Earthquake, Azimuth = 190	Plunge = 0	Magnitude = 0
External force 1, Azimuth = 0	Plunge = 0	Magnitude = 0
External force 2, Azimuth = 0	Plunge = 0	Magnitude = 0
Water Condition = 0	Surcharge = 0	

Results:

Kinematic Condition for Wedge Slide: Wedge on Intersection

Kinematic Condition for Plane Slide: No Plane Slide Expected

The edges: a, b, c are 5.01 4.70 6.03

The edges: d, e, f are 3.66 5.92 5.50

Area, Plane A = 9.17 Area, Plane B = 12.91

Area, Slope Wedge Face = 11.00 Area, Top Wedge Face = 9.84

Weight of Wedge = 326.80 Volume of Wedge = 13.07

Resultant Force = 326.80 Driving Component = 233.87

Water Force on A = 0.00 On B = 0.00

Normal Force on A = 192.09 On B = 111.77

Barton Resistance on A = 178.43 On B = 111.02

Safety Factor = 1.24

Single Wedge Results File:

C:\pfa\Kenwedge.swr

Force is kN, the strength parameters in kPa (kN/m square).

Length in meters, area in meters square, volume in meters cube.

Shear resistance is according to the Barton specification!

Figure 4.4 The deterministic analysis result of the single wedge shown in Figure 4.2.

4.2.1 Influence of Barton's strength parameters JCS , JRC and ϕ_B on safety factor

For simplicity, the influence of strength parameters on the safety factor is undertaken under dry condition. The possibility of an external water force that may come from a heavy rainfall will be considered later.

Figure 4.5 shows the influence of JCS (joint wall compressive strength) on the safety factor for three different $JRCs$ when the basic friction angle is 26° . The results show that the safety factor increases with increasing JCS in a nonlinear form. The rate of increase is greater when JCS is less than 50 MPa.

In general, the JCS has a small influence on the safety factor when the ratio of

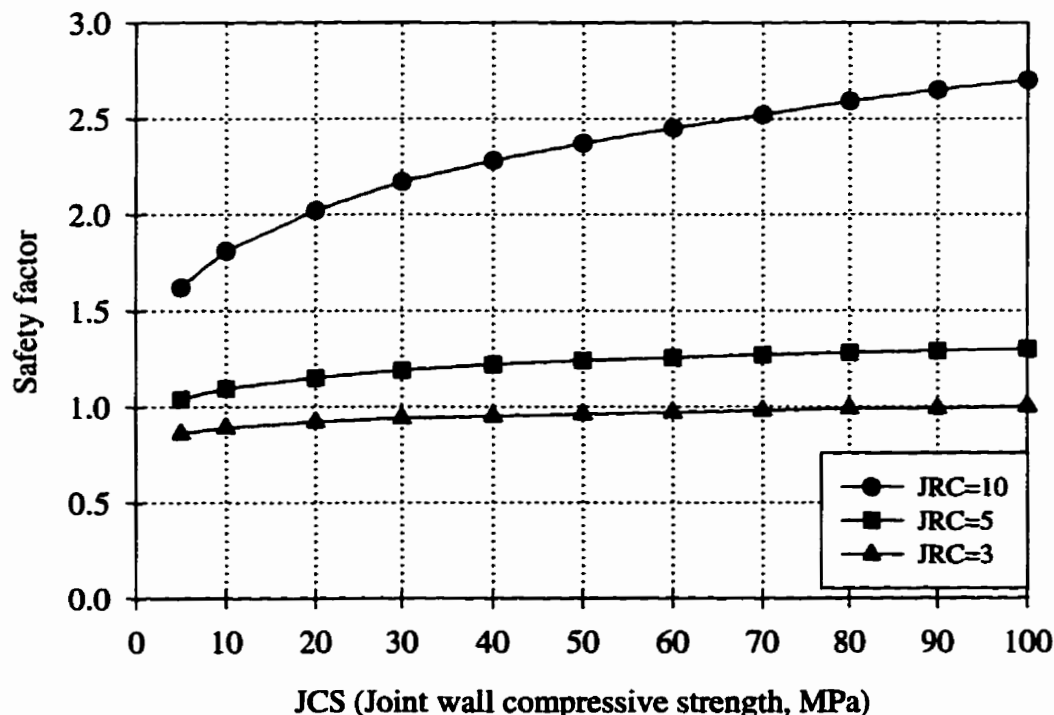


Figure 4.5 The effect of JCS on the safety factor ($\phi_B=26^\circ$)

JCS/σ_n is large. The normal stresses on the two planes of the Kenora site are only about 20 kPa, which gives a large JCS/σ_n ratio, larger than 2000. Figure 4.5 also indicates that JCS has more of an impact on the safety factor when the JRC is large. This is reasonable since with the bigger JRC values, the first term in equation (3.2) increases rapidly. Using $JRC = 5$ as originally entered into the analysis would reduce the safety factor to one if JCS is around 5 MPa (see the middle curve with $JRC = 5$ in Figure 4.5).

The effect of the basic friction angle on the safety factor is shown in Figure 4.6. The safety factor increases with the basic friction angle in a linear form. The safety factor increases at the same rate with different JCS values; the safety factor increases by about 0.04 with a one degree increase in the friction angle. Figure 4.6 also suggests that JCS and the basic friction angle have probably been overestimated. The safety factor becomes one only when JCS is lowered to 10 MPa at $\phi_B = 26^\circ$.

The influence of JRC on safety factor under different JCS values is shown in Figure 4.7. It indicates that the safety factor increases nonlinearly with increase in JRC till it reaches a value of about 14 after which the safety factor remains constant. With increasing JRC , the shear strength increases as equation (3.2). However, when the value $\arctan \tau/\sigma_n > 70^\circ$ i.e. $\phi_B + JRC \log_{10}(JCS / \sigma_n) > 70^\circ$, Barton's equation (3.2) is no longer valid. In this case, the assumption of $\phi_B + JRC \log_{10}(JCS / \sigma_n) = 70^\circ$ is made. Therefore the safety factor is constant when JRC approaches 20. For the partially failed Kenora wedge JRC should be around 4 in order to get the safety factor close to one.

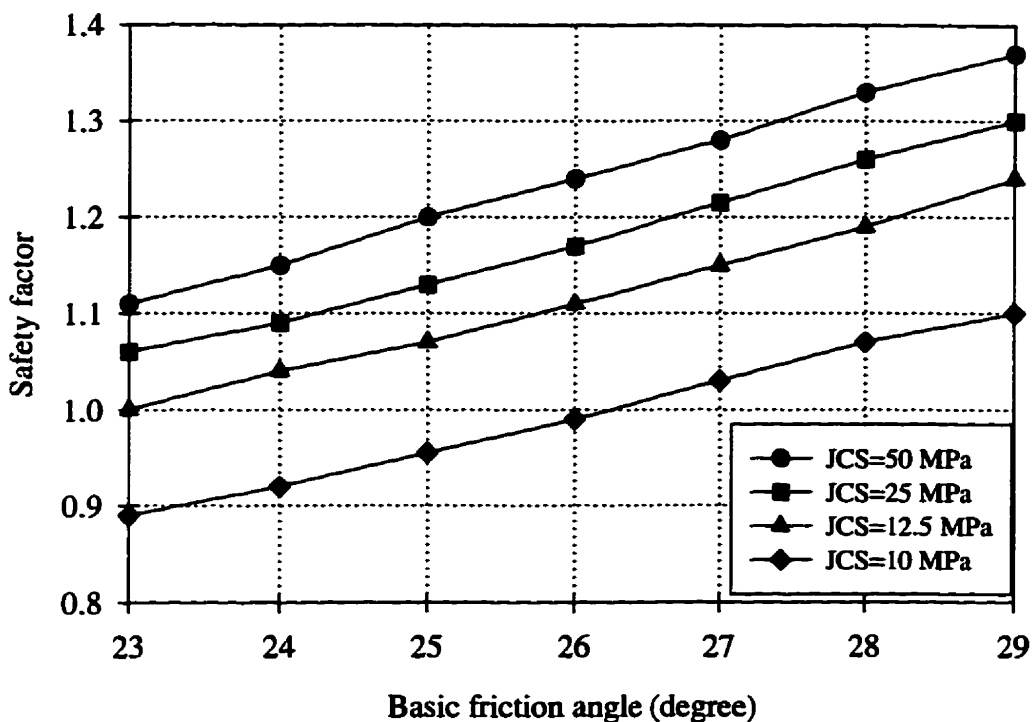


Figure 4.6 The effect of basic friction angle on the safety factor.

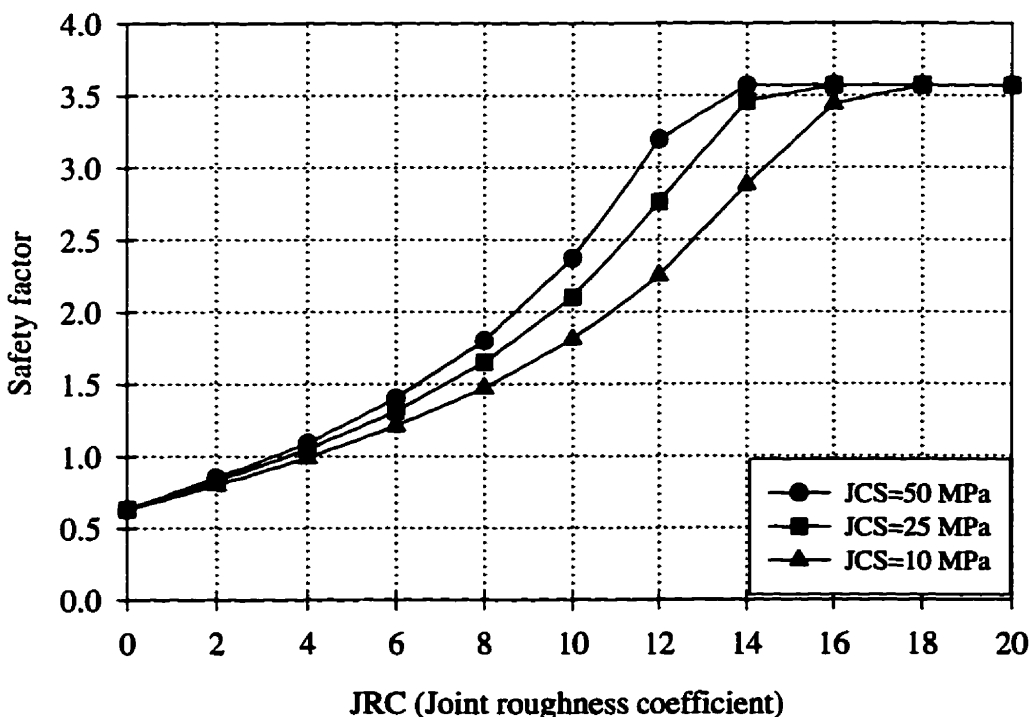


Figure 4.7 The effect of *JRC* on the safety factor ($\phi_B=26^\circ$)

4.2.2 Estimating the Barton strength parameters

From the above analyses, an appropriate set of Barton's strength parameters for the Kenora wedge would be in the range of $10 \leq JCS \leq 50$ MPa, $23 \leq \phi_B \leq 26^\circ$ and $3 \leq JRC \leq 5$. Since the JRC is already at very low value 5, there may be some room for reducing ϕ_B and JCS . Table 4.1 shows several possible combinations of strength parameters yielding a safety factor close to one.

Table 4.1 Some possible combinations of strength parameters for the partially failed Kenora wedge

	<i>JCS (Mpa)</i>	<i>JRC</i>	$\phi_b (^\circ)$	<i>Safety factor</i>
1	50	4	23	0.98
2	50	4	24	1.02
3	40	4	24	1.00
4	30	4	25	1.02
5	30	4	24	0.99
6	20	4	26	1.03
7	20	4	25	1.00
8	10	4	26	0.99

4.2.3 The influence of the Mohr-Coulomb strength parameters

The Mohr-Coulomb strength parameters are the unit cohesion c and the friction angle ϕ . By assuming the friction angle at 30° for both plane A and B, the unit cohesion c for the two planes would have to be very low, only 3.0 kPa to get the safety factor close to one. The relationship between safety factor and both the cohesion and the friction

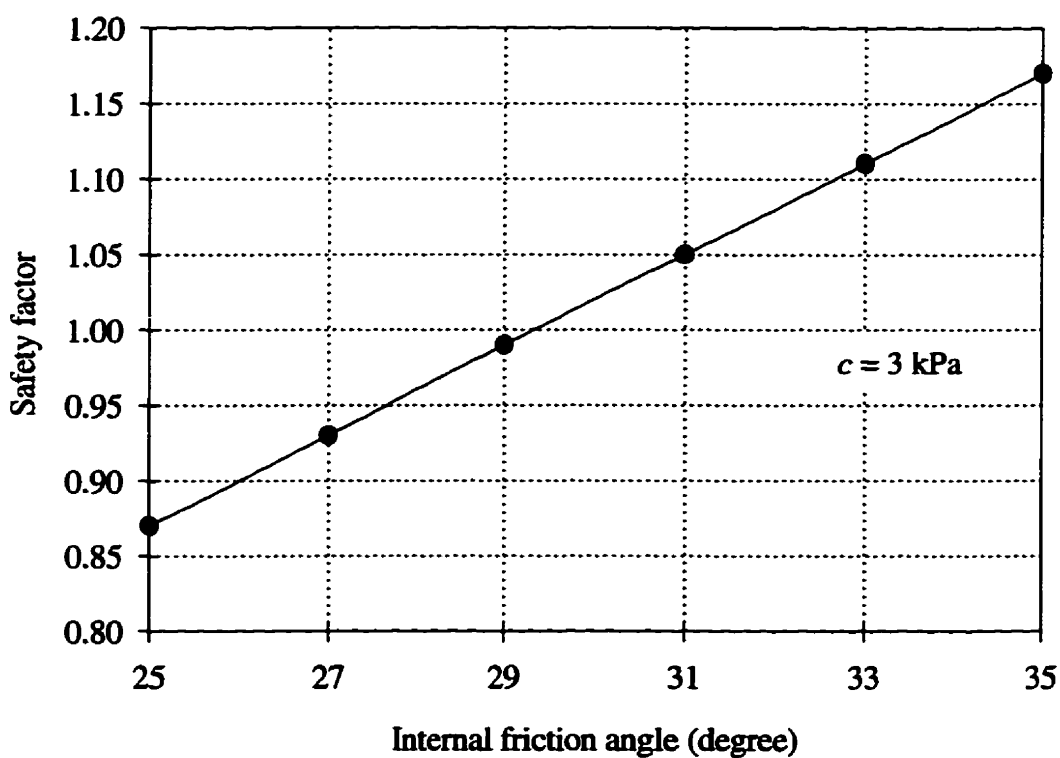
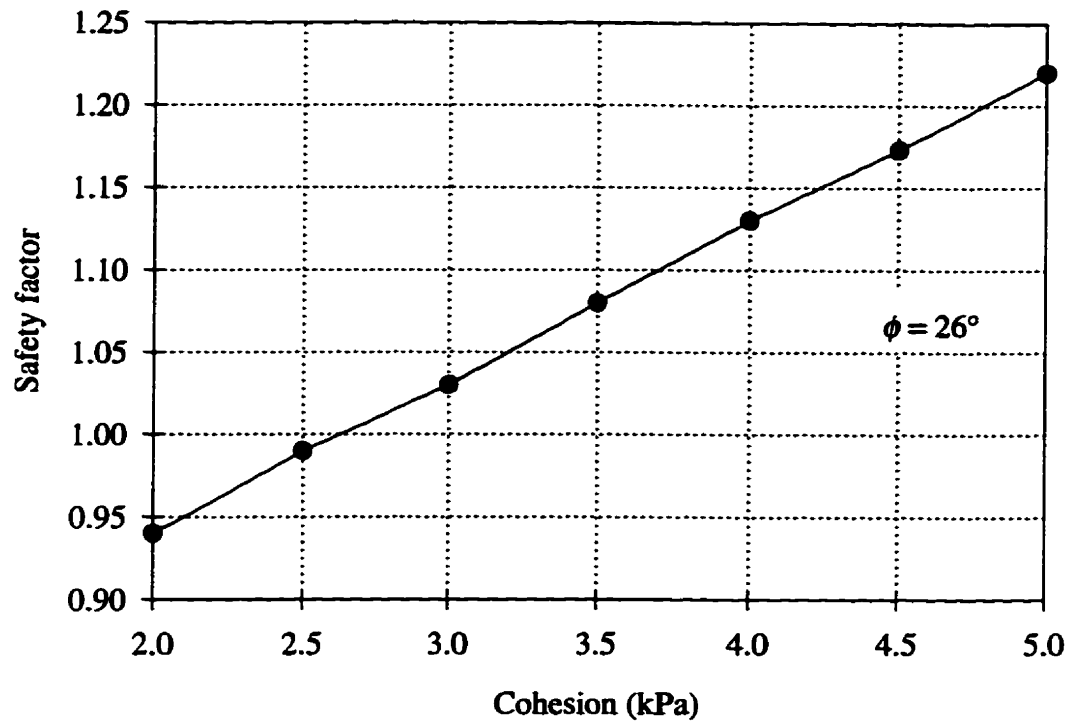


Figure 4.8 The effect of the unit cohesion and the friction angle on the safety factor of the Kenora wedge.

angle is approximately linear (Figure 4.8). Figure 4.9 plots the SF = 1 contour. Any combinations of cohesion and internal friction angle above the line generate a stable wedge, while below the line the wedges are unstable. If we assume a friction angle between $29^\circ \sim 37.5^\circ$, the cohesion of the joints would in the range of 0 to 3 kPa. These low cohesion values are perhaps consistent with the low *JRC* values of the Barton specification.

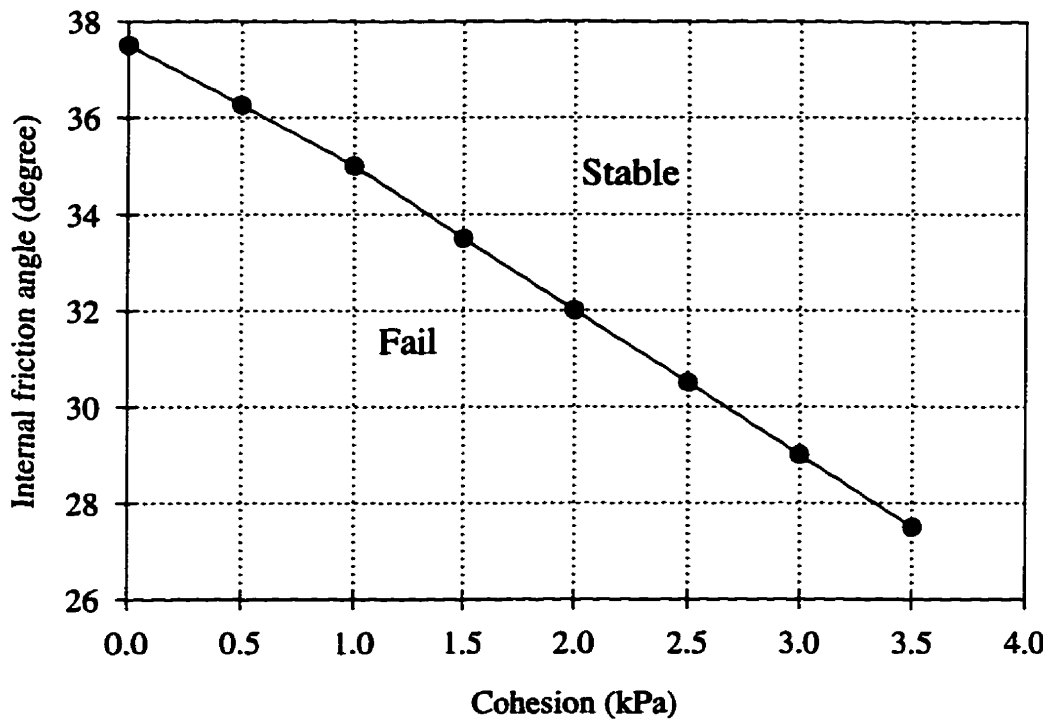


Figure 4.9 Possible combinations of the unit cohesion and the friction angle to yield a safety factor of unity.

4.2.4 The effect of the height of the slope

In the deterministic analysis of rock slopes, the cohesion and the friction angle of the joints are assumed to be constant. The safety factor however may vary depending on the weight of the wedge. The weight of the rock wedge is determined by the orientation of the joints, slope height and dip, and the unit weight. Since the orientation of the joints and the unit weight for a specific site is fixed, the safety factor becomes a function of the slope height alone. In this section, an analytical analysis of the height effect for the simple slope geometry of Figure 4.10 is conducted. The calculation of the safety factor based on the two strength criteria, the linear Mohr-Coulomb law and the non-linear Barton specification.

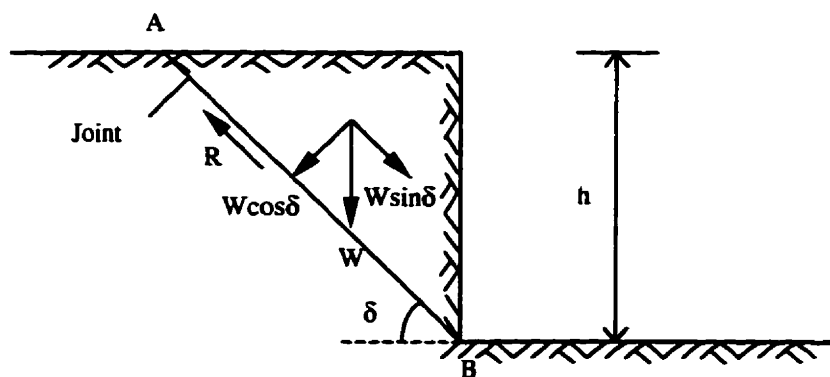


Figure 4.10 A slope with vertical excavation surface

Assume a rock slope involves a plane slide with a vertical excavation surface and a joint inclined δ with the horizontal. The unit weight of the rock is γ and the height of the slope is h . The weight of the rock wedge is calculated by taking a thickness of one meter:

$$W = \frac{h^2 \gamma}{2 \tan \delta} \quad (4.1)$$

The component of W along the sliding direction is D_p (driving force):

$$D_p = W \sin \delta = \frac{1}{2} h^2 \gamma \cos \delta \quad (4.2)$$

The component of W that acts normal to the plane is N_p :

$$N_p = W \cos \delta = \frac{h^2 \gamma \cos^2 \delta}{2 \sin \delta} \quad (4.3)$$

The base area of the sliding surface (A_p):

$$A_p = \frac{h}{\sin \delta} \quad (4.4)$$

The normal stress that acts across the sliding surface:

$$\sigma_n = \frac{N_p}{A_p} = \frac{1}{2} h \gamma \cos^2 \delta \quad (4.5)$$

For the Mohr-Coulomb strength criterion, the unit cohesion and the friction angle are equal to c_p and ϕ_p , respectively. The shear strength of the joint is calculated based on equation (3.1):

$$\tau = c_p + \sigma_n \tan \phi_p \quad (4.6)$$

The safety factor is defined as the ratio of the resisting force along the sliding direction to the drive force that induces sliding:

$$SF = \frac{\tau A_p}{D_p} \quad (4.7)$$

Substituting equation (4.2), (4.4), (4.5) and (4.6) to the equation (4.7), the safety factor:

$$SF = \frac{c_p \frac{h}{\sin \delta} + \frac{1}{2} h \gamma \cos^2 \delta (\tan \phi_p) \frac{h}{\sin \delta}}{\frac{1}{2} h^2 \gamma \cos \delta} \quad (4.8)$$

This reduces to:

$$SF = \frac{4c_p}{\gamma h \sin 2\delta} + \frac{\tan \phi_p}{\tan \delta} \quad (4.9)$$

Equation (4.9) indicates that the safety factor decreases with increasing slope height. Only the first term, the one containing the unit cohesion, is the function of the slope height.

For the Barton non-linear specification, the strength parameters of the sliding plane are JRC_p , JCS_p and ϕ_{Bp} . The driving force is the same as in equation (4.2). The shear strength is equation (3.2):

$$\tau = \sigma_n \tan(JRC_p \log_{10} \frac{JCS_p}{\sigma_n} + \phi_{Bp}) \quad (4.10)$$

The safety factor is calculated from equation (4.7). Substituting equation (4.2), (4.5), (4.6) and (4.10) to equation (4.7):

$$SF = \frac{\frac{1}{2} h \gamma \cos^2 \delta \left(\frac{h}{\sin \delta} \right) \tan(JRC_p \log_{10} \frac{2JCS_p}{h \gamma \cos^2 \delta} + \phi_{Bp})}{\frac{1}{2} h^2 \gamma \cos \delta} \quad (4.11)$$

After cancelling some items, the safety factor:

$$SF = \frac{\tan(JRC_p \log_{10} \frac{2JCS_p}{h \gamma \cos^2 \delta} + \phi_{Bp})}{\tan \delta} \quad (4.12)$$

In equation (4.12), the height of the slope is in the logarithmic term. In shallow slope problems, JCS is usually much larger than the normal stress so that the term of the

\log_{10} factor will not show a big variation. This implies that the height effect is less significant when Barton's strength criterion is used.

For the partially failed wedge (Figure 4.2), the height effect is quite different for the two strength criteria (Figure 4.11). Through the Mohr-Coulomb strength criterion, the influence of the height on the safety factor is a great deal more significant.

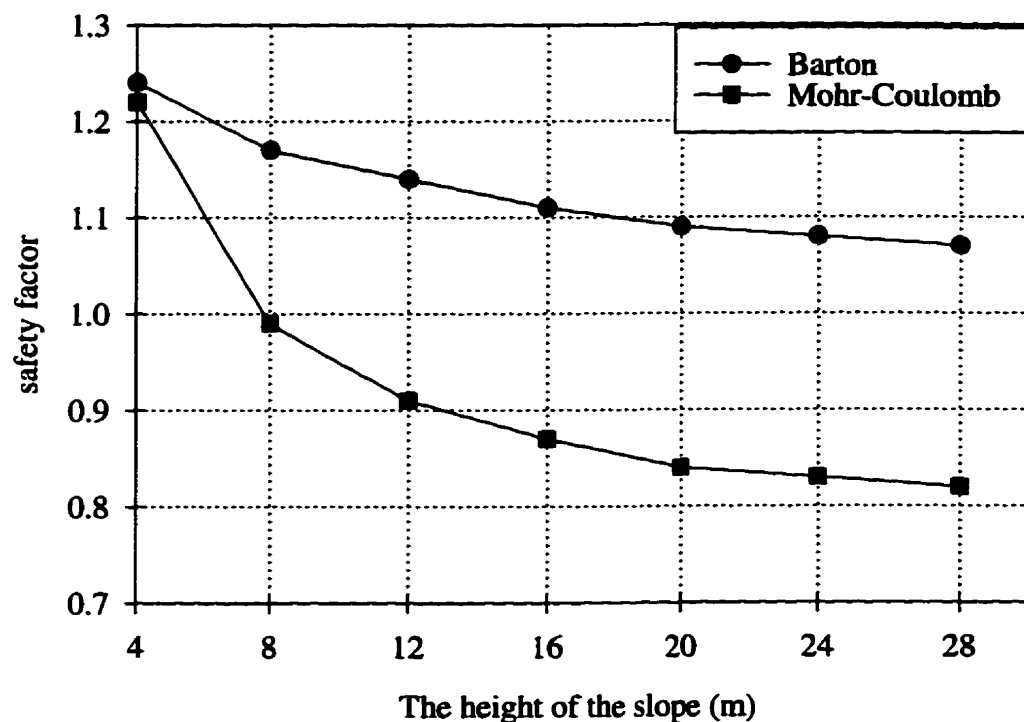


Figure 4.11 The height effect on the safety factor.

4.3 Probabilistic Analysis of A Multi Joint System

4.3.1 Probabilistic analysis

Before carrying out the probabilistic analysis for the joint system measured on the south side of 17A, a strength criterion must be selected. The Barton's non-linear strength criterion has been selected because the strength parameters defined by Barton are easier to estimate when actual test data are not available. JRC can be estimated through the visual comparison of the joint surface with standard profiles. Values for JCS and ϕ_B can be found from references (Hoek & Bray, 1977 and Barton, 1976).

The discontinuity data to be used in the simulation are listed in Table A.1 of Appendix A. The loading conditions and the strength parameters are assumed to be random variables. The probability distribution for JCS and JRC is assumed to be the normal. The probability distribution of the basic friction angle ϕ_B is taken as the triangular distribution. The range of JCS is from $1/4 \sigma_c$ to $1/2 \sigma_c$ because of the slightly weathered nature of the joint system, namely from 25 to 50 MPa. The most likely value of JCS is the mean value 37.5 MPa. The range of the basic friction angle for all joints is assumed from 23° to 26° , the most likely value is 24° . The range of JRC comes from the site investigation as shown in Table 4.2. For domain 1, the low value is 4, the high value is 6 and the most likely value is 5. For domain 2, the low value is 3, the high value is 8 and the most likely value is 5. For domain 3, the low value is 4, the high value is 7 and the most likely value is 5.

Table 4.2 Input for the random variables

	<i>Low</i>	<i>High</i>	<i>Most likely</i>	<i>Probability distribution</i>
JCS (MPa)	25	50	37.5	Normal
ϕ_B ($^{\circ}$)	23	26	24	Triangular
JRC (# 1)	4	8	5	Normal
JRC (# 2)	3	9	5	Normal
JRC (# 3)	3	6	4	Normal

The Monte Carlo simulation has been conducted under three different conditions (Table 4.3). One is under dry condition i.e. only the weight induces sliding. The other two add a water effect in the 20 % ~ 40 % and 30 % ~ 50 % range. Under dry conditions, two types of failure modes may exist, but failure occurs only in wedge slide along the intersection. The probability of failure in this failure mode is 14.3 %. The system probability of failure is 6.9 % (based on NK) and 4.0 % (based on NT) respectively. When there are water pressures acting on the rock slopes, the probability of system failure (based on NK) increase to 8.3 % (20 % ~ 40 % water level) and 9.3 % (30 % ~ 50 % water level) respectively.

Table 4.3 Monte Carlo Simulation

(A) Number of kinematically free wedges in the three failure modes				
Water level	Wedge slide along intersection	Wedge slide along single plane	Plane sliding	Total
Dry	1410	0	1513	2923
20 % ~ 40 %	1403	0	1539	2942
30 % ~ 50 %	1397	0	1546	2925

(B) Number of failed wedges in the three failure modes				
Water level	Wedge slide along intersection	Wedge slide along single plane	Plane sliding	Total
Dry	202	0	0	202
20% ~ 40%	243	0	0	243
30% ~ 50%	273	0	0	273

(C) Probability of failure (%)				
Water level	Wedge slide along Intersection	Plane sliding	System based on NK	System based on NT
Dry	14.3	0	6.9	4.0
20 % ~ 40 %	17.2	0	8.3	4.9
30 % ~ 50 %	19.8	0	9.3	5.5

Note: NK = Number of Kinematically free wedges,
 NT = Total number of wedges.

4.3.2 The factors influencing the probability of failure

4.3.2.1 The influence of water pressure

To do the sensitivity analysis for water pressure, the range of the random variables and their probability distribution are kept the same as listed in Table 4.2. The limits for the water head are zero (dry) to 100 % (the wedge is saturated to the ground surface). Figure 4.12 shows the results. For plane failure, the water level must exceed 60 % to have any effect at all. For wedge failure, the probability of failure rises slowly to about 30 %. After this it rises more rapidly.

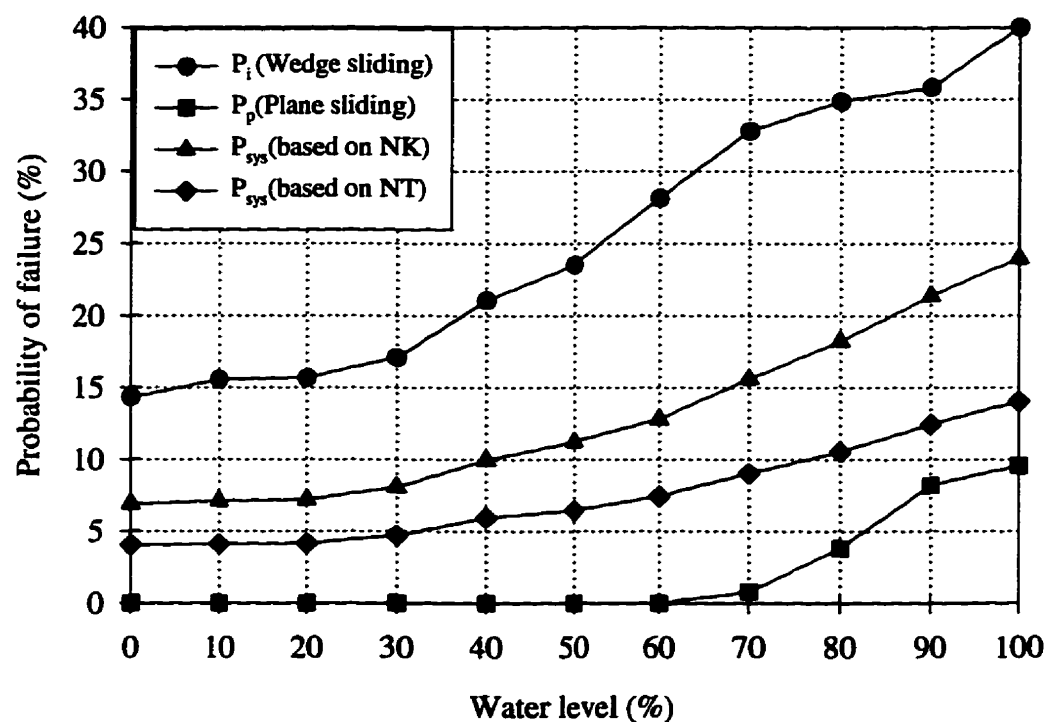


Figure 4.12 The effect of the water level on the probability of failure.

4.3.2.2 The effect of *JRC*

JRC has the most significant influence on the probability of failure in the $0 \leq JRC \leq 2$ range (Figure 4.13). When *JRC* is less than about 2, even though the ratio of JCS/σ_n is large, let's say 2000, the peak friction angle $[\phi_B + JRC \log_{10}(JCS / \sigma_n)]$ approaches the basic friction angle ϕ_B . The shear strength of joints will decrease drastically and in turn the safety factor decreases as well. When the $JRC > 4$, the probability of failure decreases at a shallow rate. Figure 4.14 shows the cumulative distribution of the safety factor in the wedge and the plane sliding modes as a function of *JRC*. In general, the safety factor increases with increasing *JRC*. Note that the safety factor in plane sliding is always greater than one even if *JRC* is zero. Thus it is the wedge sliding mode that determines the probability of failure.

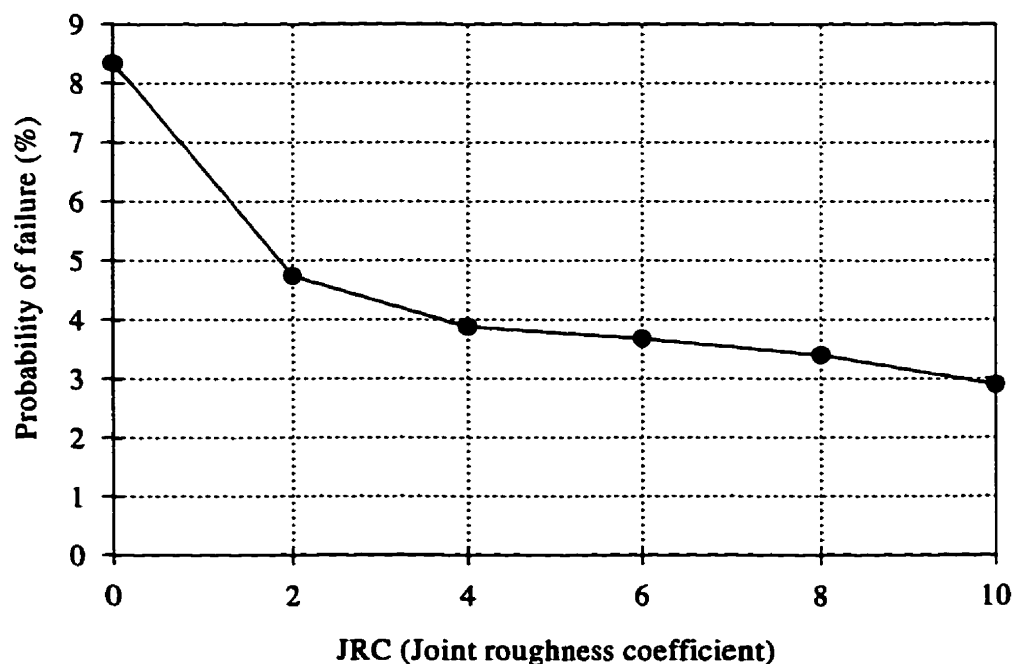


Figure 4.13 The effect of *JRC* on the probability of failure

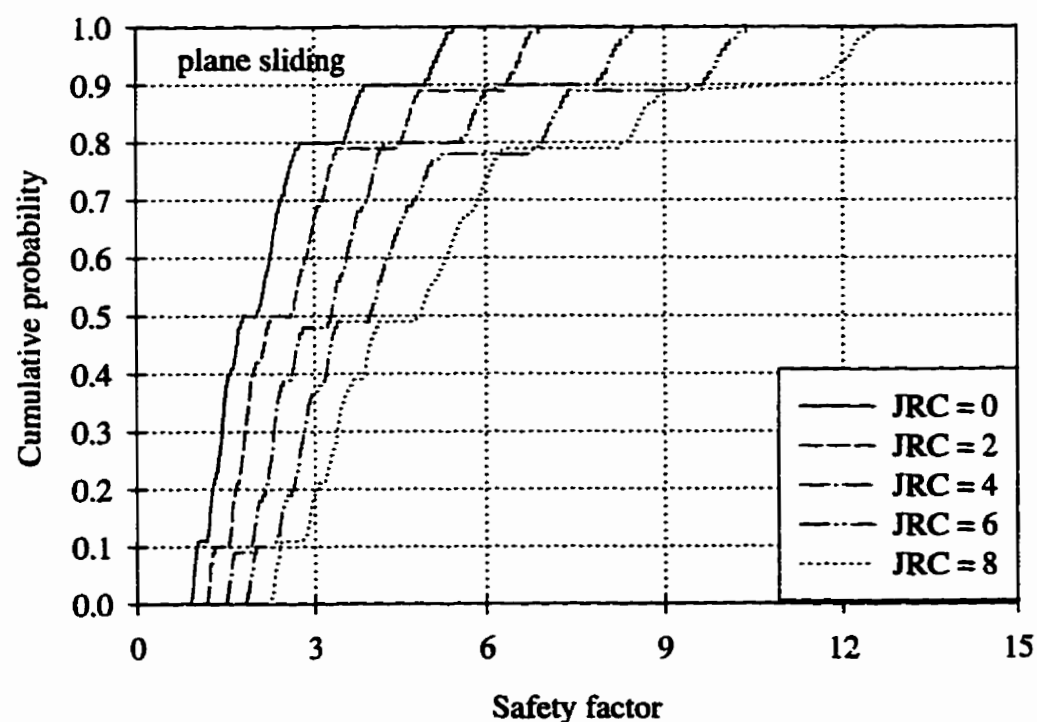
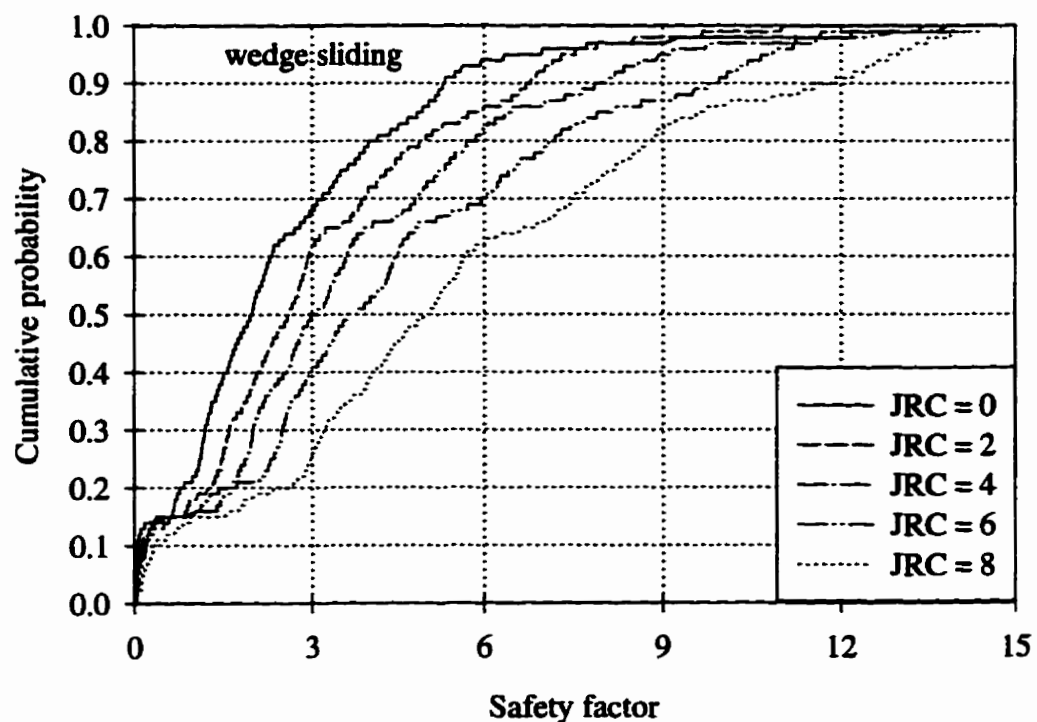


Figure 4.14 The shift of the cumulative distribution of safety factors with JRC in the wedge and the plane sliding failure modes.

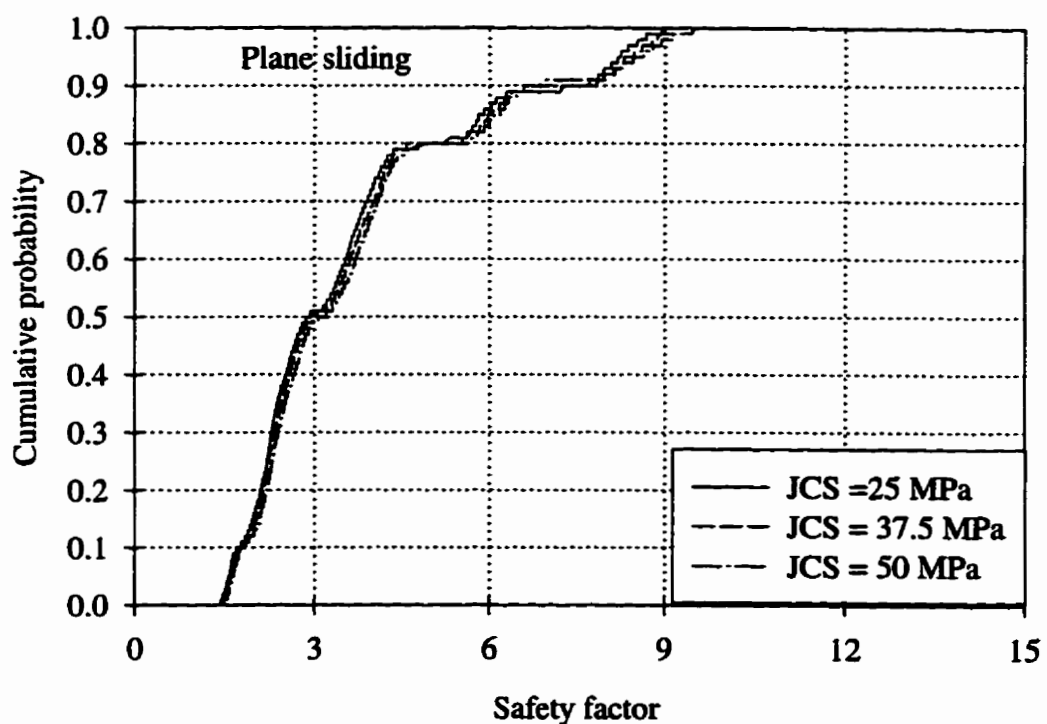
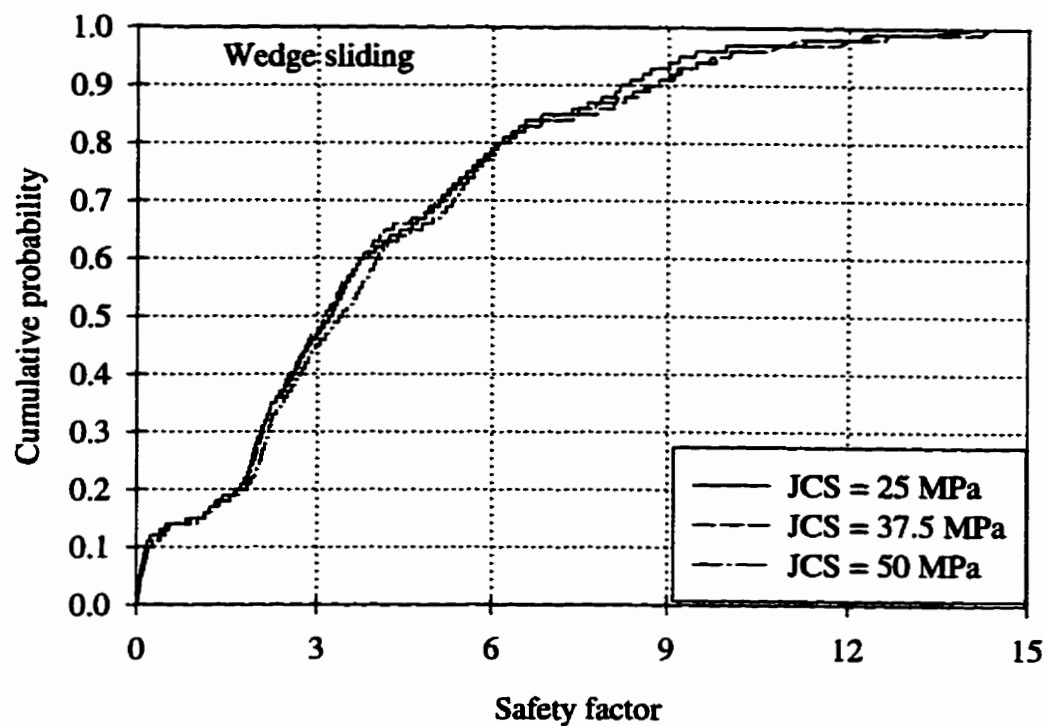


Figure 4.15 The cumulative distribution of safety factors with different JCS values in wedge sliding and plane sliding failure modes.

4.3.2.3 The effect of JCS

The cumulative distribution of the safety factor in both the wedge and the plane sliding modes is insensitive to *JCS* when taken in the 25 to 50 MPa range (Figure 4.15). The reason is that the normal stress for shallow slopes is very small when compared to *JCS*, therefore usually a big ratio of JCS/σ_n is obtained. The term $\log_{10} (JCS/\sigma_n)$ in Barton strength equation (3.2) will not change very much. Therefore increasing *JCS* will not make a significant increase in shear strength. Consequently the probability of failure decreases at a very low rate with the increasing of *JCS* (Figure 4.16).

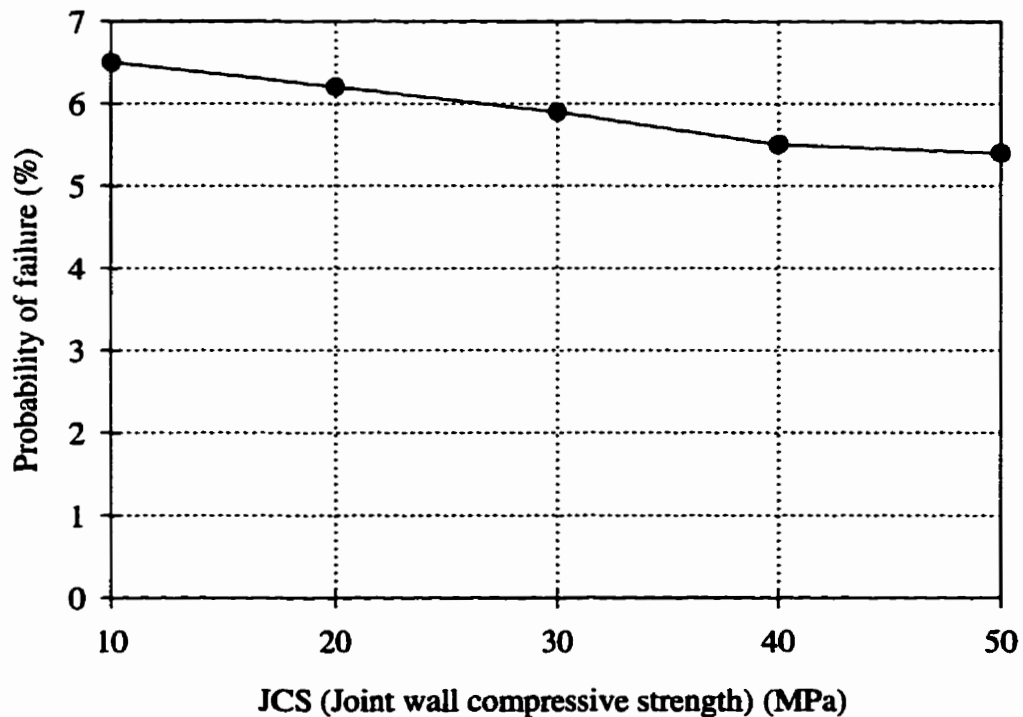


Figure 4.16 The effect of JCS on the probability of failure

4.3.3 Slope angle and the probability of failure

EzSlide makes it easy to investigate the influence of the slope angle and the trend of the highway (slope strike) on the probability of failure. The program uses 19 stations between the specified minimum and maximum limits. At each station, a full probabilistic analysis is done. At the end of the run the probability of failure is plotted against the slope angle. The investigation in this section considers water pressure as a random variable in the range of 0 % to 40 %, with the most likely water level taken at 20 %. The strength parameters are the same as in Table 4.2.

The percentage of kinematically free wedges and the probability of failure vary with increasing slope dip as shown in Figure 4.17. When the slope dip is changed from 0° to 35°, the number of kinematically free wedges increases from 0 to 60 % of the total observed wedges. However, the number of failed wedges increases only from 0 to 4.5 % of the total wedges. The slope angle does not have a significant influence on creating kinematically free wedges when the slope angle is above 35°.

4.3.4 Sensitivity of the probability of failure to slope strike

The effect of changing the slope strike on the probability of failure is shown in Figure 4.18. There is an optimum slope strike in the 240° to 380° range. The north and south walls of the highway 17A are actually at 100° and 280° respectively. The worst possible orientation of the highway would be at 200°.

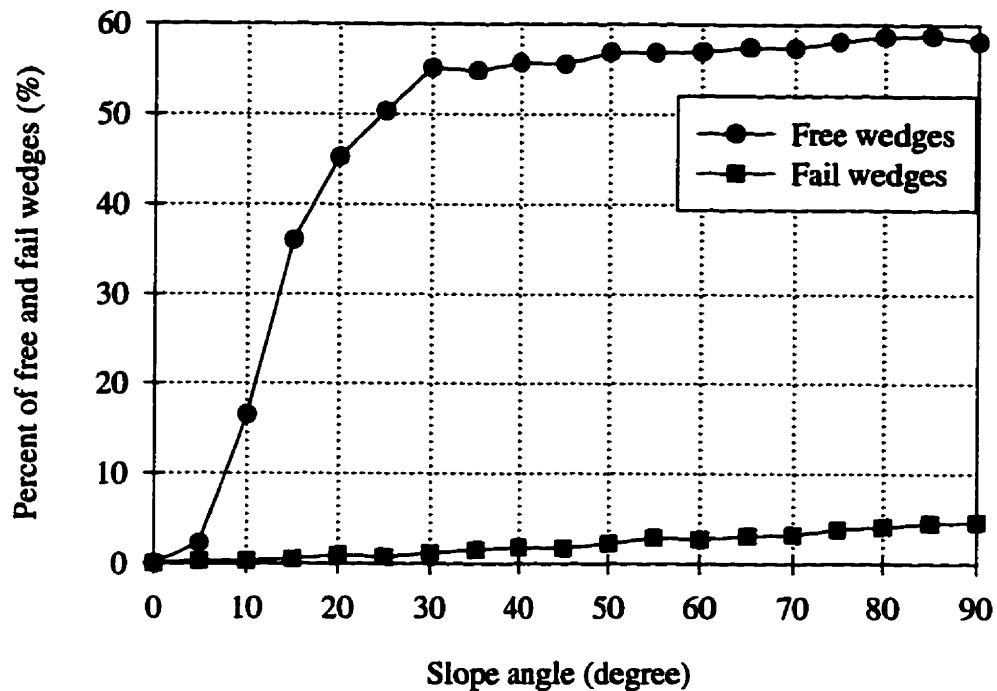


Figure 4.17 The probability of failure changes slightly with the slope dip.

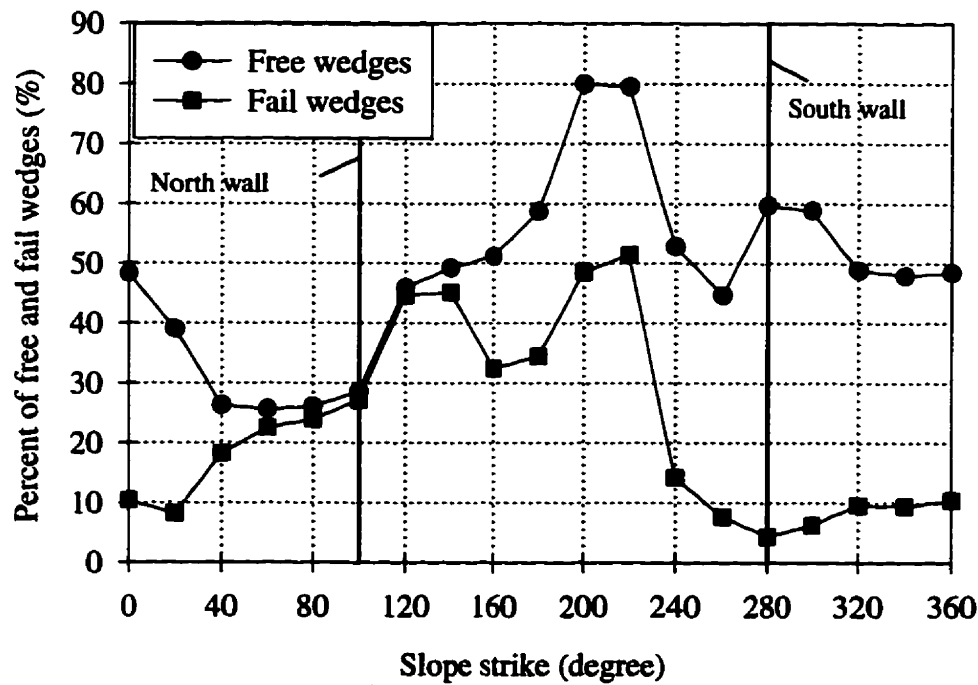


Figure 4.18 The probability of failure changes dramatically with slope strike.

4.3.5 The effect of domain control

EzSlide provides for the “Domain Control” and “No Domain Control” functions in the building of the rock wedge out of the rock joint system. When the simulation is processed under domain control, plane A and plane B come from different joint sets. In contrast, simulation under “No Domain Control” does not have this restriction, the two discontinuities can come from either the same or different joint sets.

There is a very important difference in the safety factor distributions processed through the two controls (Figure 4.19). The greatest difference is found in the most important region, at the low safety factor tail of the distribution. This is even more evident in the histogram display (Figure 4.20). Under “no domain control”, a greater

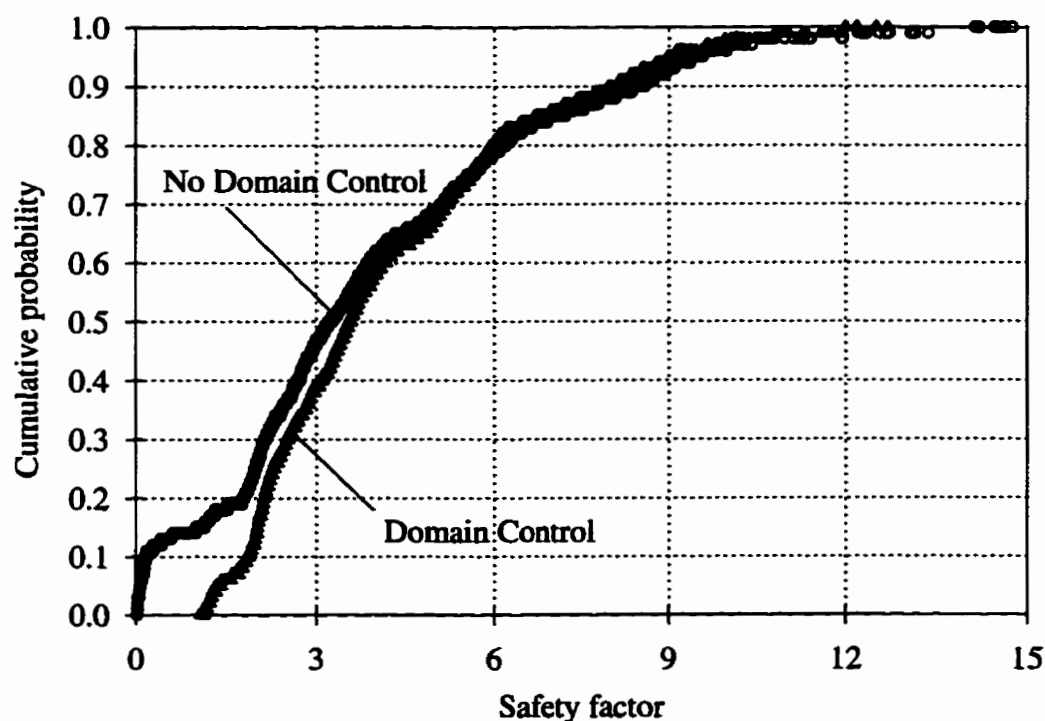


Figure 4.19 The cumulative distribution of safety factors with domain control and no domain control in the wedge sliding mode.

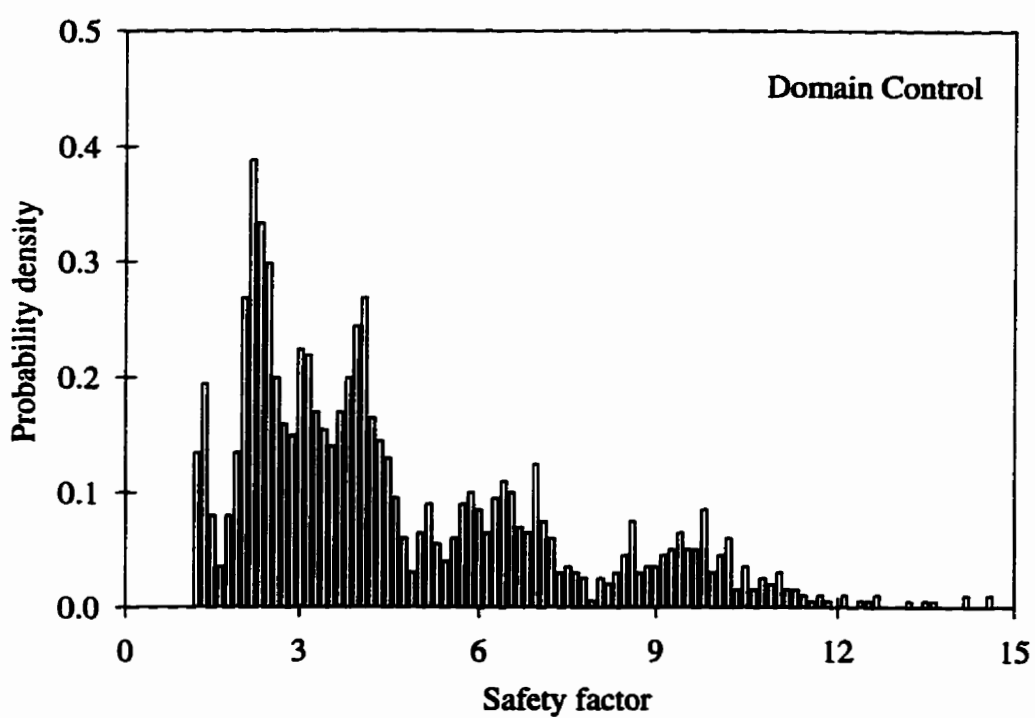
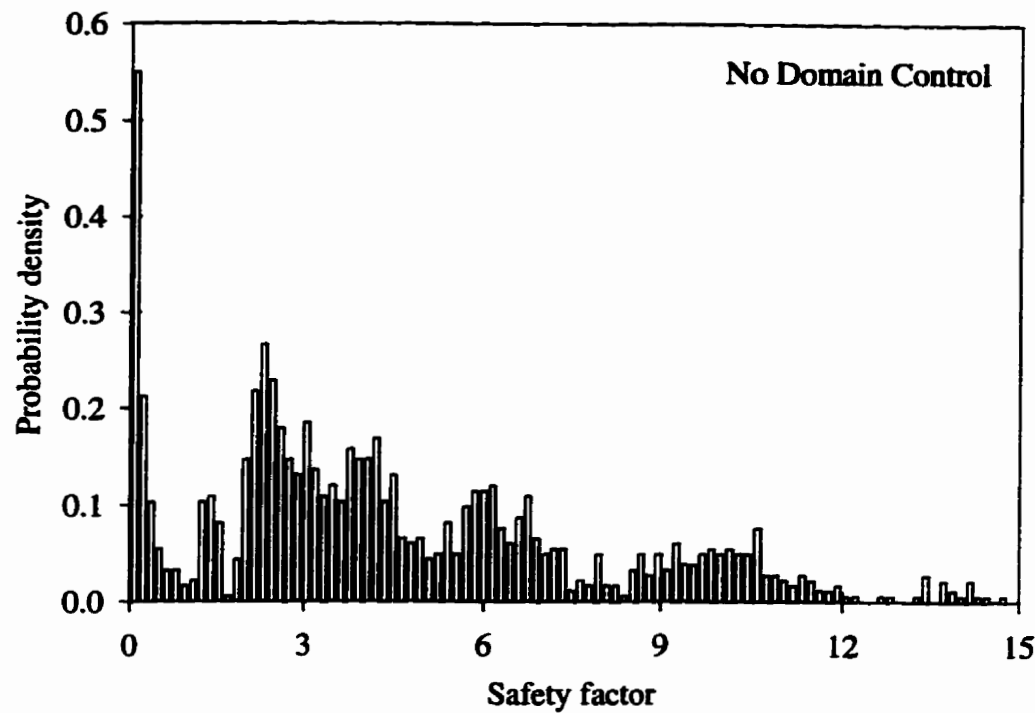


Figure 4.20 The histograms of safety factors in wedge sliding mode under “domain control” and “no domain control”.

number of failed wedges is produced. An investigation of the low safety factor wedges showed that they are formed by discontinuities that come from the same joint set (the set 2 in the Discontinuity List). The wedges have a very narrow front and a very small-enclosed angle between plane A and B (Figure 4.21). However, the low safety factor peak disappears under “domain control”. To be conservative, the user should always do simulations both ways, under both “domain” and “no domain control” and then analyze the significance of the difference by examining the size and the weight of the wedges occupying the low safety factor tail of the distribution.

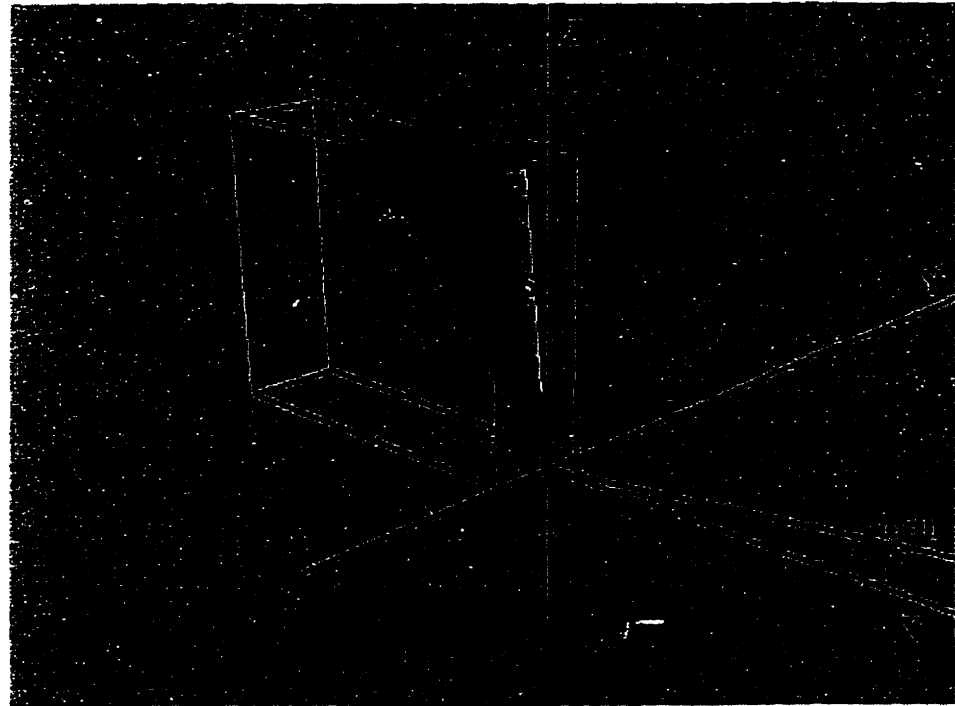


Figure 4.21 A typical failed wedge whose plane A and B comes from the same set.

4.3.6 The effect of the probability distribution type

Five probability distributions are provided for modeling the random variable in EzSlide. The user can select any one of these. This section examines the effect of changing the probability distribution for *JRC*.

In this analysis, *JRC* is assumed to be a random variable within the range from 1 to 8 with the most likely value at 4. The probability distribution of *JRC* is represented by the normal, the triangular, the Weibull, the exponential and the lognormal distributions. The difference between the truncated and non-truncated distribution is investigated as well. In a truncated distribution, the random variates outside the specified range are cut off. Figure 4.22 shows that the simulation results when using non-truncated distributions. The probability of failure with the Weibull, the lognormal and the exponential distributions are slightly higher than those with the normal and the triangular distributions. The probability of failure with truncated distributions, on the other hand, differs less (Figure 23).

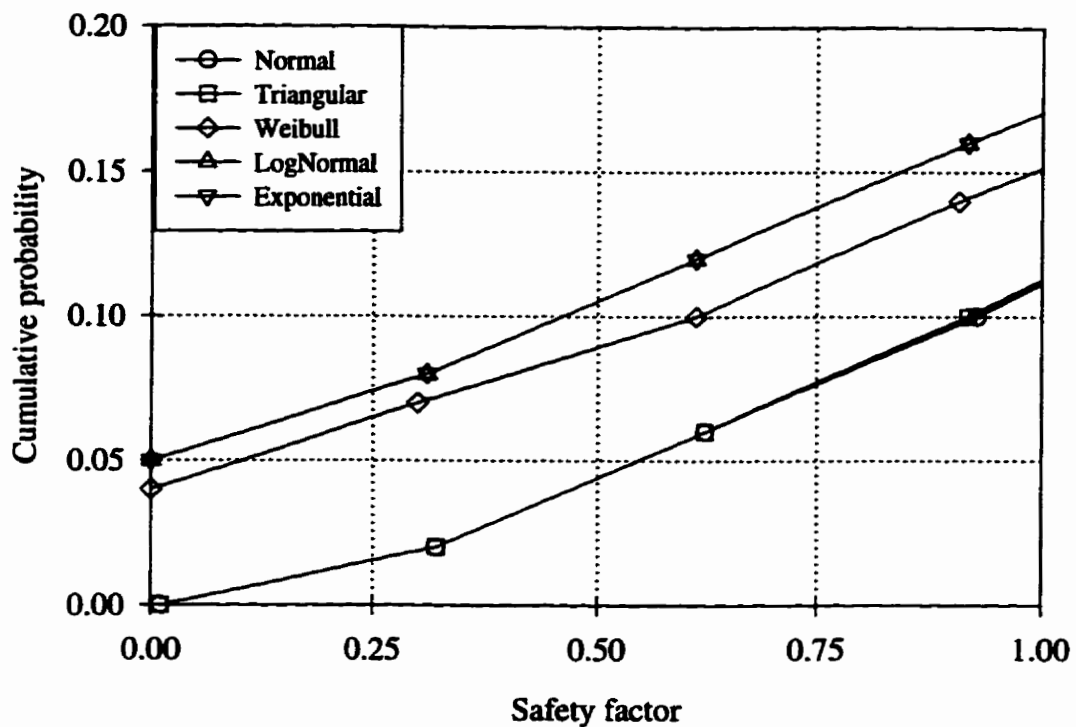


Figure 4.22 The cumulative distribution of the safety factor in the $0 < SF < 1$ range. The distribution are not truncated.

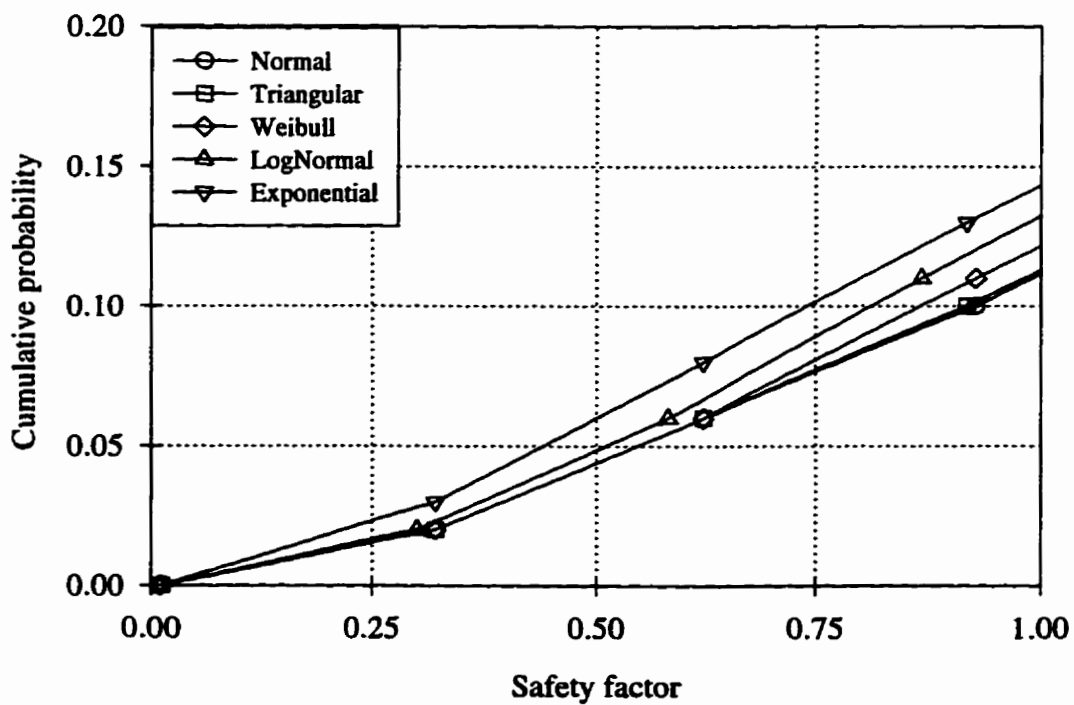


Figure 4.23 The cumulative distribution of the safety factor in the $0 < SF < 1$ range. The distributions are truncated at $1 < JRC < 8$.

In the next step, the probability of failure at a wider range of *JRC* is compared. The range of *JRC* is expanded from 1 ~ 8 to 1~ 20 with the most likely value remaining fixed at 4. For the truncated case, the probability of failure for the five different distributions is quite close. However, in the non-truncated case, the probability of failure with the Weibull, the lognormal and the exponential distributions are about 2 times as high as for the normal and the triangular distributions (Figure 4.24). The reason for this difference could be that the Weibull, the lognormal and the exponential distributions are asymmetrical distributions skewed toward the small values. In the simulation a greater number of low value variates are produced. For *JRC*, the small values will lead to lower shear strength and lower safety factors. As a result, the probability of failure will increase. The normal and the triangular distributions are symmetrical leading to an equal number of low and high variates. Therefore the probability of failure will not be affected.

The effect of changing the most likely value of *JRC* on the probability of failure is evaluated next. The range of *JRC* is fixed at 1 ~ 8, with the most likely value taken at 2 and 4, respectively. The change is of little significance (Figure 4.25). It is the range that has the greater influence.

Whether the distribution is truncated or not, the results are very similar for the normal and the triangular distributions (Figure 4.22 to 4.25). There is not much of a difference between the normal and the triangular distributions of the *JRC*. There is little point in using the normal distribution when the simple triangular distribution will do just as well. This, however, may not be the case for other types of random variables.

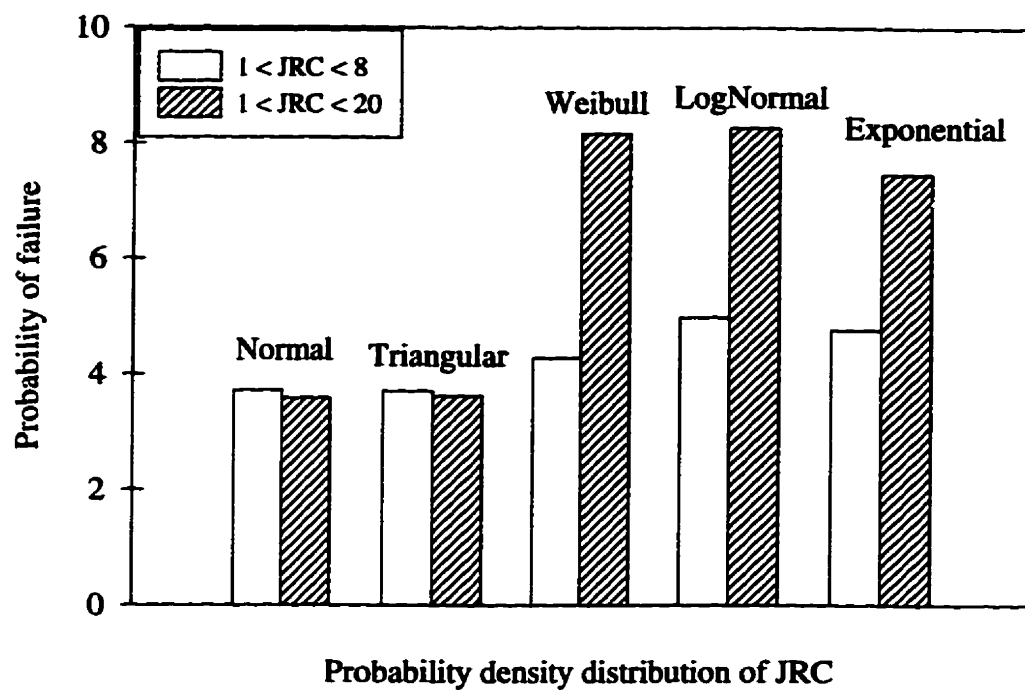


Figure 4.24 The probability of failure under different probability distributions of JRC with the same most likely value at 4, but different range of JRC .

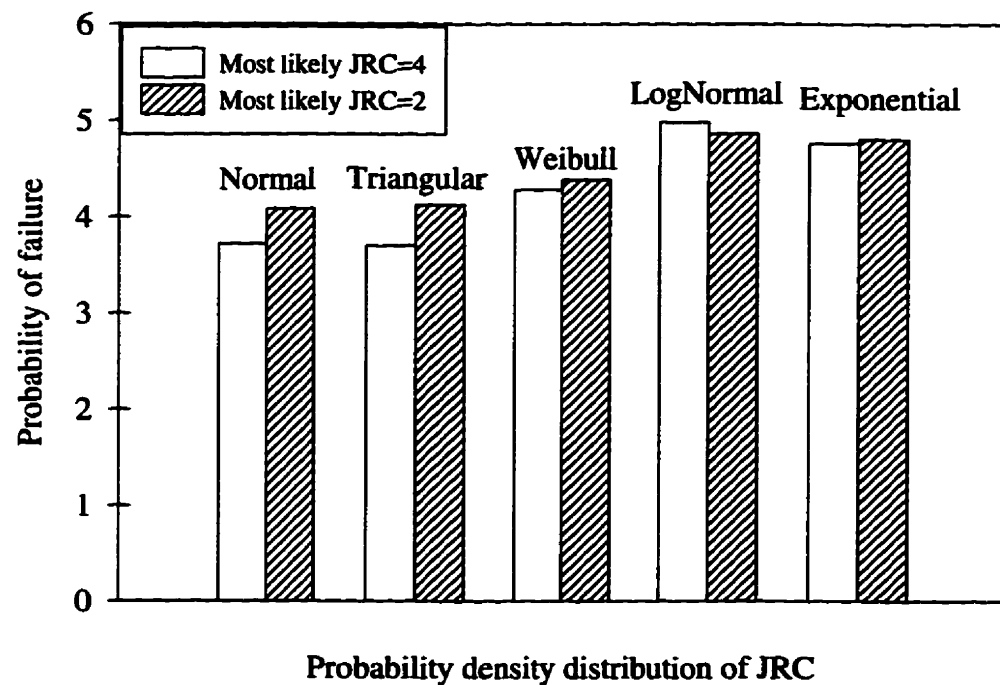


Figure 4.25 The probability of failure under different probability distributions of JRC with the same range $1 < JRC < 8$ but different most likely value of JRC , one is 2 and the other is 4.

4.4 The Safety Factor Distribution

In the literature, the commonly made assumption is that the distribution of the safety factor is normal (Savely, 1985; Call, 1985 etc.). The probability of system failure is calculated as that the part of the area under the standard normal curve where the safety factors is less than one. In this section, we take a closer look at the safety factor distribution using the Kenora joint sets. Only two failure modes exist in the Kenora rock cut (Table 4.3), wedge slide along the line of intersection and plane slide.

In the Monte Carlo simulation, the wedges are formed by a random combination of two discontinuities together with the slope face and top slope. The strength parameters and loading conditions are considered as random variables using one of the available theoretical distributions. The safety factor data including both the plane and the wedge slide modes, are widely distributed in the range of $-99.99 < SF < 99.99$ (Figure 4.26). However, almost 99% of safety factors are between 0 and 15 (Figure 4.27). Clearly, the distribution is not unimodal; the histogram would suggest the presence of at least five distinct distributions.

Figure 4.28 shows the distribution of safety factors in the wedge slide mode alone. It is again multi modal with at least four peaks within the range of 0 to 15. An investigation of the safety factor data that are less than one has found that most of the failed wedges formed by the discontinuities come from the same domain. The shape of the wedges is usually very narrow and slender (Figure 4.21).

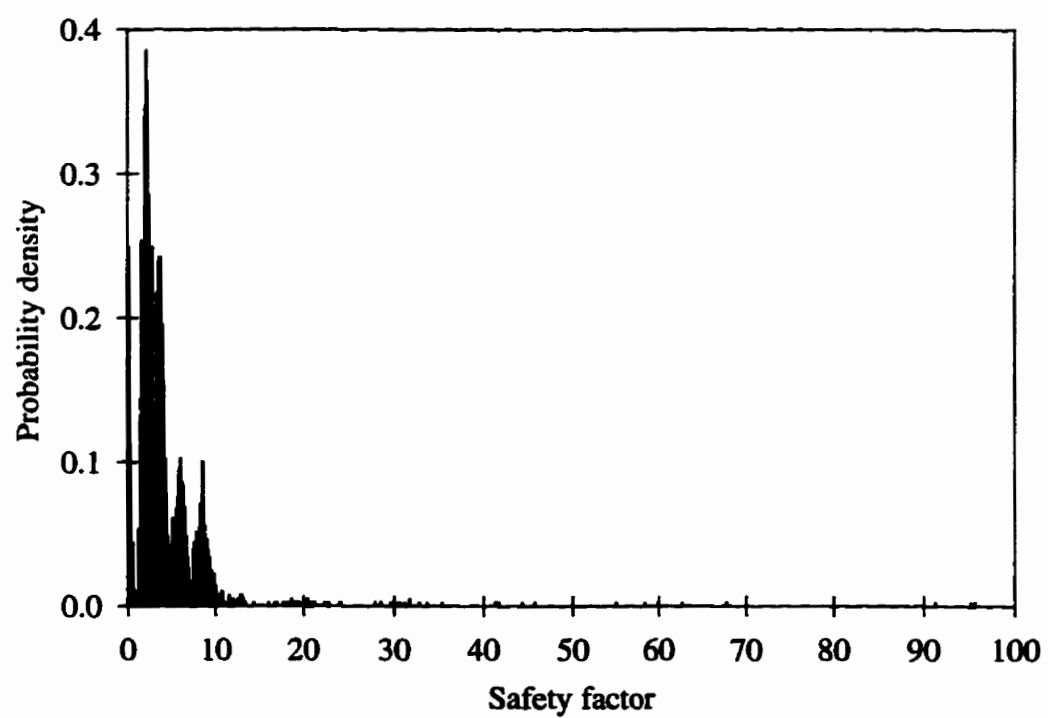
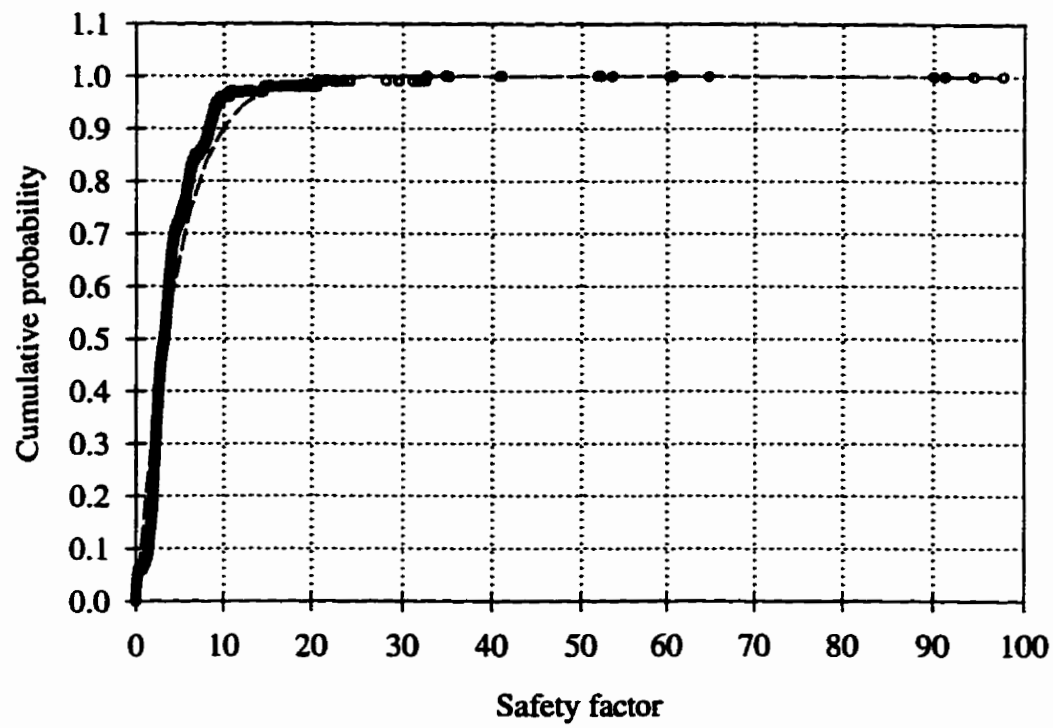


Figure 4.26 The cumulative distribution and histogram of total safety factor with $-99.99 < SF < 99.99$.

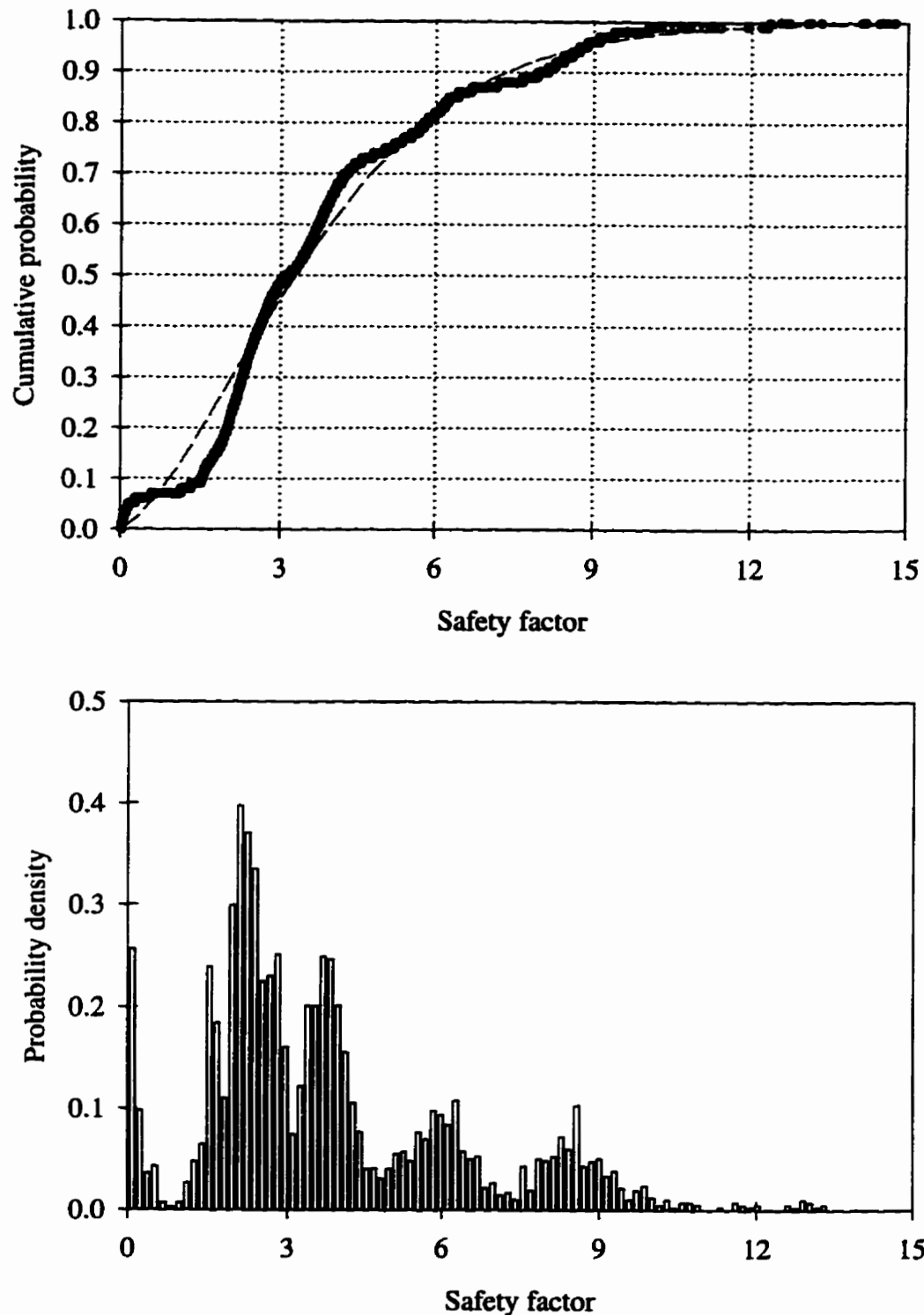


Figure 4.27 The cumulative distribution and the histogram of total safety factors with $0 < SF < 15$.

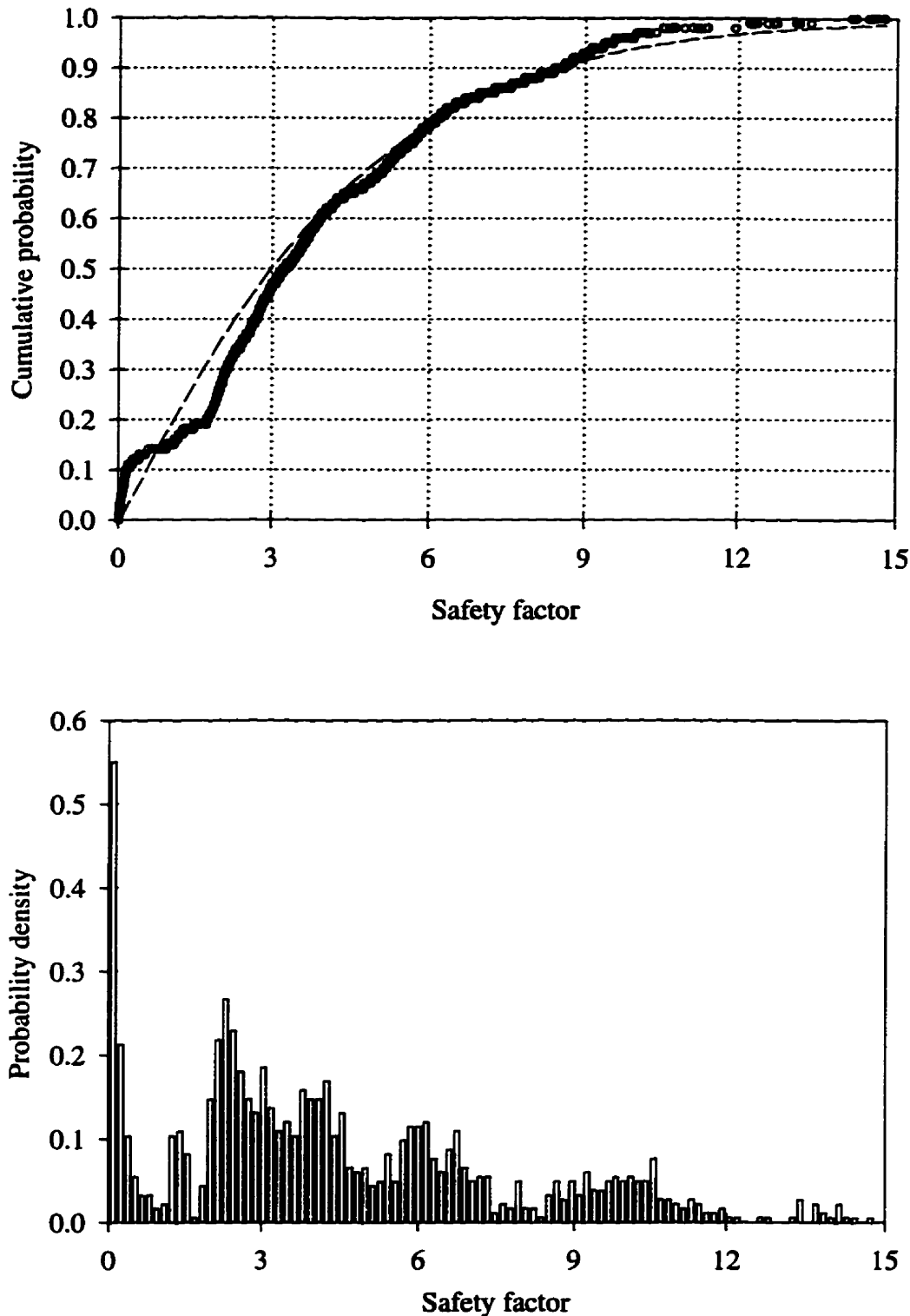


Figure 4.28 The cumulative distribution and histogram of safety factors in wedge sliding failure mode with $0 < SF < 15$.

The histogram and the cumulative distribution of the safety factor in plane sliding in the range between -99.99 and 99.99 are shown in Figure 4.28. The distribution is multi-modal. There is however less overlap among the five individual distribution. When taken separately, the safety factors in the range 1.0 ~ 1.82, 1.82 ~ 3.08, 3.1 ~ 4.8, 5.35 ~ 6.9 and 7.2 ~ 10 can be considered approximately unimodal. Figure 4.29 shows one of these for the range between 3.1 and 4.8. What is of interest that the unimodal distributions involve either only one plane or planes with very similar orientation. For example, when the safety factors are within the range of 0 ~ 1.82, only discontinuity 29 is involved. When the safety factors are within 3.1 ~ 4.8, three discontinuities 24, 26 and 38 are listed, all belonging to the same set.

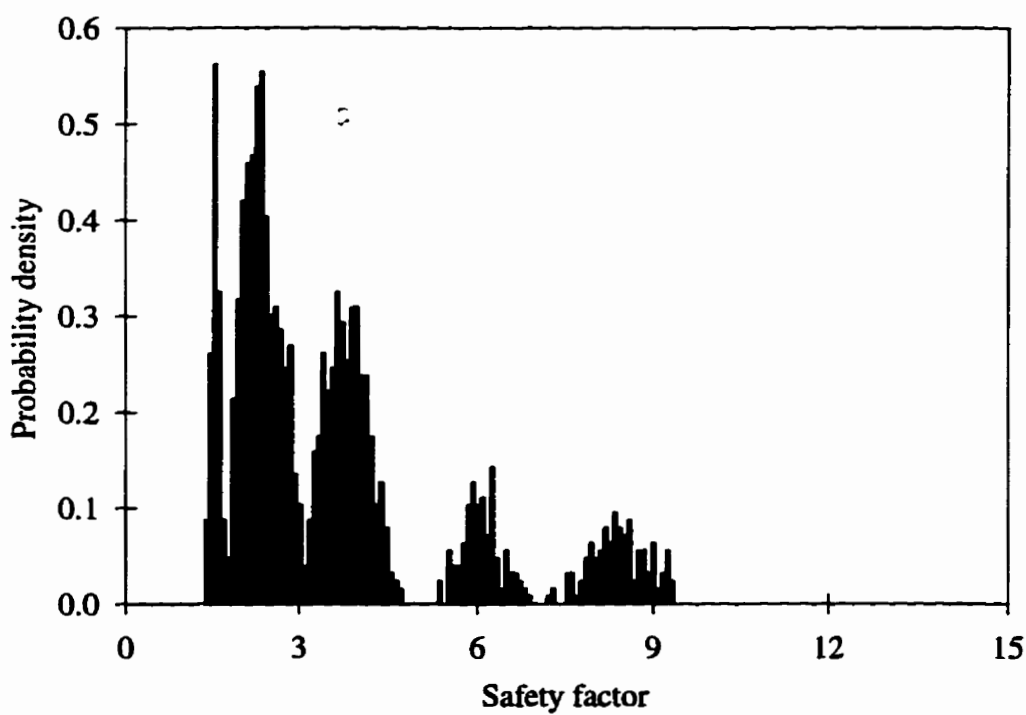
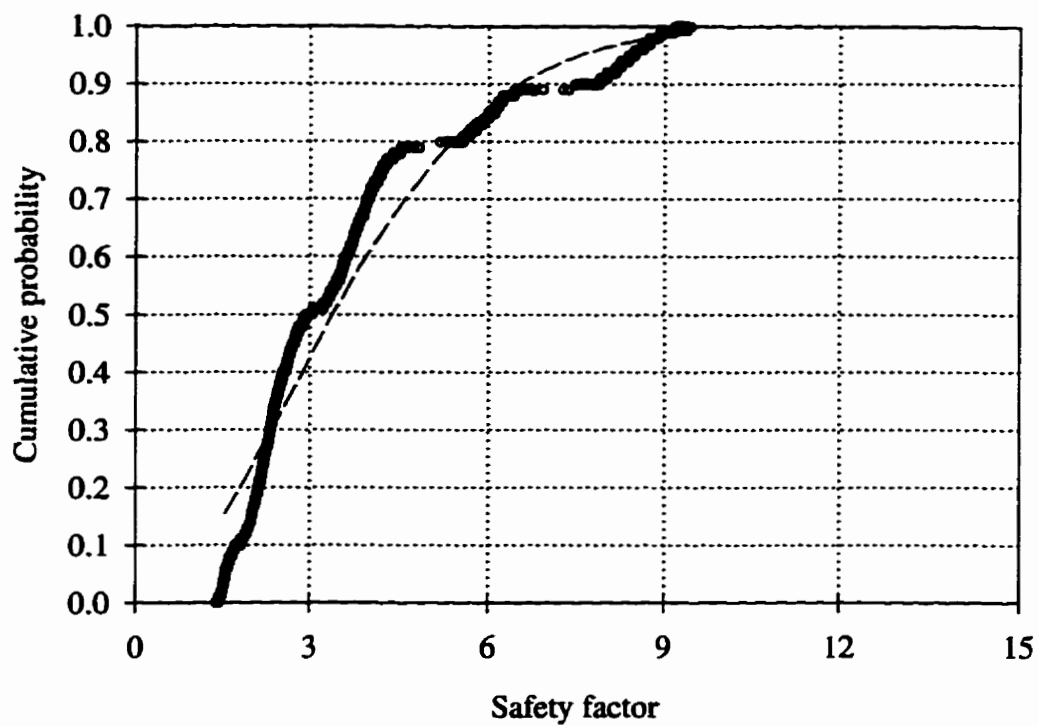


Figure 4.29 The cumulative distribution and histogram of safety factors in plane sliding failure mode with $-99.99 < SF < 99.99$.

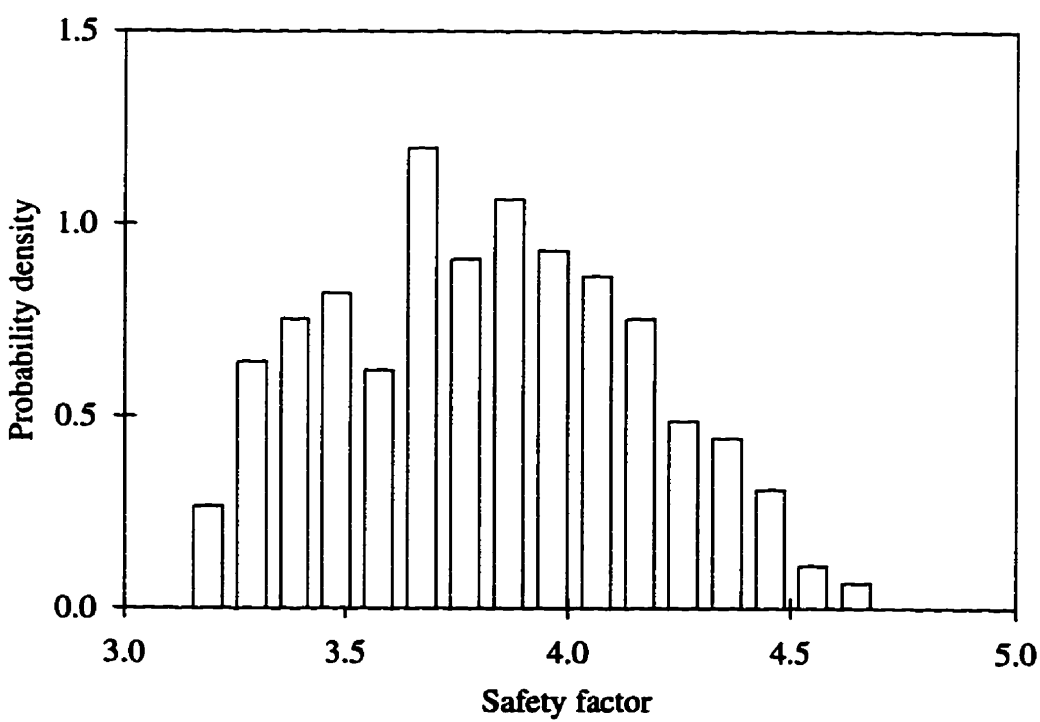
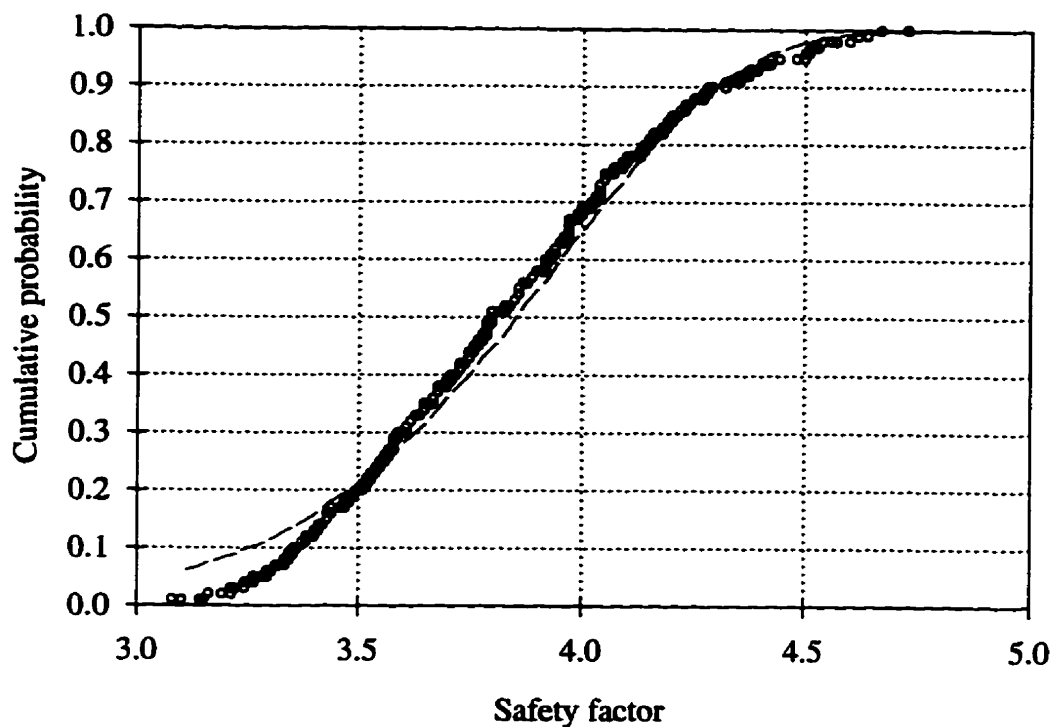


Fig. 4.30 The cumulative distribution and the histogram of safety factors in plane sliding mode with $3.1 < \text{SF} < 4.8$. Only discontinuities of the same set are forming the sliding plane.

Chapter 5

Conclusions

EzSlide is a Windows - based program with a user - friendly interface. It provides functions for conducting both a deterministic and a probabilistic analysis for sliding failure in rock slopes.

The effects of Barton's strength parameters on the safety factor of a sliding rock wedge and the probability of failure of a multi joint system have been investigated. It is evident that normal stress in shallow rock slope problems is usually much smaller than the joint *Wall Strength Coefficient JCS*. Consequently *JCS* has insignificant impact on the safety factor and the probability of failure. This is especially true when the value of *JRC* is low. The influence of the basic friction angle on the safety factor is linear. With increasing basic friction angle, the safety factor increases linearly at the same rate regardless of the value of *JCS*. The *JRC*, *Joint Roughness Coefficient*, has the most significant effect on the safety factor and the probability of failure.

The sensitivity of the probability of failure to the slope angle and the slope strike has been investigated using the Kenora rock cut. Both the safety factor and the probability of failure are more sensitive to the orientations of joints than to the variation in strength parameters.

The distribution of the safety factor data coming from the Monte Carlo simulation is multi-modal. The multi-modality comes from the fact that joint orientations do not form a continuous distribution; joints come in sets.

The orientation of discontinuities has the most dominant impact on rock slope stability. Since the orientation data of joints from a site investigation are used directly in the program EzSlide, the quality of site investigation will determine the reliability of the simulation. A careful site investigation for a joint system is suggested when using EzSlide.

Care should be taken for selecting the range of random variables, especially when the probability distribution of a random variable is assumed to be the Weibull, or the lognormal or the exponential distribution. The normal and the triangular distribution are suggested for modeling the random variable if the probability distribution of a random variable is unknown.

Appendix

Table A.1: The Discontinuity List of the rock joint system located on the south side of highway 17A west of the intersection with 659 near Kenora, Ontario (Figure 4.1)

<i>Discontinuity</i>	<i>Azimuth(°)</i>	<i>Plunge (°)</i>	<i>Domain</i>	<i>JRC</i>
1	118	0	2	4
2	117	1	2	5
3	116	0	2	5
4	117	5	2	5
5	114	5	2	5
6	116	2	2	6
7	122	1	2	6
8	116	3	2	8
9	115	2	2	6
10	110	5	2	5
11	110	10	2	5
12	112	0	2	6
13	116	10	2	7
14	112	0	2	5
15	114	2	2	8
16	111	5	2	4
17	124	5	2	6
18	114	0	2	5
19	108	10	2	6
20	112	0	2	6
21	110	2	2	7
22	180	77	3	9
23	153	82	3	4
24	190	78	3	5
25	172	72	3	4
26	194	80	3	4
27	186	73	3	5
28	204	85	3	8
29	204	65	3	6
30	146	80	3	6
31	176	80	3	5
32	154	78	3	3
33	154	72	3	4
34	190	75	3	5
35	170	74	3	7
36	197	83	3	4
37	153	79	3	4

Table A.1(continued).

<i>Discontinuity</i>	<i>Azimuth(°)</i>	<i>Plunge (°)</i>	<i>Domain</i>	<i>JRC</i>
38	198	79	3	3
39	130	46	3	4
40	132	49	3	6
41	130	60	3	7
42	138	50	3	4
43	140	55	3	4
44	150	58	3	5
45	50	30	1	4
46	44	30	1	4
47	48	38	1	5
48	38	34	1	5
49	44	25	1	6
50	46	34	1	7
51	40	40	1	7
52	54	35	1	6
53	43	30	1	5
54	16	23	1	4
55	50	25	1	7
56	43	35	1	7
57	36	25	1	5
58	224	55	3	5
59	201	72	3	5
60	202	70	3	7

Table A.2 The geometry and the estimated strength parameters of the partially failed wedge located on the north side of highway 17A (Figure 4.2)

	<i>Azimuth(°)</i>	<i>Plunge (°)</i>	<i>JCS(MPa)</i>	ϕ_B (°)	<i>JRC</i>
Slope	10	0	---	---	---
Top Slope	10	85	---	---	---
Plane A	296	36	50	26	5
Plane B	46	20	50	26	5

Height = 4 meters.

References

- Barton, N. 1976. The shear strength of rock and rock joints. International Journal of Rock Mechanics Mining Sciences & Geomechanics Abstracts, Vol. 13, pp. 255-279.
- Call, R. D. 1985. Probability of stability of open pit slopes. In Rock Masses: Edited by C. H. Dowding. Proceedings of the Geotechnical Engineering Division, American Society of Civil Engineers, Denver, Colo., pp. 56-71.
- Call, R. D., Savel, J. P., and Nicholas, D. E. 1976. Estimation of joint set characteristics from surface mapping data. Proceedings, 17th U. S. Symposium on Rock Mechanics, Snowbird, Utah, pp. 65-73.
- Carter, B. J. & Lajtai, E. Z. 1992. Rock slope stability and distributed joint systems. Canada Geotech. J. Vol. 29 pp. 53-60.
- Chowdhury, R. N. 1986. Geomechanics risk model for multiple failure along rock discontinuities. International Journal of Rock Mechanics Mining Sciences & Geomechanics Abstracts, Vol. 23, 337 – 346.
- Dershowitz, W. S. & Einstein, H. H. 1988. Characterizing rock joint geometry with joint system models. Rock Mechanics and Rock Engineering, Vol. 21, pp. 21 – 51.
- Einstein, H.H., and Baecher, G. B. 1983. Probabilistic and statistical methods in engineering geology. Specific models and examples, part I: exploration. Rock Mechanics and Rock Engineering, Vol. 16, pp. 39-72.
- Franklin, J. A. & Dusseault, M. B. 1989. Rock Engineering. McGraw-Hill Publishing Company. New York.
- Glynn, E. F., Ghosh, S. 1982. Effect of correlation on rock slope stability analyses. Proceedings, 23rd U.S. Symposium on Rock Mechanics, Berkeley, California, pp. 95 – 115.
- Goodman, R.E. 1989. Introduction to rock mechanics. 2nd edition. John Wiley & Sons, New York.
- Herget, G. 1977. "Structural Geology", Chapter 4, Pit Slope Manual, CANMET Pit Slope Project, 1972/1977, Ottawa.
- Herget, G. 1978. Analysis of discontinuity orientation for a probabilistic slope stability design. Proceedings, 19th U. S. Symposium on Rock Mechanics, Lake Tahoe, Nov., pp.42-50.
- Hoek, E., & Bray, J. W. 1977. Rock slope engineering. Second edition. The Institution of Mining and Metallurgy, London.

Kim, K. & Gao, H. 1995. Probabilistic approaches to estimating variation in the mechanical properties of rock mass. International Journal of Rock Mechanics Mining Sciences & Geomechanics Abstracts, Vol. 32, No. 2, pp. 111-120.

Lajtai, E.Z. & Carter, B. J. 1989. GEOSLIDE ---- A computer code on the IBM PC for the analysis of rock slopes. Department of Civil and Geological Engineering, University of Manitoba, Winnipeg, Canada.

Lama, R. D. & Vtukuri, V. S. 1978. Handbook on mechanical properties of rocks. Volume III, Volume IV. Trans Tech Publications.

Law, A. M. & Kelton, W. D. 1991. Simulation Modeling and Analysis. Second edition. McGraw-Hill, Inc.

Leung, C. F. & Kheok, S.C. 1987. Computer aided analysis of rock slope stability. Rock Mechanics and Rock Engineering, Vol. 20, pp. 111-122.

McMahon, B. K. 1971. A Statistical method for the design of rock slopes. Proceedings, 1st Australia - New Zealand Conference on Geomechanics, Melbourne, Australia, Vol. 1, pp. 314-321.

Piteau, D. R., Stewart, A. F., Martin, D. C. and Trenholme, B. S. 1985. A combined limit equilibrium statistical analysis of wedges for design of high rock slopes. In Rock Masses: Edited by C. H. Dowding. Proceedings of the Geotechnical Engineering Division, American Society of Civil Engineers, Denver, Colorado, pp. 93-121.

Priest, S. D. and Hudson, J. A. 1976. Discontinuity spacing in rock. International Journal of Rock Mechanics Mining Sciences & Geomechanics Abstracts, Vol. 13, pp. 135 – 148.

Quek, S.T. and Leung, C. F. 1995. Reliability-based stability analysis of rock excavations. International Journal of Rock Mechanics Mining Sciences & Geomechanics Abstracts, Vol. 32, No.6, pp. 617 - 620.

Savely, J. P. 1985. An application of probability to rock slope design. In Rock Masses: Edited by C. H. Dowding. Proceedings of the Geotechnical Engineering Division, American Society of Civil Engineers, Denver, Colo., pp. 72-92.

Singh, R. N, Denby, B. & Brown, D. J. 1985. The characteristics of coal measures instability in British surface mines. 26th US Symposium on Rock Mechanics, Rapid City, slope SD, pp. 41-48.

Sobol', I. M. 1994. A Primer for the Monte Carlo Method. CRC Press, Inc. Florida.

Tamimi, S., Amadei, B. and Frangopol, D. M. 1989. Monte Carlo Simulation of Rock Slope Reliability. Computer & Structures Vol. 33, No.6: 1495-1505.

Walker, J.R. 1987. Variate generation for probabilistic fracture mechanics and fitness-for-service studies. Whiteshell Nuclear Research Establishment, Pinawa, Manitoba. AECL-9088.

Warburton, P.M. 1981. Vector stability analysis of an arbitrary polyhedral rock block with any number of free faces. *International Journal of Rock Mechanics Mining Sciences & Geomechanics Abstracts*, Vol. 18, pp. 415-427.

Young, D.S., and Hoerger, S.F. 1988. Geostatistics applications to rock mechanics. *Proceedings, 29th U. S. Symposium on Rock Mechanics*, University of Arizona, Tucson, Arizona, pp. 271-282.

Appleman, D., Visual Basic Programming guide to the Win32 API. Ziff-Davis Press, An imprint of Macmillan Computer Publishing USA. Emeryville, California.

Feldman, P., Jennings, R., Seymour, B., Eidson, B., Palmer, P., Gillmor, S. & Pesso, J. 1993. Using Visual Basic 3. Que® Corporation.

"Programmer's Guide - Microsoft Visual Basic, Programming System for Windows – Version 4.0", Microsoft Corporation, 1995.

"Language Reference - Microsoft Visual Basic, Programming System for Windows – Version 4.0", Microsoft Corporation, 1995.

"Spread/VBX™" for Visual Basic, FarPoint Technologies, Inc., 1993.